



**Aalto University  
School of Chemical  
Engineering**

**Sami Kulju**

## **PALLADIUM-CATALYZED HETEROARYLATION OF VINYL CHLORIDES**

Master's Programme in Chemical, Biochemical and Materials Engineering  
Major in Chemistry

Master's thesis for the degree of Master of Science in Technology  
submitted for inspection, Espoo, 16 October 2017.

Supervisor

Professor Ari Koskinen

Instructor

D. Sc. (Tech.) Esa Kumpulainen

---

**Author** Sami Kulju

---

**Title of thesis** Palladium-catalyzed heteroarylation of vinyl chlorides

---

**Degree Programme** Master's Programme in Chemical, Biochemical and Materials Engineering

---

**Major** Chemistry

---

**Thesis supervisor** Professor Ari Koskinen

---

**Thesis advisor** D. Sc. (Tech.) Esa Kumpulainen

---

**Date** 16.10.2017**Number of pages** 58+28**Language** English

---

## Abstract

This master's thesis describes a method to prepare heteroarene-linked cycloalkenones. The method is a previously underutilized palladium-catalyzed coupling reaction between vinyl chlorides and non-activated heteroarenes. The reaction type is essentially the reverse of the Heck reaction.

The procedure was optimized using a reaction between imidazo[1,2-*a*]pyridine and 3-chloro-2-cyclohexenone. The optimized reagent system consists of Pd(OAc)<sub>2</sub> as catalyst, PPh<sub>3</sub> as ligand, K<sub>2</sub>CO<sub>3</sub> as base, 2-ethylhexanoic acid as acid additive and toluene as solvent. A number of other heteroarenes and another chlorocycloalkenone were used to expand the scope of the reaction, with a total of 23 successfully synthesized products. By default, the syntheses were performed at 100 °C but some substrates required a higher temperature of 120 °C. Chlorocycloalkenones were used in a moderate excess.

The most suitable substrates were fused imidazoles and substituted oxazoles and thiazoles. Yields of over 80% were obtained from several substrates and most yields ranged between 50% and 80%. Ester and nitrile functionalities were tolerated. Unsubstituted thiazole reacted unselectively at two sites.

As such, the developed method has potential uses in small-scale medicinal chemistry and other fine chemical industries. The use of non-activated heteroarenes complies with the green chemistry principles. In addition, vinyl chlorides are conveniently synthesized and are relatively stable compared to other vinyl halides.

---

**Keywords** C-H activation, palladium, heteroarenes, heteroarylation, vinyl chlorides, DoE

---

---

**Tekijä** Sami Kulju

---

**Työn nimi** Palladiumkatalysoitu vinyylidikloridien heteroarylointi

---

**Koulutusohjelma** Master's Programme in Chemical, Biochemical and Materials Engineering

---

**Pääaine** Chemistry

---

**Työn valvoja** Professori Ari Koskinen

---

**Työn ohjaaja** TkT Esa Kumpulainen

---

**Päivämäärä** 16.10.2017

---

**Sivumäärä** 58+28

---

**Kieli** englanti

---

## Tiivistelmä

Tässä diplomityössä esitellään menetelmä heteroareenikytkettyjen sykloalkenonien valmistamiseksi. Menetelmä on aiemmin vähän käytetty palladiumin katalysoima kytKentäreaktio vinyylidikloridien ja aktivoimattomien heteroareenien välillä. Reaktiotyyppiä voi pitää käänteisenä Heck-reaktioon nähden.

Menetelmä optimoitiin käyttäen reaktiota imidatso[1,2-a]pyridiinin ja 3-kloro-2-sykloheksenonin välillä. Optimoidussa reagenssiyhdistelmässä oli katalyyttinä Pd(OAc)<sub>2</sub>, ligandina PPh<sub>3</sub>, emäksenä K<sub>2</sub>CO<sub>3</sub>, happolisäaineena 2-etyyliheksaanihappo ja liuottimena tolueni. Yhteensä 23 tuotetta valmistettiin onnistuneesti käyttäen erilaisia heteroareeneja ja toista klorosykloalkenonia. Useimmat synteesit tehtiin 100 °C:n lämpötilassa, mutta osa lähtöaineista vaati 120 °C:n lämpötilan. Klorosykloalkenoneja käytettiin ylimäärin.

Soveltuvimpia lähtöaineita olivat bisykliset imidatsolit sekä substituoidut oksatsolit ja tiatsolit. Useat reaktiot tuottivat yli 80 %:n saannon, ja useimmat saannot olivat 50 ja 80 %:n välillä. Esteri- ja nitrilifunktionaalisuudet kestivät reaktio-olosuhteissa. Substituoidun tiatsolin reagoi epäselektiivisesti kahdesta paikasta.

Menetelmä soveltuu sellaisenaan pienen mittakaavan lääkeainekemian ja muun hienokemian käyttöön. Aktivoimattomien heteroareenien käyttö on vihreän kemian periaatteiden mukaista. Lisäksi vinyylidikloridit ovat helposti saatavilla ja ne ovat suhteellisen stabiileja muihin vinyylialideihin verrattuna.

---

**Avainsanat** C-H-aktivointi, palladium, heteroareenit, heteroarylointi, vinyylidikloridit, DoE

---

## **Preface**

The experimental work for this master's thesis was carried out at the department of Medicinal Chemistry at Orion Pharma, Espoo, between February and May 2017. I appreciate the opportunity to work on this fascinating topic that was conceived by my advisor Dr. Esa Kumpulainen. I also wish to thank Prof. Ari Koskinen, all the helpful people in the labs, and my family and friends.

Helsinki, 16 October 2017

Sami Kulju



## Abbreviations

Ad	adamantyl
Ar	(hetero)aromatic group
B	base
BINAP	2,2'-bis(diphenylphosphino)-1,1'-binaphthyl
bipy	2,2'-bipyridine
Boc	<i>tert</i> -butoxycarbonyl
CMD	concerted metalation-deprotonation
CPME	cyclopentyl methyl ether
Cy	cyclohexyl
DCE	1,2-dichloroethane
DFT	density functional theory
DIPEA	<i>N,N</i> -diisopropylethylamine
dipp	1,3-bis(diisopropylphosphino)propane
DMA	dimethylacetamide
DME	1,2-dimethoxyethane
DMF	dimethylformamide
DoE	design of experiments
dppb	1,4-bis(diphenylphosphino)butane
EHA	2-ethylhexanoic acid
EMD	electrophilic metalation-deprotonation
Het	heterocycle
HMG-CoA	3-hydroxy-3-methylglutaryl-coenzyme A
HRMS	high resolution mass spectrometry
IMes	1,3-bis(2,3,6-trimethylphenyl)imidazolium chloride
L	ligand
LC	liquid chromatography
[M]	metal complex

mNP	3-nitrophenyl
mp	melting point
MS	mass spectrometry
NMP	<i>N</i> -methyl-2-pyrrolidone
NMR	nuclear magnetic resonance
NOE	nuclear Overhauser effect
NOESY	nuclear Overhauser effect spectroscopy
[O]	oxidizer
oPBA	<i>o</i> -phenylbenzoic acid
R	any atom or group of atoms
S <sub>E</sub> Ar	electrophilic aromatic substitution
SM	starting material
TADDOL	$\alpha,\alpha,\alpha',\alpha'$ -tetraaryl-2,2-disubstituted 1,3-dioxolane-4,5-dimethanol
OTf	triflate, trifluoromethanesulfonate
Piv	pivaloyl
TMEDA	tetramethylethylenediamine
TMS	tetramethylsilane
UPLC	ultra performance liquid chromatography
UV	ultraviolet
vis	visible light
X	(pseudo)halogen
Y	heteroatom
Z	heteroatom

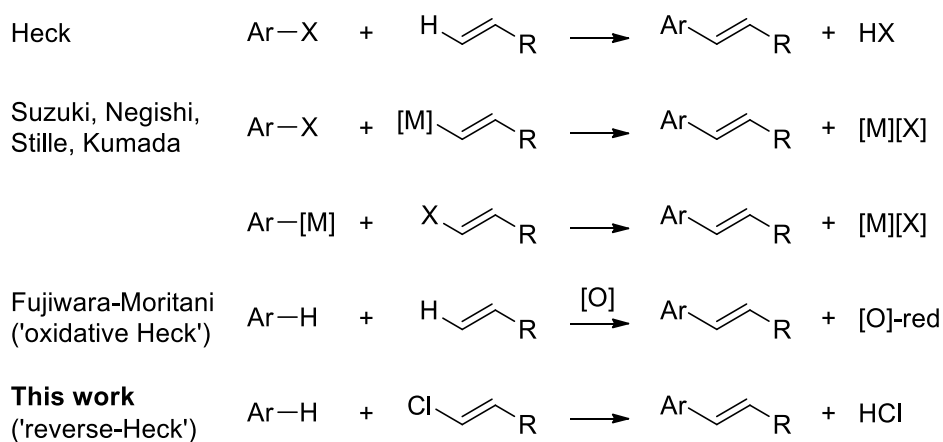
## Table of Contents

<b>1</b>	<b>Introduction.....</b>	<b>1</b>
<b>2</b>	<b>Applications of vinyl heteroarenes .....</b>	<b>3</b>
<b>3</b>	<b>C–H arylation of vinyl halides .....</b>	<b>5</b>
3.1	Proposed mechanisms .....	5
3.2	Regiochemistry of the double bond .....	8
3.3	Stereochemistry of the double bond.....	11
3.4	Effect of the (pseudo)halide .....	12
3.5	Regiochemistry of the arene.....	14
3.6	Reactions with heteroarenes.....	16
3.7	Reactions with arenes.....	24
<b>4</b>	<b>Results and discussion .....</b>	<b>27</b>
4.1	Model reaction .....	27
4.2	Optimization of reaction conditions.....	29
4.3	Scope and limitations .....	34
<b>5</b>	<b>Conclusions and outlook .....</b>	<b>39</b>
<b>6</b>	<b>Experimental.....</b>	<b>40</b>
6.1	Starting materials .....	40
6.2	Coupling reactions .....	41
<b>7</b>	<b>References.....</b>	<b>54</b>
	<b>Appendices.....</b>	<b>59</b>

## 1 Introduction

Palladium-catalyzed coupling reactions have long been recognized as some of the most powerful and versatile ways of forming carbon–carbon bonds. A particularly reliable class of these reactions is a coupling of an aryl or vinyl halide with an organometallic reagent. Both of the coupling partners have to be functionalized, which increases synthetic complexity as well as byproducts. In accordance with the green chemistry principles, the focus in palladium-catalyzed reactions has turned to reactions that do not have these limitations. Much attention has recently been paid to C–H activation reactions in which at least one reactive center is a simple carbon–hydrogen bond. In 2011 alone over 500 papers were published on the topic.<sup>1</sup>

An emerging subject in the field of C–H activation is a coupling of non-activated heteroarenes with vinyl halides. Vinyl heteroarenes are in themselves common motifs in pharmaceutical compounds; in addition, the double bond can act as a scaffold onto which further functionalities can be built. The novel strategy is the reverse of the Heck reaction which couples aryl halides with alkenes (Scheme 1). Another related C–H activation reaction is the Fujiwara-Moritani reaction which was first described using stoichiometric palladium a few years prior to the Heck reaction.<sup>2</sup> Later iterations use an external oxidizer which regenerates the active catalyst, hence the reaction is also called the oxidative Heck reaction. The reduced form of the oxidizer is obtained as a byproduct.



**Scheme 1. Palladium-catalyzed aryl–vinyl coupling reactions. Any acid byproducts are usually neutralized with base. X = Cl, Br, I, OTf; [M] = B(OR)<sub>2</sub>, ZnX, SnR<sub>3</sub>, MgX.**

This thesis aims to develop a C–H activation procedure coupling heteroarenes with vinyl chlorides. Vinyl chlorides are uncommon coupling partners due to their low reactivity; however, they are usually more available and less expensive than other vinyl halides. Non-activated heteroarenes are also attractive substrates in cases where the heteroarene has no available activated analogues. The optimized procedure is applied to different heteroarenes and vinyl chlorides.

The second chapter of this thesis presents potential applications of the method. Chapter 3 is a detailed review on the reaction class in question. Proposed mechanisms are presented and existing literature is discussed more closely. Properties unique to the reverse-Heck reaction are considered in detail and compared to the Heck and oxidative Heck reactions. Chapters 4 to 6 summarize the experimental part of the thesis.

## 2 Applications of vinyl heteroarenes

Many active pharmaceutical ingredients contain a side chain double bond connected to a heteroaromatic ring. Examples of such vinyl heteroarenes are presented in Figure 1. The examples contain a variety of heterocycles including thiophene, thiazole, imidazole, quinoline, pyrrole, pyridine, indole and pyrimidine as well as both electron-rich and electron-deficient double bonds. Ixabepilone is an amide analogue of the epothilones, bacterial metabolites that have been studied as potential anticancer drugs.<sup>3</sup> Other examples include the antiparasitic drug pyrantel,<sup>4</sup> the antihypertensive drug eprosartan,<sup>5</sup> the antiasthmatic drug montelukast,<sup>6</sup> the anticancer drugs sunitinib<sup>7</sup> and abiraterone acetate<sup>8</sup> and the lipid-lowering HMG-CoA reductase inhibitors fluvastatin<sup>9</sup> and rosuvastatin.<sup>10</sup>

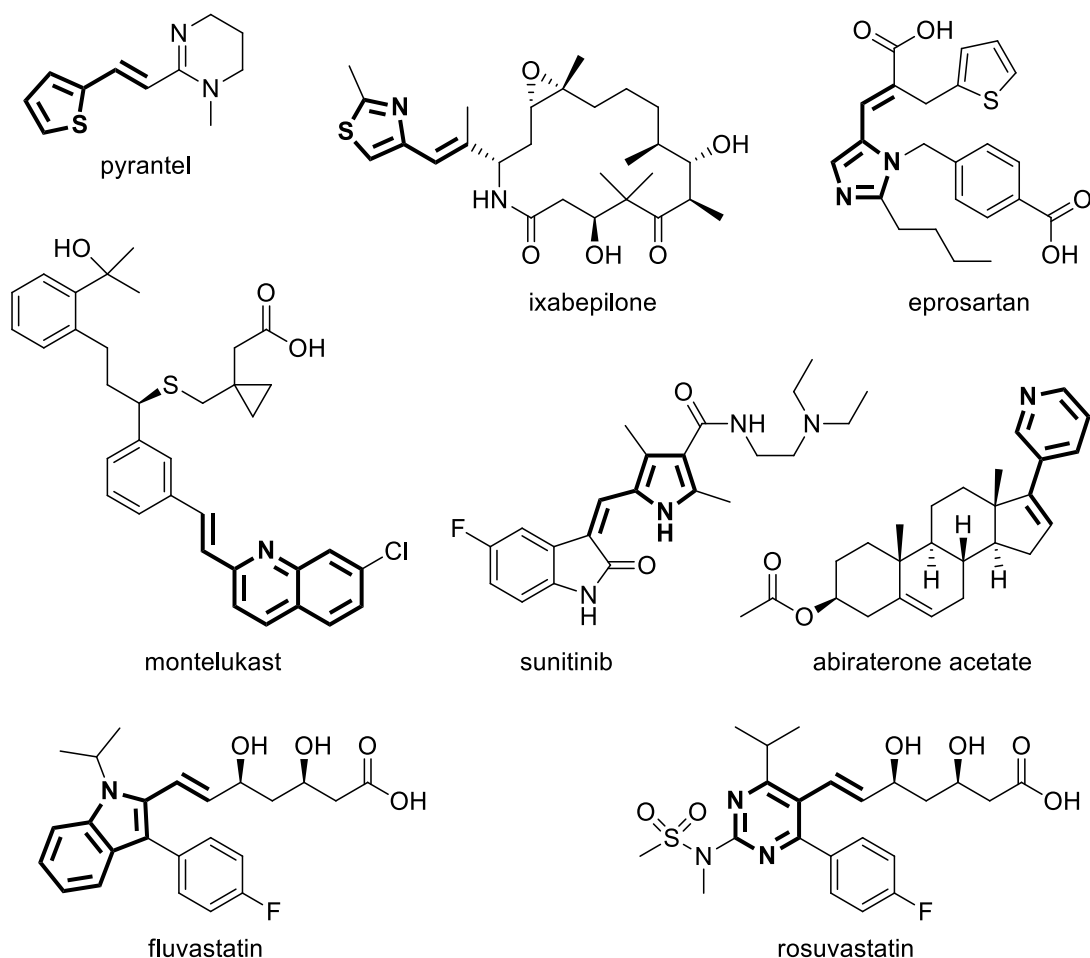
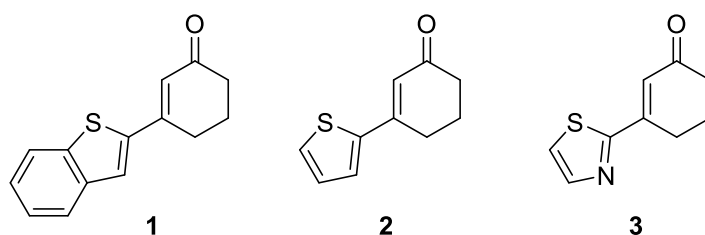


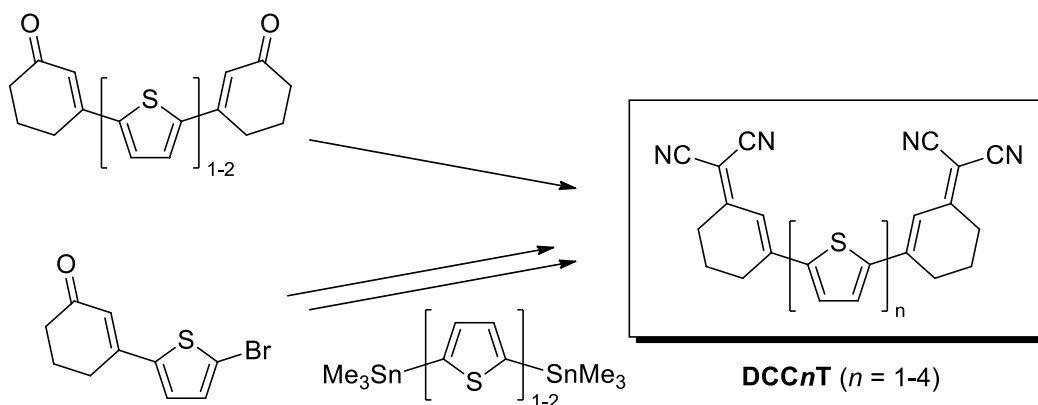
Figure 1. Pharmaceutical molecules that contain vinyl heteroarene units.

Modern statin drugs typically have such a side chain double while in the older types of statins a saturated linkage has usually provided optimal activity.<sup>11</sup> Similarly, the reduced derivative of abiraterone acetate was an order of magnitude less potent than its precursor.<sup>8</sup>

Some interest has also been directed toward heteroarene-coupled cyclohexenones which are the focus of the experimental part of this thesis. Gilbertson and co-workers screened multiple related small molecule inhibitors of anthrax edema factor and reported moderate activity (Figure 2).<sup>12</sup> The compounds were synthesized using a Suzuki-type reaction with yields ranging from low to good. Bäuerle and co-workers developed a series of dicyanomethylene-capped oligothiophenes DCCnT that function as small molecule semiconductors (Scheme 2).<sup>13</sup> Thiophene-coupled cyclohexenones served as important intermediates. These acceptor–donor–acceptor-type oligomers outperformed previous derivatives and have potential applications in organic solar cells.



**Figure 2.** Examples of small molecule inhibitors of anthrax edema factor screened by Gilbertson and co-workers.<sup>12</sup>



**Scheme 2.** Syntheses of small molecule semiconductors DCCnT from thiophene-coupled cyclohexenones.<sup>13</sup>

### 3 C–H arylation of vinyl halides

In the last couple of decades a handful of papers have been published on a new type of vinyl–aryl coupling reaction, C–H arylation of vinyl halides. These reactions have combined some of the best qualities of the existing techniques: few byproducts, easily obtained starting materials, good regioselectivity, and good functional group tolerance. Since a vinyl halide is coupled with a non-activated arene, the method has been called the inverse- or reverse-Heck reaction.<sup>14,15</sup> This chapter discusses the reverse-Heck reaction in detail, concentrating on differences to the other Heck-type reactions. Although some authors have not distinguished the reverse-Heck reaction from the Heck reaction, it can be argued that the differences in regio- and stereoselectivity justify calling it its own type.

Subchapters 3.6 and 3.7 elaborate on representative reactions that did not come up on previous subchapters. As the thesis mainly focuses on heteroarenes, reactions of arenes are discussed in a more general sense. Common strategies to achieve regioselectivity are discussed.

Similar reactions have also been performed using copper<sup>16</sup> and cobalt<sup>17</sup> catalysts instead of palladium. Other palladium-catalyzed reactions have been performed using a copper cocatalyst<sup>18,19</sup> or a strong organometallic base (e.g. BuLi<sup>20</sup> or a Grignard reagent<sup>21</sup>). The latter types can be considered to belong to the organometal–halide coupling reactions. This thesis focuses on reactions using palladium as the sole metal catalyst. Some borderline cases using an intermediate strength base (e.g. *t*-BuOLi<sup>22</sup>) are included.

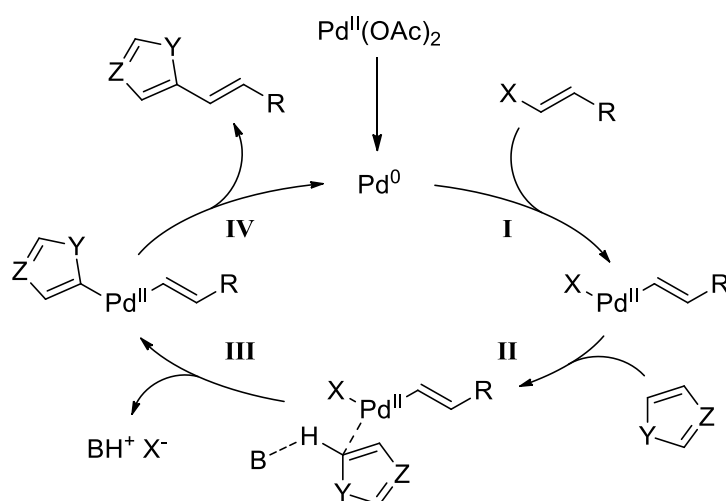
#### 3.1 Proposed mechanisms

Two essentially different mechanisms have been proposed for the reverse-Heck reactions: one catalyzed by Pd<sup>0</sup> (Scheme 3) and the other catalyzed by Pd<sup>II</sup> (Scheme 4). The actual C–H activation step (metalation-deprotonation) and other details that affect the regio- and stereochemical outcome are discussed in the following subchapters. In the presented general catalytic cycles spectator ligands (e.g. solvent



or  $\text{PPh}_3$ ) are omitted and an unspecified base B is present. Base is however not used in some actual procedures: for example, Daugulis and Zaitsev used  $\text{AgOTf}$  to precipitate the halide.<sup>15</sup> Fagnou and co-workers also reported that the addition of a soluble proton transfer agent such as pivalic acid significantly increased reactivity in C–H heteroarylations of aryl halides.<sup>23</sup>

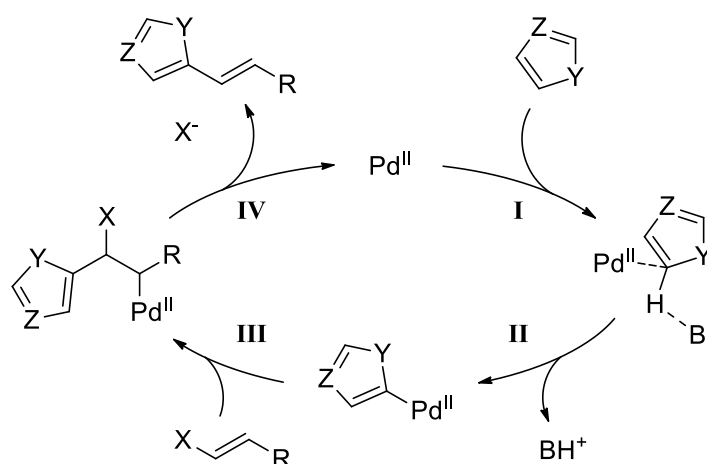
The  $\text{Pd}^0$  mechanism (Scheme 3) was proposed by Trauner and Hughes<sup>24</sup> based on the work on aryl–aryl coupling reactions by Miura and co-workers.<sup>25</sup> Later similar mechanisms have been proposed by Berteina-Raboin and co-workers,<sup>26</sup> Lautens and Chai,<sup>27</sup> Cramer and Albicker,<sup>28</sup> Li and co-workers,<sup>29</sup> Chen and co-workers<sup>30</sup>, Zhang and co-workers<sup>31</sup> and Xi and co-workers.<sup>32</sup> The mechanism consists of oxidative addition of the vinyl halide to  $\text{Pd}^0$  to generate a  $\text{Pd}^{\text{II}}$  intermediate (I), C–H activation of the heteroarene (II and III) and reductive elimination (IV) to yield the product and regenerate the  $\text{Pd}^0$  catalyst.  $\text{Pd}^0$  is in the first place generated from  $\text{Pd}^{\text{II}}(\text{OAc})_2$  via reduction by a phosphine ligand, an amine or an olefin.<sup>33</sup> The mechanism resembles the Heck reaction<sup>34</sup> in the oxidation state of palladium and the order in which the C–X and C–H bonds are activated, however the exact steps differ: the Heck reaction requires *syn* addition of palladium to the alkene, C–C bond rotation and *syn*  $\beta$ -hydride elimination.



**Scheme 3.** The  $\text{Pd}^0$  mechanism for the heteroarylation of a vinyl halide. Y, Z = heteroatoms.

The  $\text{Pd}^{\text{II}}$  mechanism (Scheme 4) has been proposed by Daugulis and Zaitsev,<sup>15</sup> Bouillon and co-workers<sup>35</sup> and Ye and co-workers.<sup>36</sup> It consists of C–H activation of

the heteroarene (**I** and **II**), *syn* insertion to the vinyl halide (**III**) and *anti*  $\beta$ -halide elimination (**IV**). The oxidation state of palladium stays the same throughout the cycle. The mechanism resembles that of the oxidative Heck reaction<sup>2</sup> except for the last step: the oxidative Heck reaction requires C–C bond rotation, *syn*  $\beta$ -hydride elimination and reductive elimination to afford  $\text{Pd}^0$  which is oxidized to  $\text{Pd}^{\text{II}}$  by an external oxidizer. The reverse-Heck reaction does not require an external oxidizer because the heteroatom ligand can eliminate without reduction.



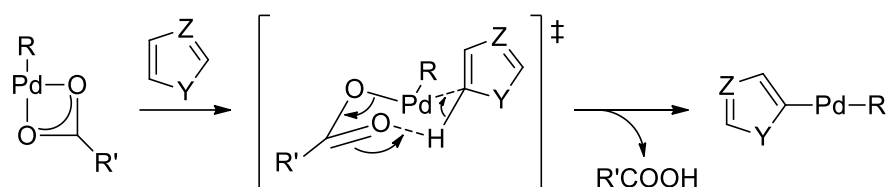
**Scheme 4.** The  $\text{Pd}^{\text{II}}$  mechanism for the heteroarylation of a vinyl halide. Y, Z = heteroatoms.

An important difference between the mechanisms is the way the palladium complex adds to the vinyl halide. In the  $\text{Pd}^0$  mechanism the double bond stays untouched while in the  $\text{Pd}^{\text{II}}$  mechanism the palladium complex inserts across the double bond. It is easy to see that in the  $\text{Pd}^0$  mechanism the regio- and stereochemistries of the double bond stay unchanged but the same also applies to the other mechanism as will be discussed in the following subchapters. Experimental results support this retention hypothesis so both mechanisms are possible.

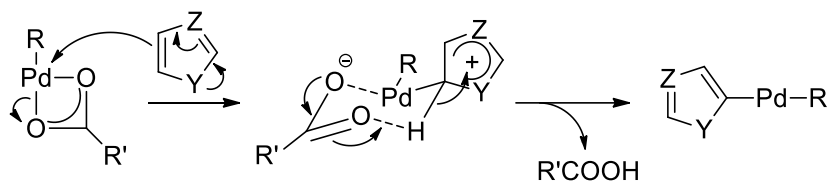
The exact nature of the C–H activation step depends on the base, additive and the (hetero)arene. In Scheme 5 two possible C–H activation pathways are presented: the concerted metalation-deprotonation (CMD) and the electrophilic metalation-deprotonation (EMD).<sup>37</sup> A carboxylic acid  $\text{R}'\text{COOH}$  is added as a proton transfer agent to form the six-membered transition state; a four-membered transition state is also possible with other bases. In the one-step CMD pathway, the aromatic C–H bond is cleaved at the same time as the Pd–C bond is formed. The most acidic C–H

bond is typically activated. In the two-step EMD pathway, the (hetero)arene first attacks in an  $S_EAr$  fashion to palladium, and the C–H bond is cleaved only after the Pd–C bond is formed. The C–H bond is activated at the most nucleophilic site of the arene. The reactions can thus lead to different products depending on the C–H activation mechanism if the most acidic and the most nucleophilic sites differ. Electron-deficient arenes are often thought to react via the CMD pathway and electron-rich arenes via the EMD pathway. However, the issue may not be so obvious as Fagnou and co-workers demonstrated that a wide range of (hetero)arenes, including electron-rich ones, proceed via the CMD pathway.<sup>38</sup>

#### Concerted metalation-deprotonation



#### Electrophilic metalation-deprotonation

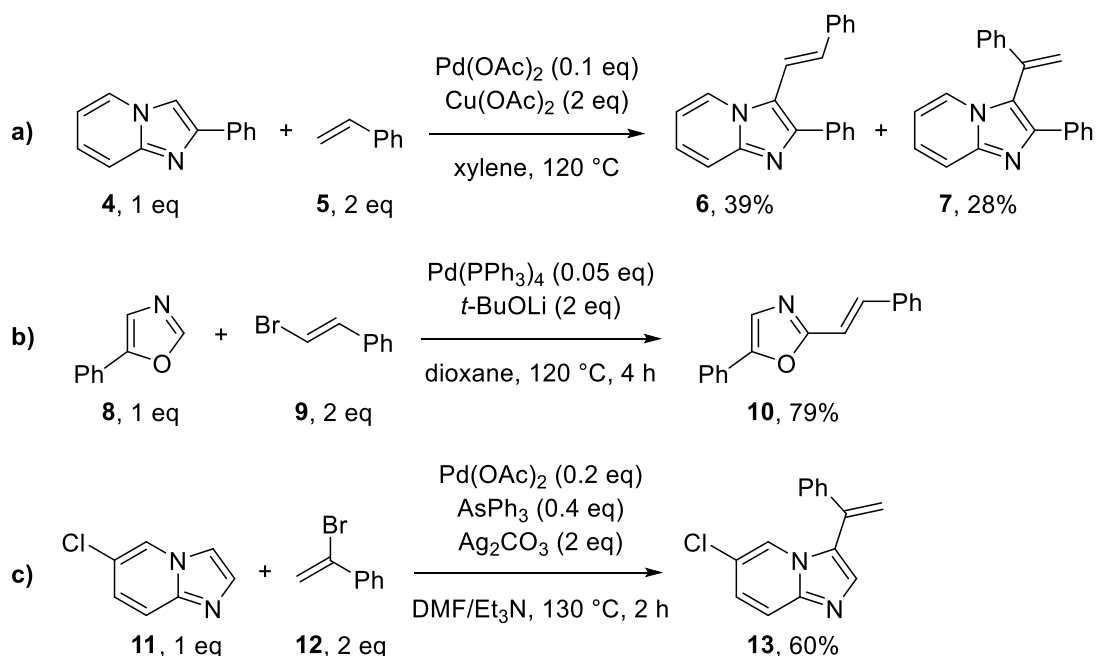


Scheme 5. Two potential pathways for C–H activation. Y, Z = heteroatoms.

### 3.2 Regiochemistry of the double bond

The traditional Heck reactions usually proceed smoothly with alkenes substituted with electron-withdrawing groups. On the other hand, electron-neutral or electron-rich alkenes have often yielded a wide variety of side-products such as diarylated products, regioisomers, double bond isomers and mixtures of *cis* and *trans* isomers.<sup>39</sup> Some useful regio- and stereocontrolled Heck reactions have been developed but they may require extreme conditions or intricate catalyst systems. In contrast, the reverse-Heck reaction is in many ways inherently regio- and stereospecific. These two subchapters discuss the regiochemistry of the vinyl halide coupling partner and the stereoselectivity of the resulting double bond.

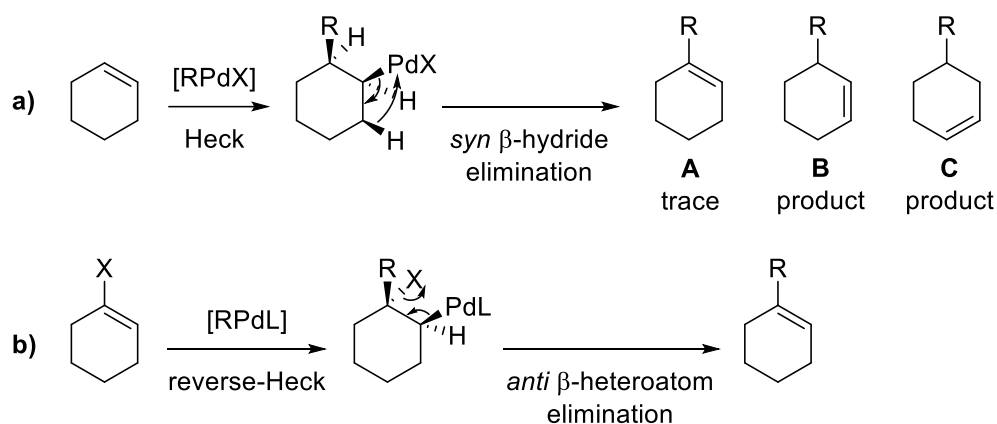
The existing coupling methods have little control over the heteroaryl addition site when using unpolarized vinyl compounds. For example, an oxidative Heck reaction between an imidazo[1,2-*a*]pyridine and styrene reported by Berteina-Raboin and co-workers (Scheme 6a) led to two double bond isomers **6** and **7**.<sup>40</sup> In contrast, reverse-Heck reactions appear to always couple with the halide-bearing carbon atom: for example, the reaction between an oxazole and  $\beta$ -bromostyrene reported by Piguel and co-workers produced the desired  $\beta$ -coupling product **10** in good yield (Scheme 6b).<sup>22</sup> Even the other product **13** could be made via the reverse-Heck reaction as reported in another article by Berteina-Raboin (Scheme 6c).<sup>26</sup>



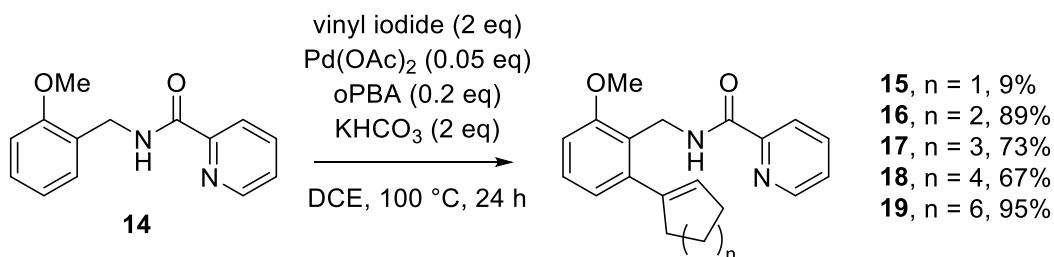
**Scheme 6.** a) Heteroarylation of styrene via the oxidative Heck reaction.<sup>40</sup> b) and c) Heteroarylations of bromostyrenes via the reverse-Heck reaction.<sup>22,26</sup>

Another regiochemical difference is in the position of the double bond. In the Heck and oxidative Heck reactions, *syn*  $\beta$ -hydride elimination next to the inserted group is possible only after a C–C bond rotation. With cyclic olefins (Scheme 7a) this rotation is not possible and the elimination occurs at the opposite side, forming the allylic product **B**.<sup>41</sup> Moreover, the palladium hydride can add to the allylic product and isomerize it to homoallylic product **C**, a process known as double bond migration. The vinylic products **A** have only been achieved with rather specific catalyst–ligand systems and long reaction times<sup>42</sup> or with cyclic enones via a palladium enolate

intermediate.<sup>43</sup> However, regioselectivity is not a problem with the reverse-Heck reactions. Unlike hydrides, heteroatoms are eliminated *anti* which is convenient because the halide always ends up opposite to the palladium after *syn* insertion (Scheme 7b). The *anti* arrangement of  $\beta$ -heteroatom elimination was confirmed experimentally by Lu and Zhu<sup>44</sup> and with DFT calculations by Lin and co-workers.<sup>45</sup> In fact, no competitive *syn*  $\beta$ -hydride elimination occurred at all when there was a good *anti*  $\beta$ -leaving group.<sup>44</sup> Chen and co-workers obtained coupling products from vinyl iodides of various ring sizes in good to excellent yields (Scheme 8), with the exception of the five-membered ring (product **15**).<sup>14</sup> Regioselectivity in the aromatic ring was achieved using a chelating picolinamide group in the *ortho* position (see Section 3.5 for more information).



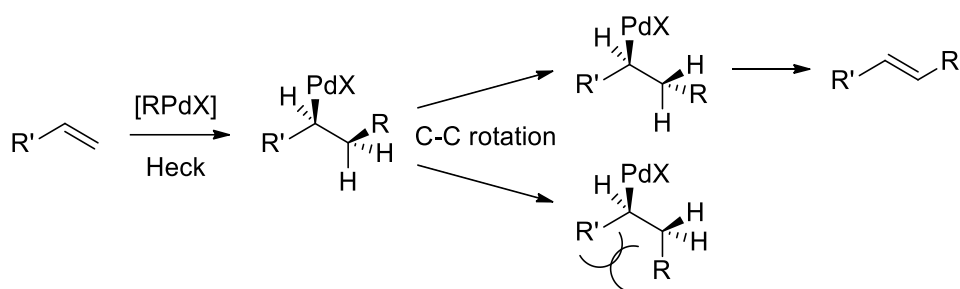
Scheme 7. a) The Heck reaction of cyclohexene. b) The reverse-Heck reaction of cyclohexenyl iodide.



Scheme 8. Chelate-assisted reverse-Heck reactions with various cyclic vinyl iodides.<sup>14</sup>

### 3.3 Stereochemistry of the double bond

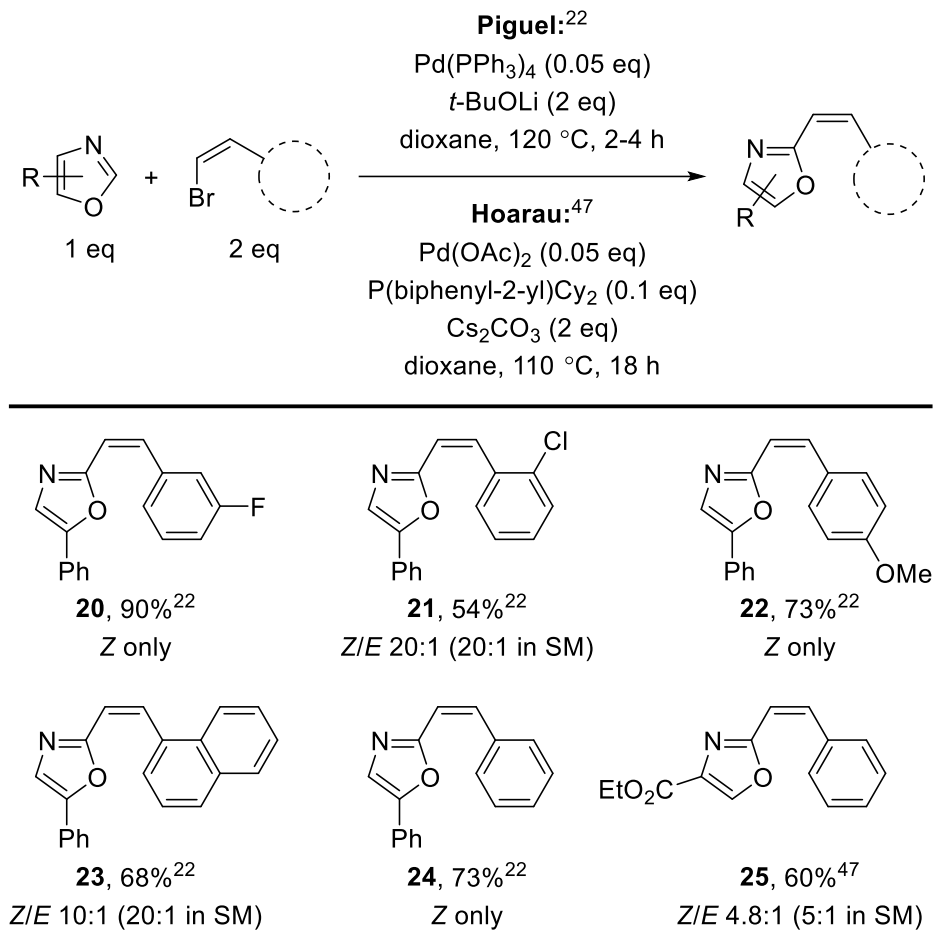
Heck reactions typically have an excellent *trans* selectivity with monosubstituted alkenes. The molecule is free to rotate in such a conformation that places the substituents farthest from each other, after which *syn*  $\beta$ -hydride elimination leads to the *trans* product (Scheme 9).<sup>39</sup> For this reason the *cis* product is usually difficult to obtain. It can in some cases be favored with chelating ligands: for example, Milstein and co-workers managed to synthesize stilbene in a 7:81 *E/Z* ratio using 1,3-bis(diisopropylphosphino)propane (dipp) as ligand.<sup>46</sup>



Scheme 9. The Heck reaction of a monosubstituted alkene leading to the *trans* product.

In contrast, in reverse-Heck reactions the *anti*  $\beta$ -heteroatom elimination is always possible right after insertion to the double bond (Scheme 7b) so the reaction preserves whichever configuration the double bond was in. Indeed, excellent *cis* selectivities have been obtained using (*Z*)- $\beta$ -bromostyrene derivatives (Table 1) by Piguel and co-workers<sup>22</sup> and Hoarau and co-workers.<sup>47</sup> The *cis* selectivities were consistently over 90% and most *trans* products were explained by contamination in starting materials. According to Piguel, any formed *trans* product was the result of thermal isomerization. A compromise had to be made between conversion and isomerization as prolonged heating resulted in larger ratios of the *trans* product. On the other hand, Hoarau obtained essentially the same *Z/E* ratio as in starting materials after 18 hours of reaction and isomerization was not significant (product **25**).

**Table 1. Reactions between substituted oxazoles and various (*Z*)- $\beta$ -bromostyrene derivatives by Piguel and co-workers<sup>22</sup> and Hoarau and co-workers.<sup>47</sup>**



Yields and *Z/E* ratios in starting materials and products are presented.

### 3.4 Effect of the (pseudo)halide

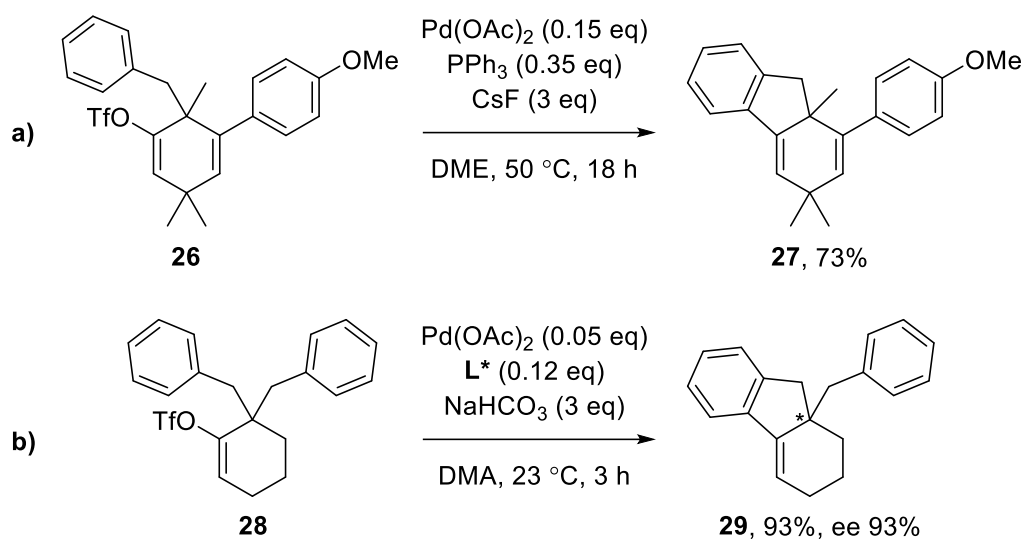
Heck reactions using aryl chlorides are typically considerably slower than those using aryl bromides and iodides. The rate of oxidative addition is limited by the bond dissociation energy.<sup>48</sup> For example, the experimental C–X bond dissociation energies in phenyl halides are 97, 84 and 67 kcal/mol for Cl, Br and I.<sup>49</sup> The limitations are similar in reverse-Heck reactions. The proposed mechanisms require either oxidative addition to a C–X bond (Scheme 3) or  $\beta$ -elimination of a halide (Scheme 4). The bond dissociation energies of vinyl halides are slightly lower than those of aryl halides: for example, 91 and 81 kcal/mol for X = Cl and Br in CHXCH<sub>2</sub>.<sup>49</sup> Despite this advantage, published reactions of vinyl chlorides are uncommon. Chlorides

would be very attractive substrates because they are usually more available and less expensive to make than other halides.<sup>50</sup> The lower reactivity also makes them more shelf-stable. For these reasons vinyl chlorides were chosen as substrates for the experimental part of this thesis.

Aryl triflates are the most common pseudohalides in Heck reactions and their reactivities are similar to those of aryl bromides.<sup>48</sup> On the other hand, reverse-Heck reactions with vinyl triflates have been performed at exceptionally low temperatures and with short reaction times. In 2002 Willis and co-workers published an intramolecular arene–vinyl triflate coupling that was conducted at 50 °C (Scheme 10a).<sup>51</sup> In 2009 Cramer and Albicker published a similar enantioselective reaction occurring at room temperature in only three hours, yielding the product in excellent yield and enantioselectivity (Scheme 10b).<sup>28</sup> Since this striking difference in performance between triflates and halides is not explained by relative reactivities, another possibility is the mechanism. The Heck reaction is known to occur via either a neutral or a cationic pathway.<sup>48</sup> In the neutral pathway (analogous to steps **II** and **III** in Scheme 3) the halide is coordinated to the palladium complex during the C–H activation, which is the usual case. However, non-coordinating counterions such as triflates initiate the cationic pathway in which the counterion is dissociated prior to the C–H activation, making a cationic palladium complex.<sup>48</sup> Cramer and Albicker proposed that this cationic complex should undergo rapid association with a carboxylate ion to form the crucial cyclic intermediate in Scheme 5.<sup>28</sup>

Another documented approach to initiate the cationic pathway is to use a silver salt as a halide scavenger.<sup>52</sup> Daugulis and Zaitsev used silver triflate to scavenge the bromide (Scheme 17a, Section 3.7).<sup>15</sup> The reaction was complete after 1.5 hours at 90 °C. The coupling was unsuccessful using sodium triflate. When using iodide substrates, silver salts can also overcome the catalyst poisoning effect caused by accumulation of iodide.<sup>53</sup>





**Scheme 10.** Intramolecular reverse-Heck with vinyl triflates by Willis and co-workers<sup>51</sup> and Cramer and Albicker.<sup>28</sup> L\* is a TADDOL-based chiral phosphine ligand.

### 3.5 Regiochemistry of the arene

This section discusses factors that govern the regiochemical outcome of C–H activation in heteroarenes and arenes. Most of the research on the subject has been done in the context of aryl halide arylations. The principles are assumed to apply to vinyl halide arylations as well.

Heteroarenes are typically inherently selective in specific sites. These sites correspond to the most nucleophilic or acidic sites depending on the C–H activation mechanism (Section 3.1). The most favorable C–H activation sites of monocyclic electron-rich heteroarenes are compiled in Figure 3, as reported by Gorelsky and co-workers,<sup>37</sup> Ess and co-workers<sup>54</sup> and Fagnou and Leclerc.<sup>55</sup> Five-membered heteroarenes are predominantly activated at the C2 or C5 site when the heteroatom with a delocalized lone pair is assigned to 1. Similarly, pyridine *N*-oxide and diazine *N*-oxides are activated at the C2 or C6 site. The regioselectivity is also influenced by any ring fusions and substituents present on the heterocycle and used reagents but the C2/C5 selectivity holds true remarkably well. The C2 and C5 sites often exhibit comparable reactivity and it is a difficult task to differentiate between them if both are unsubstituted. However, in some cases carefully selected reagents and conditions have afforded the C2 or C5 arylated products in excellent selectivities.<sup>56</sup>

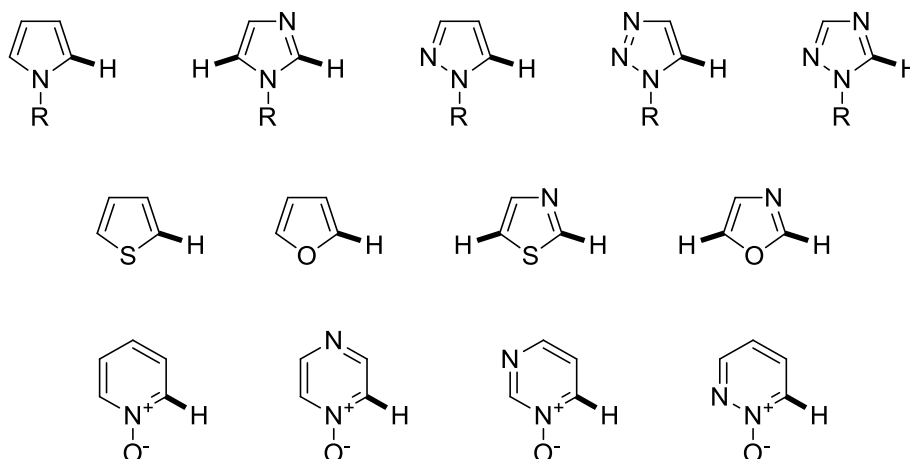
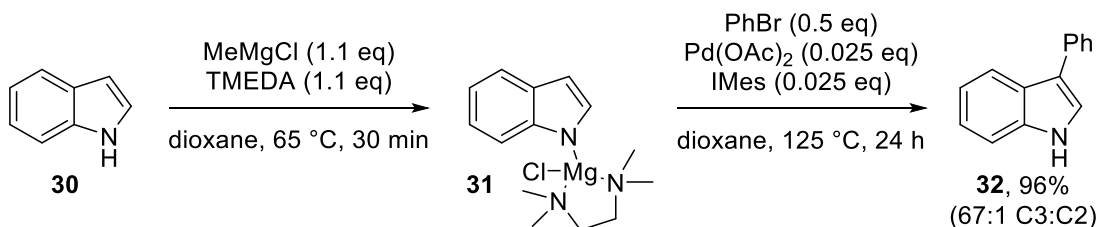


**Figure 3. Most favorable positions for C–H activation of electron-rich heteroarenes. Bold C–H bonds are preferentially activated.**

Some attention has been directed toward C3 and C4 activation of heteroarenes as reviewed by Doucet and co-workers.<sup>57</sup> Most often C3/C4 selectivity has been achieved by blocking the more favorable sites or in intramolecular reactions. Also, pyrroles and indoles have been selectively activated at the C3 site by using bulky or cationic substituents on the nitrogen. For example, Sames and co-workers reported that the congested MgCl/TMEDA-substituted indole gave almost exclusively the C3 product in 96% yield (Scheme 11).<sup>58</sup>



**Scheme 11. C3 arylation of indole with a bulky cationic substituent. Reaction yield based on PhBr.**<sup>58</sup>

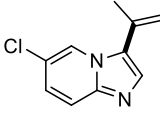
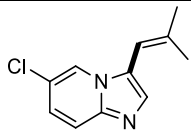
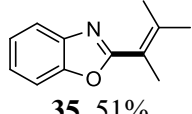
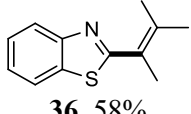
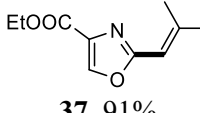
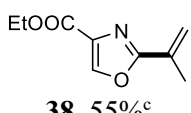
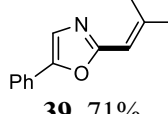
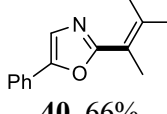
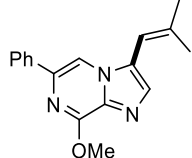
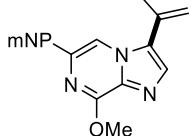
In contrast to heteroarenes, benzene rings usually have little control over C–H activation regioselectivity. There are limited cases in which a simple arene has been selectively functionalized as reviewed by Glorius and co-workers.<sup>59</sup> In other cases, reliable selectivity has been achieved with either coordinating groups or blocking groups. Coordinating groups are arene substituents that coordinate to the palladium complex and deliver the coupling partner to a specific site, almost always the *ortho*

position. Common coordinating groups are amides and pyridines.<sup>59</sup> Another strategy is to block all but one site with inert substituents. Popular examples are perfluorobenzenes which have often been used in aryl–aryl coupling reactions.<sup>60</sup> The role of the fluoride substitution is twofold: besides blocking other possible activation sites, the substituents withdraw electron density from the ring and thus make it more reactive in the CMD pathway.<sup>60</sup>

### 3.6 Reactions with heteroarenes

Open-chained haloalkenes are some of the most studied substrates in reverse-Heck reactions. As discussed in Section 3.2, simple alkenes are rarely usable in traditional Heck-type reactions which would be an incentive to develop their reactions. Published heteroarylations of aliphatic vinyl halides are compiled in Table 2 with reagents, conditions and two representative products. The reactions have given fair to excellent yields (51–91%) and good regioselectivities with respect to both the vinyl compound and the heteroarene. The only exception is product **38** which was accompanied with 28% of the double coupling product.<sup>47</sup> Reaction conditions are usually harsh with temperatures over 100 °C and long reaction times, but in some cases the reaction was complete in only 2 or 4 hours. Polar solvents and carbonate bases are typical as well. The vinyl halide is usually a bromide which is a compromise between availability and reactivity. For example, vinyl chlorides were not reactive under Piguel’s conditions (Entry 4).<sup>22</sup> However, Hoarau and co-workers have reported two single reactions with vinyl chlorides yielding 91% and 65% (products **37** and **41**).<sup>47,61</sup> In fact, vinyl chloride seemed to be a more selective coupling partner and did not yield any double coupling product. Hoarau’s conditions were later used by Fürstner and co-workers in their total synthesis of enigmazole A, a macrolide isolated from marine sponge *Cinachyrella enigmatica* (Scheme 12).<sup>62</sup>

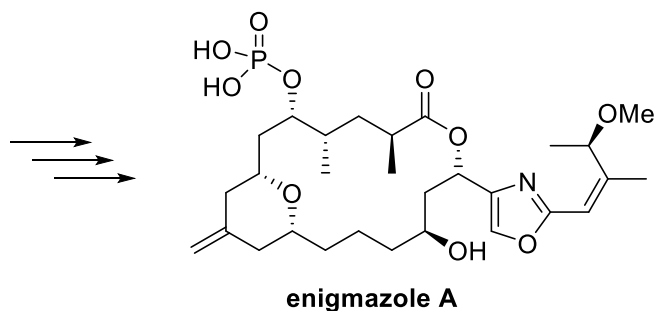
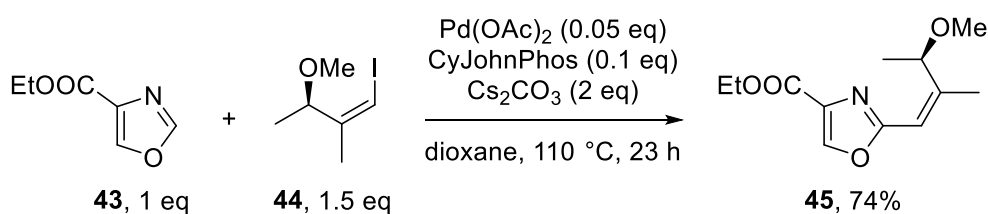
**Table 2. Heteroarylations of various open-chained haloalkenes.**

Entry	Halide <sup>a</sup>	Reagents <sup>a</sup>	Conditions	Products <sup>b</sup>	
1 <sup>26</sup>	Br (2)	Pd(OAc) <sub>2</sub> (0.2) AsPh <sub>3</sub> (0.4) Ag <sub>2</sub> CO <sub>3</sub> (2)	DMF+Et <sub>3</sub> N 130 °C 2 h	 <b>33</b> , 71%	 <b>34</b> , 56%
2 <sup>63</sup>	Br (0.5)	PdCl(C <sub>3</sub> H <sub>5</sub> )dppb (0.05) Cs <sub>2</sub> CO <sub>3</sub> (2)	DMF 140/120 °C 20 h	 <b>35</b> , 51%	 <b>36</b> , 58%
3 <sup>47</sup>	Cl/Br (2)	Pd(OAc) <sub>2</sub> (0.05) CyJohnPhos (0.1) Cs <sub>2</sub> CO <sub>3</sub> (2)	dioxane 110 °C 18 h	 <b>37</b> , 91%	 <b>38</b> , 55% <sup>c</sup>
4 <sup>22</sup>	Br (2)	Pd(PPh <sub>3</sub> ) <sub>4</sub> (0.05) <i>t</i> -BuOLi (2)	dioxane 120 °C 4 h	 <b>39</b> , 71%	 <b>40</b> , 66%
5 <sup>61</sup>	Cl/Br (3)	Pd(OAc) <sub>2</sub> (0.05) CyJohnPhos (0.1) Cs <sub>2</sub> CO <sub>3</sub> (5)	dioxane 120 °C 18 h	 <b>41</b> , 65%	 <b>42</b> , 60% <sup>d</sup>

Bold bonds are formed. Vinyl halide coupling partners are specified in the Halide column.

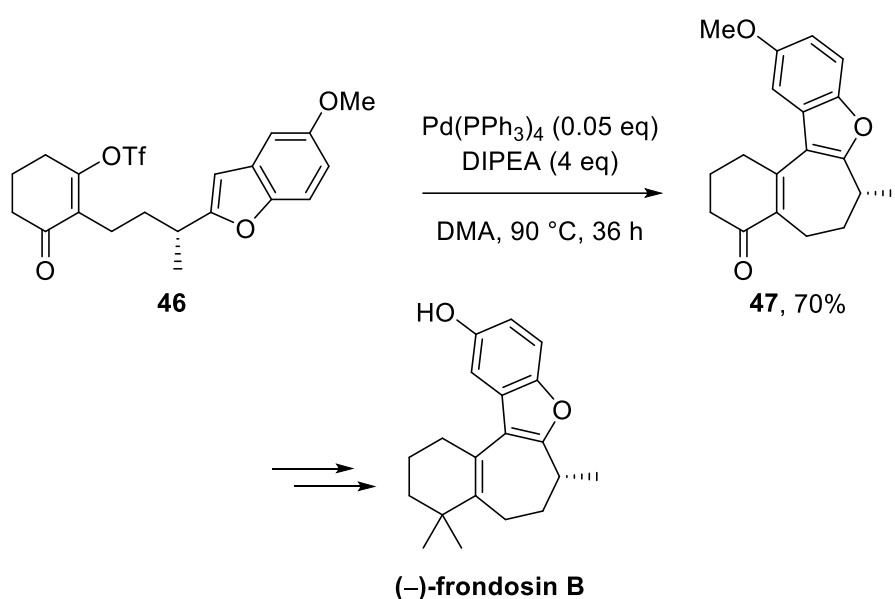
<sup>a</sup> Equivalents in parentheses. <sup>b</sup> Isolated yields based on the limiting starting material.

<sup>c</sup> 2,5-divinylated product isolated in 28% yield. <sup>d</sup> mNP = 3-nitrophenyl.



**Scheme 12. Heteroarylation of a vinyl iodide as a step in the total synthesis of enigmazole A.**<sup>62</sup>

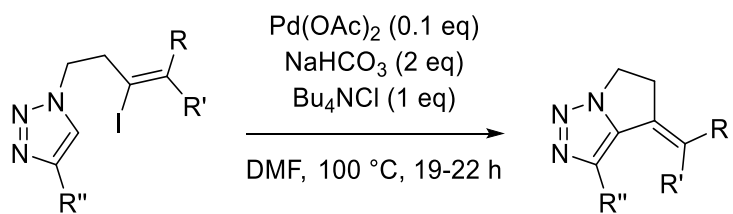
In contrast to electron-neutral alkenes, alkenes with electron-withdrawing groups usually react cleanly in Heck reactions. However, their use in reverse-Heck reactions of heteroarenes is rare. The only close example is an intramolecular reaction between enone triflate and benzofuran reported by Trauner and Hughes in 2004 (Scheme 13).<sup>24</sup> Compared to the triflate coupling reactions reported by Willis and co-workers and Cramer and Albicker (Scheme 10), this reaction needed a higher temperature (90 °C) and reaction time (36 h). The product was used in the synthesis of (–)-frondosin B, the enantiomer of a marine terpenoid that has possible applications against autoimmune disorders.



**Scheme 13.** Intramolecular heteroarylation of a vinyl triflate as a step in the total synthesis of (–)-frondosin B.<sup>24</sup>

Huang and co-workers used intramolecular reverse-Heck reactions between 1,2,3-triazole and vinyl iodide as part of their synthesis of 4-alkylidene-5,6-dihydro-4*H*-pyrrolo[1,2-*c*][1,2,3]triazoles (Table 3).<sup>64</sup> Previous syntheses of pyrrolotriazoles had been limited and involved thermal intramolecular cycloadditions. The products were obtained in fair to very good yields (52–85%). However, substrates containing a vinyl hydrogen (R = H) only gave alkyne products via elimination. Tetrabutylammonium chloride was presumably added as a phase transfer catalyst.

**Table 3. Intramolecular reverse-Heck reactions yielding pyrrolotriazoles.**<sup>64</sup>

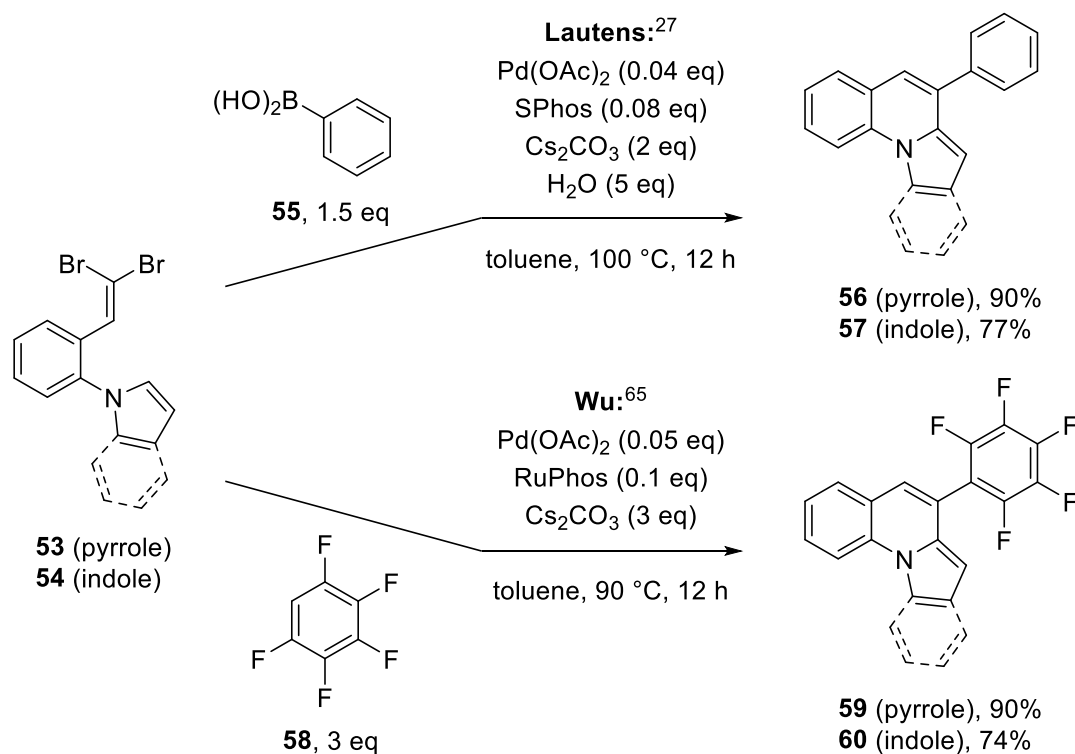
<div><div></div><div><div>Pd(OAc)<sub>2</sub> (0.1 eq) NaHCO<sub>3</sub> (2 eq) Bu<sub>4</sub>NCl (1 eq) DMF, 100 °C, 19-22 h</div></div></div>			
Product	R / R' / R''	Time (h)	Yield (%)
<b>48</b>	Ph / Ph / C <sub>5</sub> H <sub>11</sub>	20	85
<b>49</b>	Ph / Ph / CH <sub>2</sub> OMe	19	52
<b>50</b>	<i>p</i> -ClC <sub>6</sub> H <sub>4</sub> / <i>p</i> -ClC <sub>6</sub> H <sub>4</sub> / C <sub>5</sub> H <sub>11</sub>	22	58
<b>51</b>	<i>p</i> -FC <sub>6</sub> H <sub>4</sub> / <i>p</i> -FC <sub>6</sub> H <sub>4</sub> / C <sub>5</sub> H <sub>11</sub>	22	70
<b>52</b>	Me / Ph / C <sub>5</sub> H <sub>11</sub>	20	71

Several research groups have used *gem*-dibromovinyl compounds in one-pot reactions that combine intramolecular reverse-Heck reactions with other palladium-catalyzed coupling reactions. The combination is exceptionally favorable for several reasons. The *trans* halogen is less sterically hindered and thus more reactive in intermolecular reactions while the intramolecular heteroarene can only react with the *cis* halogen. Besides, *gem*-dihalovinyl compounds are more reactive toward palladium complexes than the corresponding monohalovinyl compounds.<sup>27</sup>

Lautens and Chai were the first to report a one-pot reverse-Heck–Suzuki reaction in 2009 (Scheme 14, upper arrow).<sup>27</sup> Syntheses of substituted pyrrole[1,2-*a*]quinolines (e.g. **56**) succeeded in good to excellent yields from dibromovinyl pyrrole system **53**. Various Suzuki reagents including aryl, alkyl and alkenyl boronic acids gave good results. The indole derivative **54** also gave the product **57** in good yield; however, other ring systems such as furans, thiophenes, pyrazoles and tetrazoles were not successful. Water was observed to have an important role on the rate of the Suzuki reaction but not on the rate of the reverse-Heck reaction.

Later, Wu and co-workers targeted similar products in their one-pot double reverse-Heck reaction (Scheme 14, lower arrow).<sup>65</sup> The intermolecular coupling partners were a wide range of non-activated perfluorobenzenes, other electron-deficient benzenes and a tetrafluoropyridine. The ligand was changed to RuPhos, another Buchwald ligand (see Figure 5 in Section 4.2 for structures). Yields ranged from

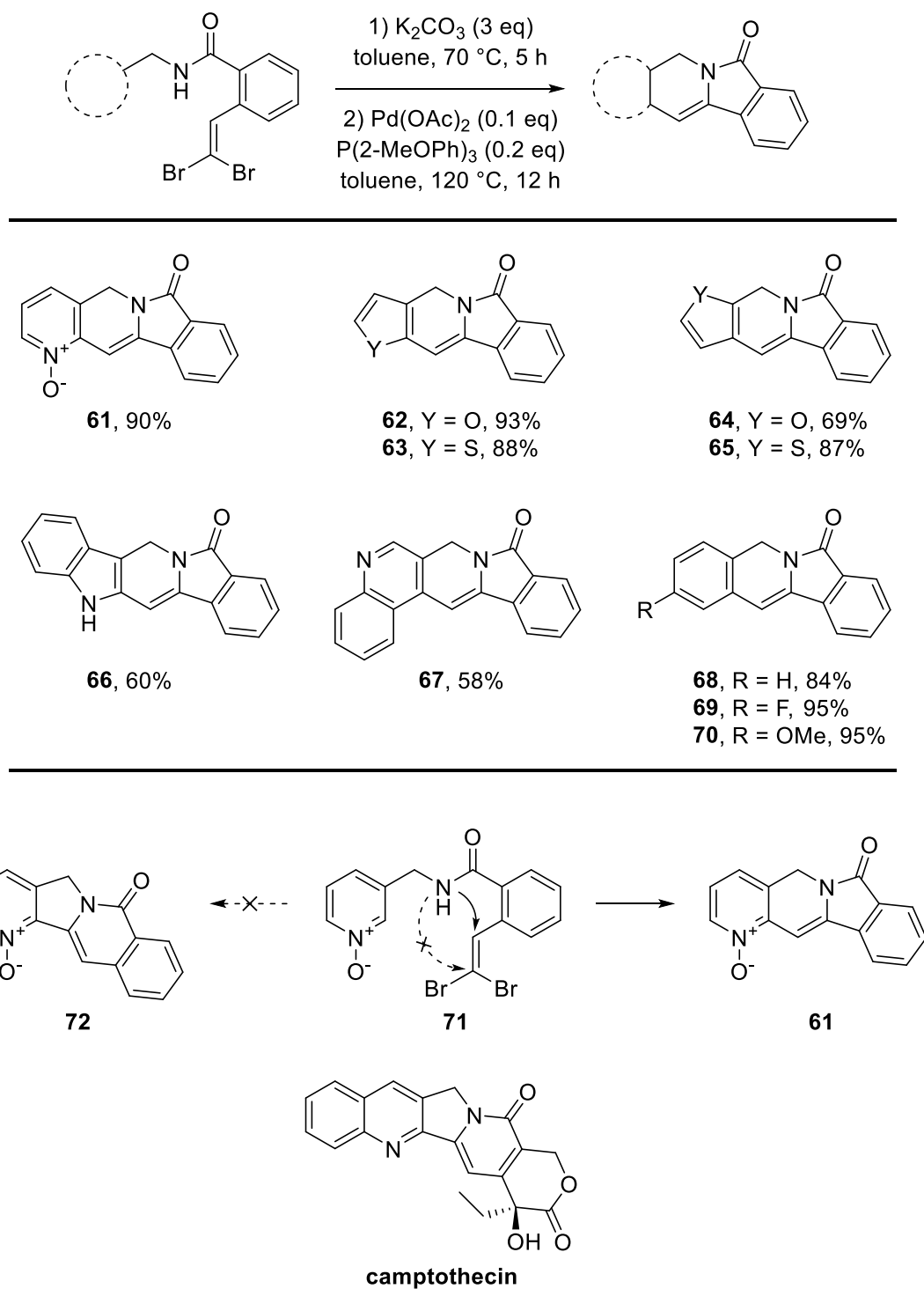
good to excellent: for example, the perfluorinated derivatives of Lautens and Chai's products (**59** and **60**) were obtained in comparable yields. Reverse-Heck reactions of perfluorobenzenes are discussed further in the next section.



**Scheme 14.** One-pot coupling reactions of *gem*-dibromovinyl compounds reported by Lautens and Chai<sup>27</sup> and Wu and co-workers.<sup>65</sup>

Chen and co-workers developed an intramolecular one-pot reverse-Heck–amination procedure using *gem*-dibromovinyl compounds.<sup>30</sup> The amination first occurred at a lower temperature using potassium carbonate, after which the palladium-catalyzed coupling reaction was performed immediately without work-up. The intramolecular reverse-Heck reaction was successfully performed on pyridine *N*-oxide, furan, thiophene, indole, quinoline and various substituted benzenes (Table 4). Furan and thiophene were also coupled on the less favorable C3 site (products **64** and **65**). Pyridine coupled unselectively at the C2 and C4 sites. Interestingly, the amine coupling occurred on the opposite side of the double bond to the bromide (Scheme 15). The expected product **72** could have provided access to derivatives of camptothecin, a quinolone alkaloid which has exhibited anticancer activity. Several camptothecin derivatives have been approved for use in cancer chemotherapy.<sup>66</sup>

**Table 4. One-pot reverse-Heck–amination procedure reported by Chen and co-workers.<sup>30</sup>**

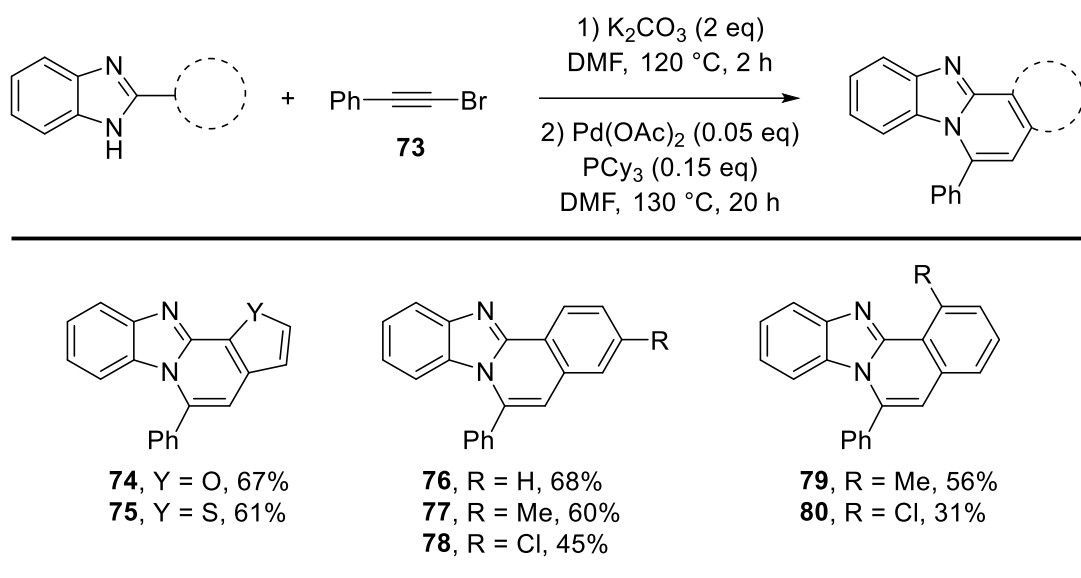


**Scheme 15. Site of amination in Chen's one-pot reaction procedure. The desired product resembles the camptothecin framework.<sup>30</sup>**



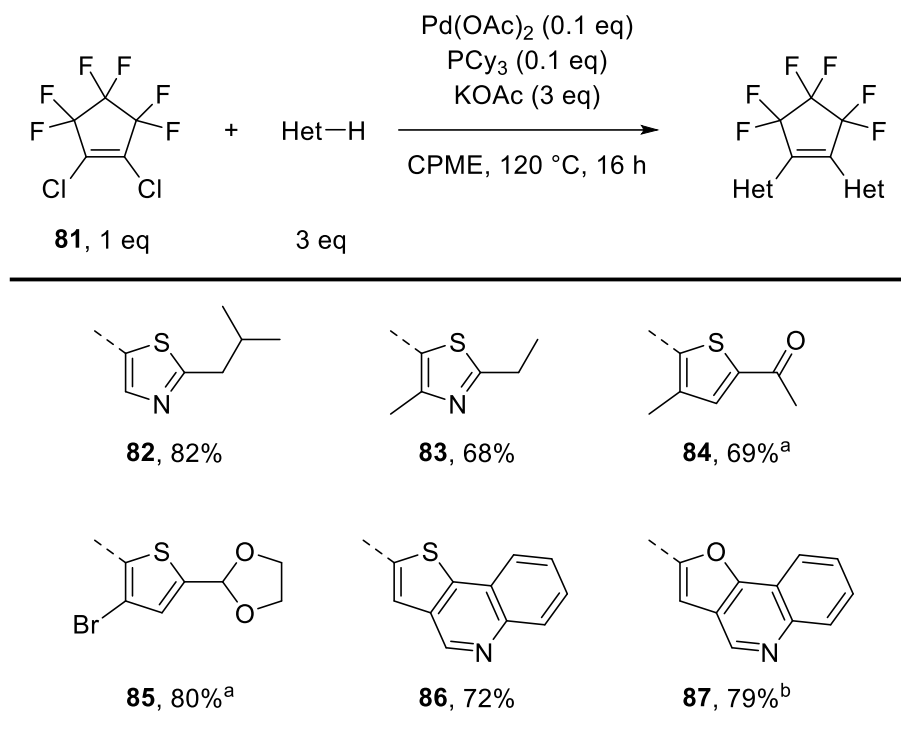
Li and co-workers developed a similar sequential one-pot reaction combining the reverse-Heck reaction and nucleophilic addition to alkyne (Table 5).<sup>29</sup> The vinyl bromide intermediate is first formed using potassium carbonate, after which an aromatic C–H bond is activated using a typical palladium catalyst system. Furan and thiophene were activated at the less favorable 3-position (products **74** and **75**). In addition, various substituted benzenes were used. Asymmetric *meta*-substituted benzenes were not selective and yielded mixtures of products. Urabe and co-workers have also studied similar reactions between sulfonamides and bromoacetylenes.<sup>67,68</sup>

**Table 5. One-pot nucleophilic addition–reverse-Heck reaction reported by Li and co-workers.**<sup>29</sup>



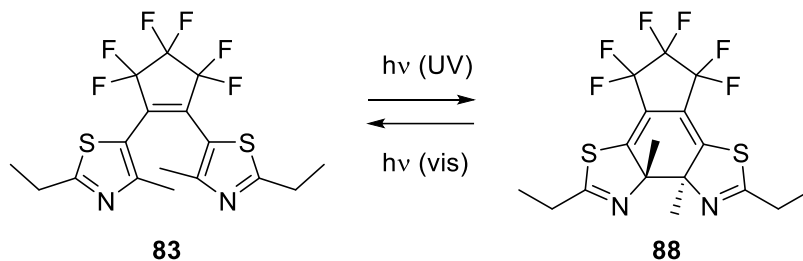
Reverse-Heck reactions have also been developed for dihalogen compounds that do not have a geminal relationship. For example, Doucet and co-workers reported a double coupling reaction of 1,2-dichloroperfluorocyclopentene (Table 6).<sup>69</sup> Various thiazoles, thiophenes and furans were employed to form the symmetric diarylated products. Chloro- and bromosubstituted thiophenes were successfully coupled without cleavage of the arene–halogen bond (e.g. product **85**). The diarylethene products function as molecular switches due to their controllable cyclization upon UV light irradiation. For example, product **83** switched to the closed form **88** after irradiation with 350 nm UV light and was regenerated after irradiation with 450 nm visible light (Scheme 16).

**Table 6. Syntheses of diarylethene derivatives reported by Doucet and co-workers.<sup>69</sup>**



For each product are shown the starting material and the coupling site.

<sup>a</sup> PdCl(C<sub>3</sub>H<sub>5</sub>)dppb (0.05 eq) as catalyst. <sup>b</sup> Reaction time 24 h.

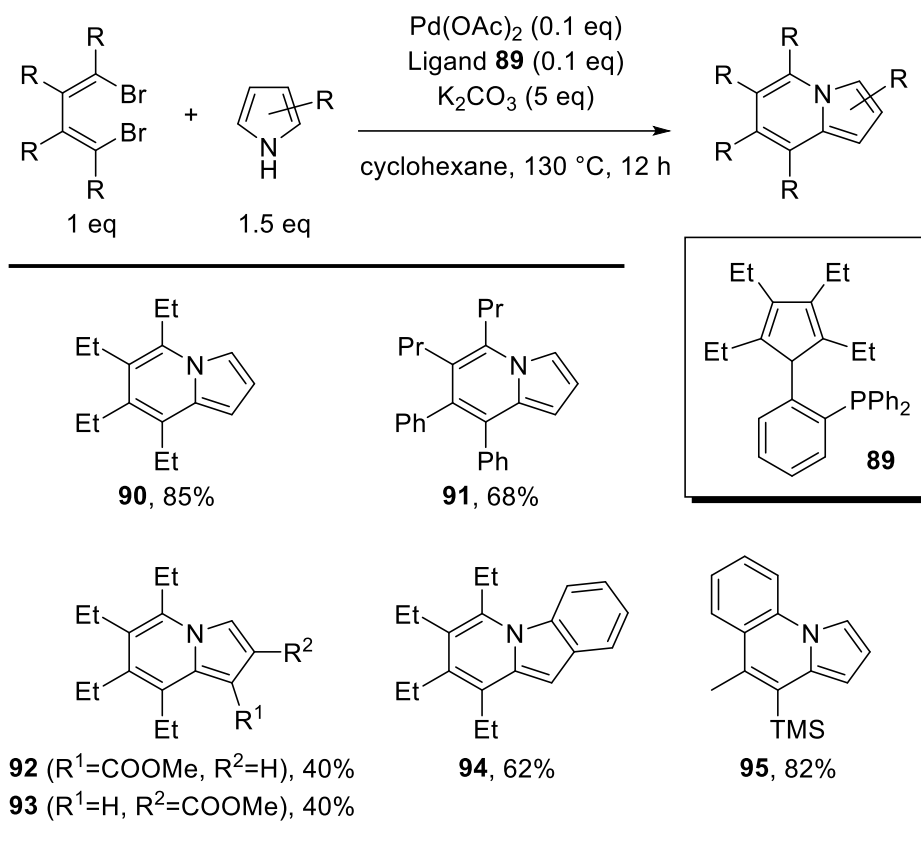


**Scheme 16. Switching between the open and closed forms of product 83.**

Xi and co-workers used the reverse-Heck method in a novel indolizine synthesis from pyrroles and 1,4-dibromo-1,3-butadienes (Table 7).<sup>32</sup> The mechanism involves an intermolecular C–N coupling followed by an intramolecular reverse-Heck reaction. The procedure worked well with an asymmetrically substituted butadiene (product **91**) as the amination took place selectively at the alkyl-substituted vinyl bromide. However, asymmetric methyl pyrrole-3-carboxylate gave products **92** and **93** as an inseparable 1:1 mixture. Interestingly, a styrene-type dibromide containing both an aryl and a vinyl bromide gave product **95** as a single isomer. Apparently amination of the aryl bromide took place first, even though vinyl bromides are

generally more reactive than aryl bromides. The crowded cyclopentadiene phosphine ligand **89** gave significantly better yields than any of the other tested ligands, including PPh<sub>3</sub> and CyJohnPhos.

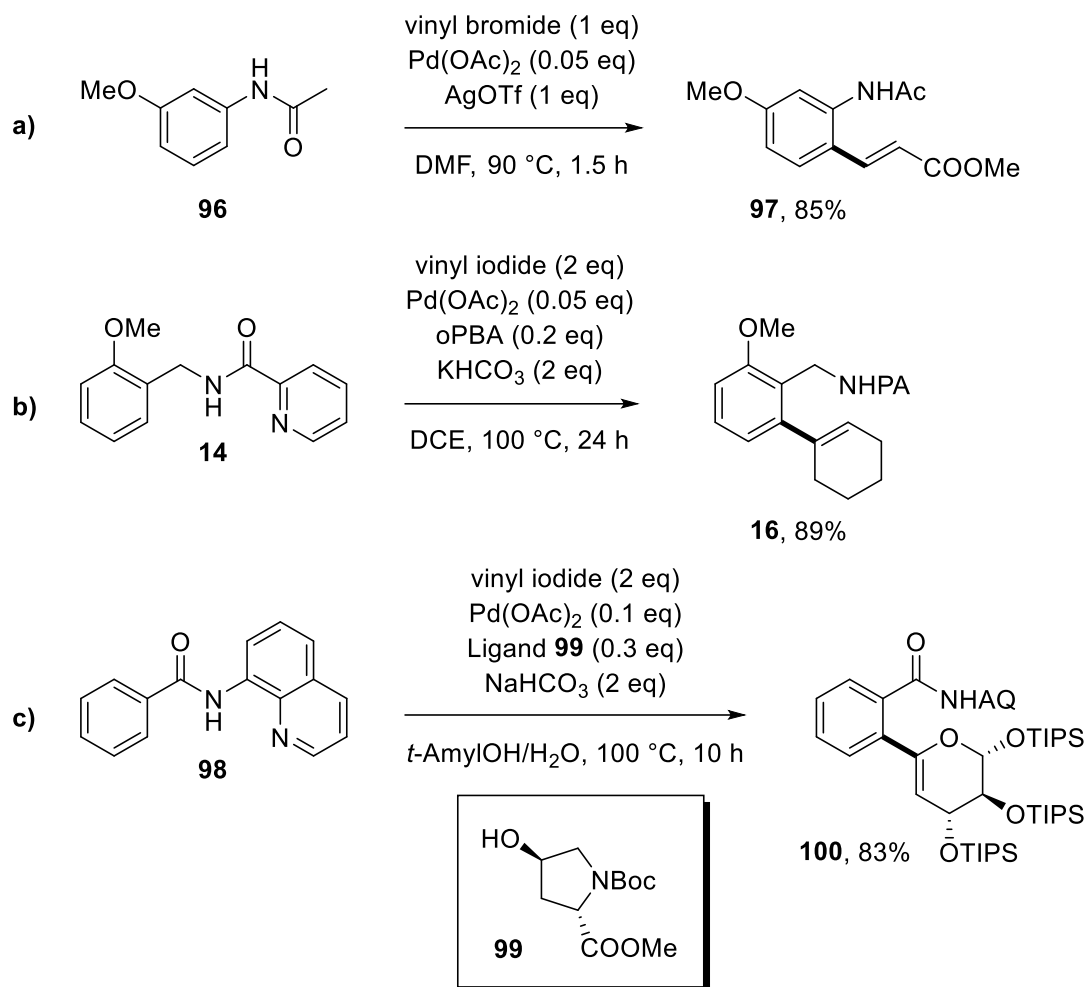
**Table 7. Syntheses of substituted indolizines reported by Xi and co-workers.<sup>32</sup>**



### 3.7 Reactions with arenes

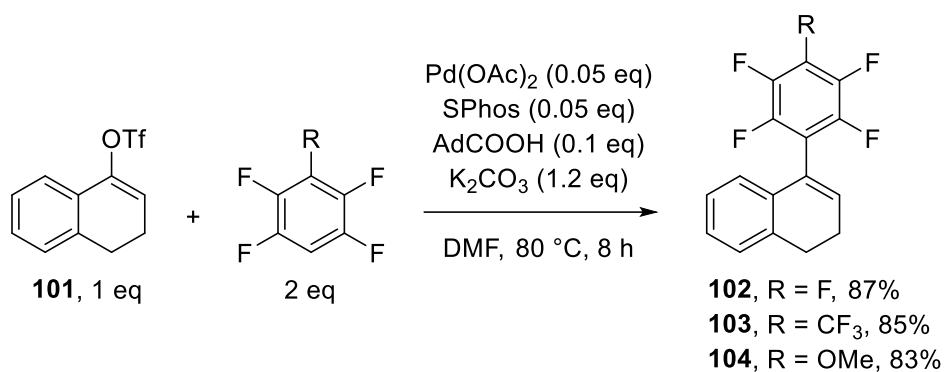
Directing groups provide some of the most common ways of making regioselective reverse-Heck reactions of benzene derivatives. Some approaches are compiled in Scheme 17. Daugulis and Zaitsev used an acetamide substituent which coordinates to the palladium complex through the oxygen atom (Scheme 17a).<sup>15</sup> Another commonly used simple amide is pivalamide which was used by Daugulis and Zaitsev as well as by Bouillon and co-workers.<sup>35</sup> Chen and co-workers used a benzyl picolinamide which coordinates to the catalyst through two nitrogen atoms (Scheme 17b).<sup>14</sup> A related quinolyl benzamide substrate was used by Ye and co-workers in their efficient aryl–glycol coupling procedure (Scheme 17c).<sup>36</sup> Ye's ligand was an unusual

amino acid derivative which led to high monoselectivity. In other cases, reagents and conditions were similar to those used in heteroarene reactions.



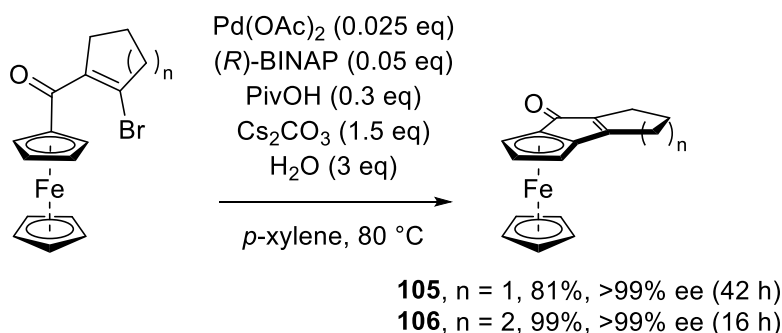
Scheme 17. Different *ortho*-directing groups used in reverse-Heck reactions.

Perfluorobenzenes are popular substrates in aryl–aryl coupling reactions but their use in reverse-Heck reactions is less common. Besides Wu and co-workers (Scheme 14), Zhang's research group has also studied reactions of perfluorobenzenes with vinyl halides (Scheme 18).<sup>31</sup> In addition to pentafluorobenzene, two common derivatives were used to give the trifluoromethylated product **103** and the methoxylated product **104** in very good yields. Adamantanecarboxylic acid (AdCOOH) was used as a proton transfer agent. A single coupling reaction of pentafluorobenzene with 1-chlorocyclopentene was also reported by Kwong and co-workers.<sup>70</sup>



**Scheme 18.** Perfluorobenzylations of a vinyl triflate.<sup>31</sup>

Intramolecular reactions are a third type of reliable regioselective reactions of arenes. For example, You and co-workers synthesized a series of planar ferrocene derivatives via intramolecular *ortho* coupling with a vinyl bromide (Scheme 19).<sup>71</sup> As the vinyl bromide tether is too short to reach any other site, only one regioisomer is observed. Using (*R*)-BINAP as a chiral ligand afforded the products practically as single enantiomers. In this case, addition of water had a positive effect on the reverse-Heck reaction rate.



**Scheme 19.** Intramolecular coupling reactions of ferrocenes by You and co-workers.<sup>71</sup>

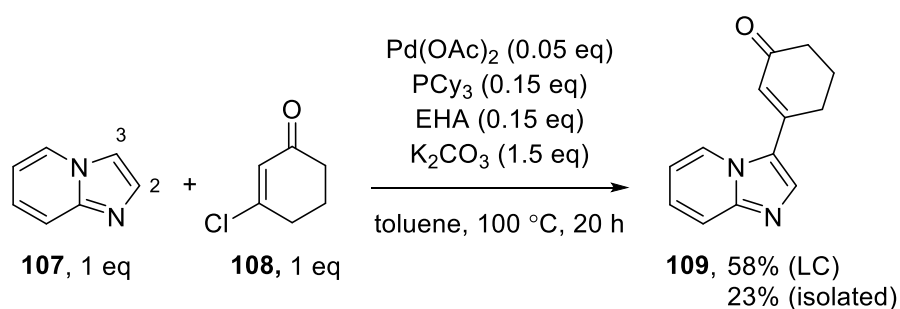
Other intramolecular reactions between arenes and vinyl bromides have been reported by Grigg and co-workers,<sup>72</sup> Willis and co-workers<sup>73</sup> and Ohgane and co-workers.<sup>74</sup>

## 4 Results and discussion

This chapter summarizes the experimental work that was done on the thesis. The aim was to develop a widely applicable method for coupling heteroarenes with vinyl chlorides. Once a suitable model reaction had been optimized, the scope of the method was expanded with a number of different heteroarenes and another vinyl chloride. Experimental procedures and analysis data are presented in Chapter 6.

### 4.1 Model reaction

The reaction between imidazo[1,2-*a*]pyridine **107** and 3-chloro-2-cyclohexenone **108** (Scheme 20) was chosen as the model reaction. The reagent system has been proven to be applicable for several C–H activation reactions in our laboratory: tricyclohexylphosphine (PCy<sub>3</sub>) as ligand, 2-ethylhexanoic acid (EHA) as additive and potassium carbonate as base.<sup>75,76</sup> The unoptimized reaction gave a promising 58% yield and 73% conversion measured with LC and the product **109** was isolated as a yellow solid in 23% yield after careful purifications. The chromatogram was reasonably clean and the components were sufficiently resolved so the reaction was considered well suited for optimization. 3-Chloro-2-cyclohexenone was found to be stable for months when stored in a freezer.



**Scheme 20. The unoptimized model reaction. The used numbering system is shown.**

The product was obtained as a single isomer, although <sup>1</sup>H-NMR showed traces (<5%) of a similar compound which is possibly the other regioisomer. The obtained isomer was identified using NOESY (Appendix 2). A nuclear Overhauser effect was observed between the vinylic proton and one of the pyridine protons as well as the

allylic protons and the imidazole proton (Figure 4). These effects confirm that the vinyl chloride coupling occurred at the imidazole C3 position. In contrast, no NOE was observed between the allylic and pyridine protons or between the vinylic and imidazole protons. The product is thus evidently locked in the *s-trans* conformation. This is an interesting result that warrants detailed conformational analysis.

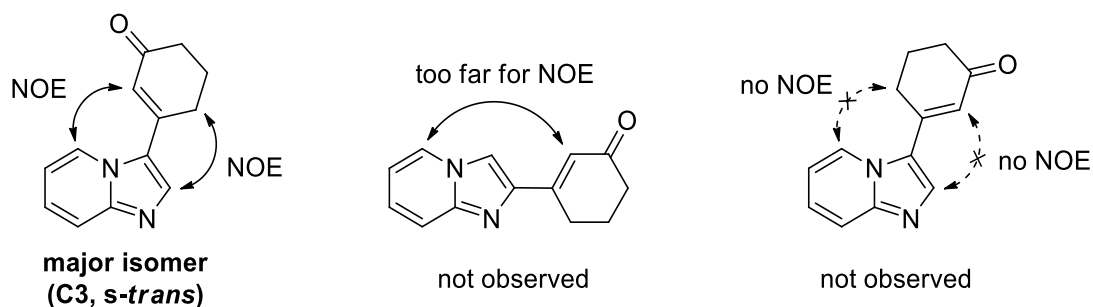
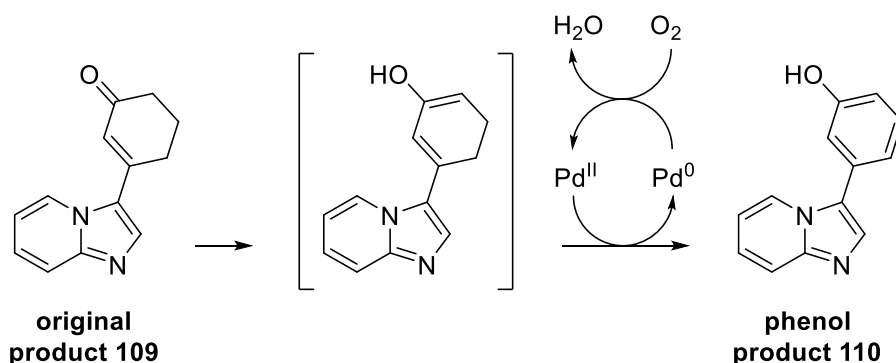


Figure 4. The major isomer and its conformation were determined by NOESY.

When the reaction was exposed to a too high oxygen concentration, a phenol product was observed (Scheme 21). This product was isolated as a white solid in 36% yield using the unoptimized conditions. The side reaction was minimized by careful flushing with inert gas, but the phenol product quickly formed whenever heating was continued in the presence of oxygen. The reaction corresponds to the catalytic Saegusa-Ito oxidation but interestingly it is very favorable even without the commonly used silyl enol ether intermediate.<sup>77</sup> The synthetic significance of the reaction was duly noted but for now, it was considered an unwanted side reaction.



Scheme 21. Proposed pathway to the phenol product. An *in situ* formed enol is oxidized by Pd<sup>II</sup> which is regenerated by oxygen.

## 4.2 Optimization of reaction conditions

The performed optimization reactions are summarized in Tables 9 and 10. Yields of the desired product and phenol side-product and conversions of imidazo[1,2-*a*]pyridine are reported. The chromatographic analysis is explained in Appendix 1. Structures of acid additives and complex ligands are presented in Figure 5.

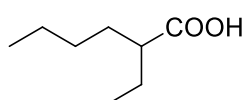
First, the significance of each component was confirmed. An experiment without a catalyst (Entry 2) gave no product so the reaction is palladium-catalyzed. An experiment without ligand resulted in more phenol byproduct than the desired product (Entry 3) and an experiment without acid additive resulted in a low conversion (Entry 4). The ligand effect is an interesting result and suggests that oxidation of the product to phenol occurs even at low oxygen concentrations but requires a phosphine-free palladium complex. When a ligand is used, the phenol product is observed only at high oxygen concentrations when phosphines are oxidized to phosphine oxides.

Alternative solvents, bases, additives and ligands were screened using a design of experiments (DoE) approach which allows a wide exploration of the chemical space with few experiments. A DoE software (JMP 13) was used to plan a 16-experiment design (Entries 7 to 22) from the selected components (Table 8). The components were compiled from similar reactions in the literature and from own experience. In order to simplify the design and reduce redundant experiments, multiple related components (e.g.  $\text{Cs}_2\text{CO}_3$  in addition to  $\text{K}_2\text{CO}_3$ ) were not included; instead, they were tested during a second iteration for only the most promising components. Some less probable ligands were tested separately (Entries 5 and 6). The only non-phosphine ligand, bipy, produced the phenol which supports the hypothesis that the oxidation is inhibited by phosphine ligands.

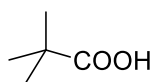


**Table 8. Components selected for the experimental design.**

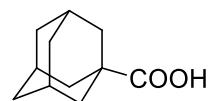
Solvent	Base	Additive	Ligand
toluene	K <sub>2</sub> CO <sub>3</sub>	EHA	PCy <sub>3</sub>
NMP	K <sub>3</sub> PO <sub>4</sub>	PivOH	PPh <sub>3</sub>
DMF	KOAc	AdCOOH	CyJohnPhos
anisole	DIPEA		cataCXium A
dioxane			



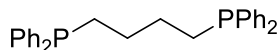
**EHA**  
2-ethylhexanoic acid



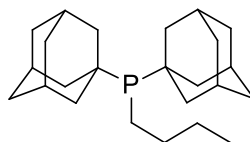
**PivOH**  
pivalic acid



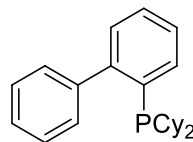
**AdCOOH**  
adamantanecarboxylic acid



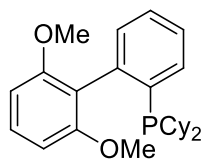
**dppb**  
1,4-bis(diphenylphosphino)  
butane



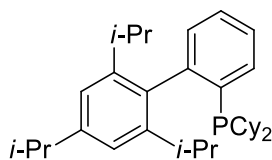
**cataCXium A**  
butyldi-1-adamantyl-  
phosphine



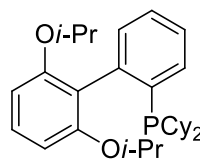
**CyJohnPhos**  
(2-biphenyl)dicyclohexyl-  
phosphine



**SPhos**  
2-dicyclohexylphosphino-  
2',6'-dimethoxybiphenyl



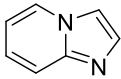
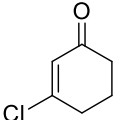
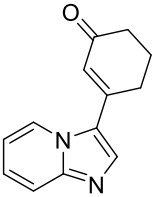
**XPhos**  
2-dicyclohexylphosphino-  
2',4',6'-triisopropylbiphenyl



**RuPhos**  
2-dicyclohexylphosphino-  
2',6'-diisopropoxybiphenyl

**Figure 5. Structures of acid additives and complex ligands.**

**Table 9. Optimization of reaction components.**

<div style="display: flex; align-items: center; justify-content: space-around;"> <div style="text-align: center;">  <p><b>107</b>, 1 eq, 0.5 mmol</p> </div> <div style="text-align: center;">  <p><b>108</b>, 1 eq</p> </div> <div style="text-align: center;"> <p> <math>\text{Pd}(\text{OAc})_2</math> (0.05 eq)            Ligand (0.15 eq)            Additive (0.15 eq)            Base (1.5 eq)         </p> <p>Solvent, 100 °C, 20 h</p> </div> <div style="text-align: center;">  <p><b>109</b></p> </div> </div>						
Entry	Solvent	Base	Additive	Ligand	Yield (%) <sup>a</sup>	Conv. (%) <sup>a</sup>
1	toluene	K <sub>2</sub> CO <sub>3</sub>	EHA	PCy <sub>3</sub>	58 (3)	73
2 <sup>b</sup>	toluene	K <sub>2</sub> CO <sub>3</sub>	EHA	PCy <sub>3</sub>	0	n/a
3	toluene	K <sub>2</sub> CO <sub>3</sub>	EHA	none	27 (37)	91
4	toluene	K <sub>2</sub> CO <sub>3</sub>	none	PCy <sub>3</sub>	30	40
5	toluene	K <sub>2</sub> CO <sub>3</sub>	EHA	dppb	22	22
6	toluene	K <sub>2</sub> CO <sub>3</sub>	EHA	bipy	39 (34)	95
7	toluene	DIPEA	AdCOOH	CyJohnPhos	2	9
8	toluene	K <sub>3</sub> PO <sub>4</sub>	AdCOOH	cataCXium A	27	34
9	toluene	KOAc	PivOH	PPh <sub>3</sub>	42	61
10	NMP	K <sub>2</sub> CO <sub>3</sub>	AdCOOH	PCy <sub>3</sub>	66	68
11	NMP	DIPEA	PivOH	PPh <sub>3</sub>	10	12
12	NMP	KOAc	EHA	cataCXium A	71	78
13	DMF	K <sub>2</sub> CO <sub>3</sub>	EHA	PPh <sub>3</sub>	21	34
14	DMF	DIPEA	AdCOOH	cataCXium A	2	10
15	DMF	K <sub>3</sub> PO <sub>4</sub>	PivOH	PCy <sub>3</sub>	3	2
16	DMF	KOAc	AdCOOH	CyJohnPhos	53	56
17	anisole	K <sub>2</sub> CO <sub>3</sub>	PivOH	cataCXium A	54	66
18	anisole	K <sub>3</sub> PO <sub>4</sub>	EHA	CyJohnPhos	51	50
19	anisole	KOAc	AdCOOH	PCy <sub>3</sub>	2	5
20	dioxane	K <sub>2</sub> CO <sub>3</sub>	PivOH	CyJohnPhos	56	56
21	dioxane	DIPEA	EHA	PCy <sub>3</sub>	1	5
22	dioxane	K <sub>3</sub> PO <sub>4</sub>	AdCOOH	PPh <sub>3</sub>	57	67
23	NMP	K <sub>2</sub> CO <sub>3</sub>	EHA	CyJohnPhos	66	68
24	toluene	K <sub>2</sub> CO <sub>3</sub>	EHA	CyJohnPhos	60	60
25	xylenes	K <sub>2</sub> CO <sub>3</sub>	EHA	CyJohnPhos	60	62
26	CPME	K <sub>2</sub> CO <sub>3</sub>	EHA	CyJohnPhos	57	63
27	NMP	Cs <sub>2</sub> CO <sub>3</sub>	EHA	CyJohnPhos	13	29
28	NMP	K <sub>2</sub> CO <sub>3</sub>	EHA	Sphos	60	69
29	NMP	K <sub>2</sub> CO <sub>3</sub>	EHA	Xphos	14	14
30	NMP	K <sub>2</sub> CO <sub>3</sub>	EHA	RuPhos	59	59

<sup>a</sup> Chromatographic results (see Appendix 1). Phenol products in parentheses. <sup>b</sup> No catalyst.

The yields obtained from the screening experiments (Entries 1 and 7–22) were collected in the DoE software and a Standard Least Squares model was fit into the data. According to the prediction profiles (Figure 6) the best combination is NMP,  $K_2CO_3$ , EHA and CyJohnPhos. NMP and dioxane are both hazardous solvents so toluene was kept as an option. Acid additives performed identically and EHA was selected because it is inexpensive and easy to use being a liquid at room temperature. Another set of experiments was run using related solvents, another carbonate base and other Buchwald ligands (Entries 23 to 30). However, none of the solvents or ligands gave significantly better results than the original conditions. Cesium carbonate (Entry 27) gave a surprisingly low conversion considering it has often been used in similar reactions (Table 2, Section 3.6).

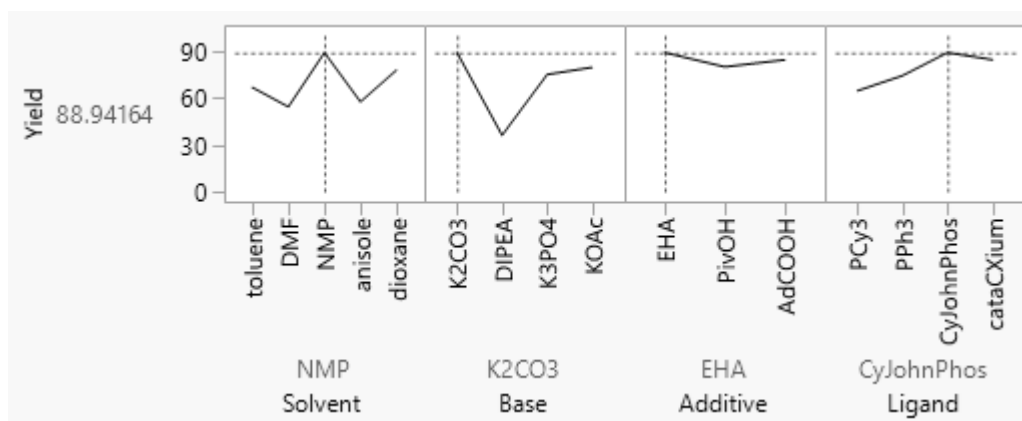


**Figure 6. Prediction profiles and the best predicted reagent combination.**

Overall, the results show that there is little difference between the performances of the best solvents and ligands. Toluene was chosen as the solvent because it is easy to evaporate and relatively green.<sup>78</sup> Triphenylphosphine is by far the least expensive ligand so it was taken into further consideration. By increasing the ratio of vinyl chloride to heteroarene, the conversion could be increased (Table 10, Entries 31–33). However, the formation of a C2-C3 double coupling product led to decreased yields with vinyl chloride equivalents over 1.5. By using the bulkier ligand CyJohnPhos, this side product could be avoided altogether. Catalyst loading could be lowered to 2% with no decrease in activity or selectivity (Entries 32, 34 and 35) so the higher price of the ligand became less of a problem. Using these conditions on a 3 mmol scale, the product **109** was isolated in 86% yield (Entry 39).

With most other substrates the use of CyJohnPhos resulted in drastically reduced conversions. In contrast, PPh<sub>3</sub> and PCy<sub>3</sub> performed well and almost identically. Triphenylphosphine was recognized as the most widely applicable ligand.

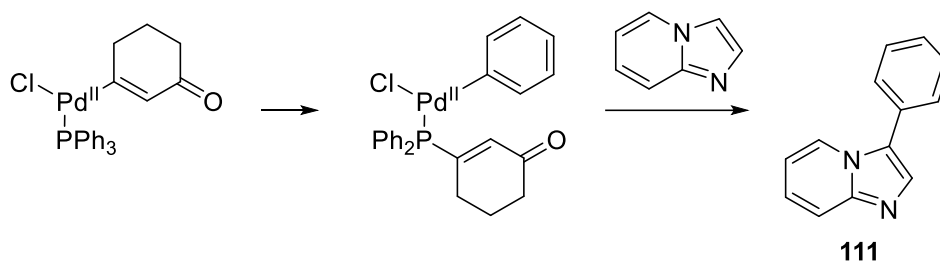
**Table 10. Optimization of starting material ratio, ligand and catalyst loading.**

$\text{Pd(OAc)}_2$  (0.01-0.05 eq)  
Ligand (0.03-0.15 eq)  
EHA (0.15 eq)  
 $\text{K}_2\text{CO}_3$  (1.5 eq)  
toluene, 100 °C, 20 h

Entry	<b>108</b> eq	Ligand	$\text{Pd(OAc)}_2$ eq	Ligand eq	Yield (%) <sup>a</sup>	Conv. (%) <sup>a</sup>
31	1	PPh <sub>3</sub>	0.05	0.15	55	82
32	1.5	PPh <sub>3</sub>	0.05	0.15	63	98
33	2	PPh <sub>3</sub>	0.05	0.15	56	100
34	1.5	PPh <sub>3</sub>	0.03	0.09	64	97
35	1.5	PPh <sub>3</sub>	0.02	0.06	68	99
36	1.3	PPh <sub>3</sub>	0.02	0.06	71	88
37	1.3	CyJohnPhos	0.02	0.06	75	89
38	1.3	CyJohnPhos	0.01	0.03	66	90
<b>39<sup>b</sup></b>	<b>1.5</b>	<b>CyJohnPhos</b>	<b>0.02</b>	<b>0.06</b>	<b>85</b>	<b>86</b>

<sup>a</sup> Chromatographic results (see Appendix 1). <sup>b</sup> On 3 mmol scale. Isolated yield 86%.

Aryl scrambling is a well-known side reaction that sometimes occurs in palladium-catalyzed coupling reactions when triphenylphosphine is used as a ligand.<sup>79</sup> After oxidative addition, the aryl or vinyl group can be exchanged with one of the phenyl groups in the ligand (Scheme 22). The reaction continues normally, resulting in phenyl coupling product **111**. Only traces of these products were observed in the experiments) so aryl scrambling does not appear to be significant under these conditions.



**Scheme 22.** Formation of a phenyl coupling product via aryl scrambling.

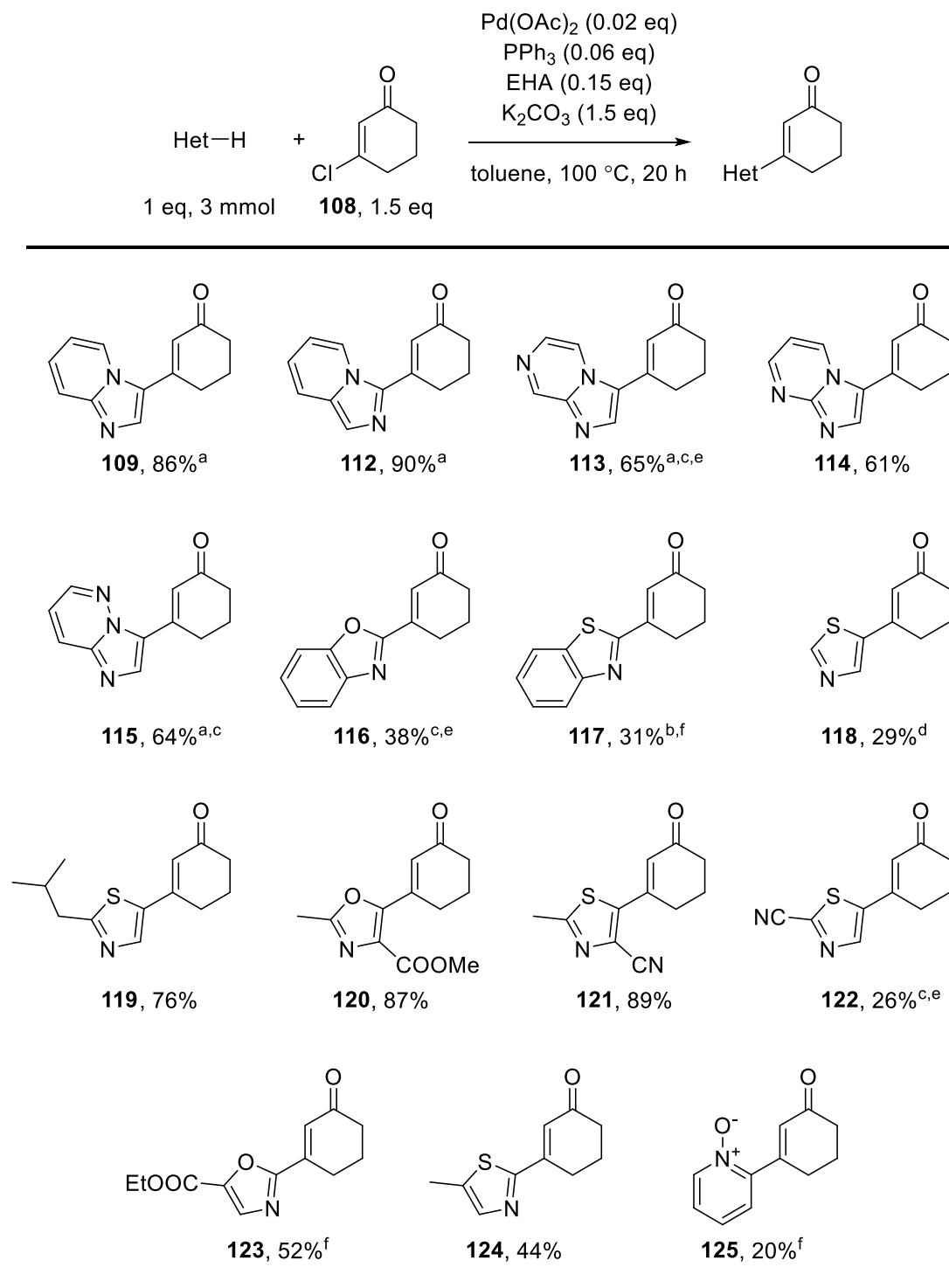
### 4.3 Scope and limitations

The performance of the optimized procedure was examined using different heteroarenes (Table 11). The coupling reactions were performed on 3 mmol or 0.5 mmol scale. All products were isolated and purified with flash chromatography.

Fair to excellent yields (61–90%) were obtained from various fused imidazoles (products **109** and **112–115**). In general, fused imidazoles benefited from the use of CyJohnPhos; only imidazo[1,2-*a*]pyrimidine coupled more efficiently with triphenylphosphine (product **114**). Benzoxazole and benzothiazole gave disappointing conversions and were prone to coupling on the benzene ring if the amount of vinyl chloride was increased (products **116** and **117**).

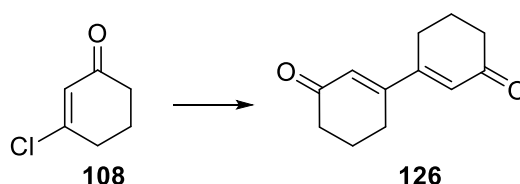
Monocyclic thiazoles and oxazoles gave fair to very good yields provided that either of the positions C2 and C5 had been blocked (products **119–124**). Coupling at the C5 position was consistently more favorable, giving yields of 76–89% compared to yields of 44% and 52% at the C2 position. Unsubstituted thiazole coupled predominantly at the C5 position (product **118**), although the double coupling product was also isolated in 15% yield. These results are in accordance with the relative energies of the C–H bonds (Section 3.5). Esters and cyano groups were well tolerated (products **120–123**) but 2-cyano-substituted thiazole yielded a mixture of products (product **122**). Pyridine *N*-oxide coupled poorly at the C2 position (product **125**).

**Table 11. Heteroarylations of 3-chloro-2-cyclohexenone.**



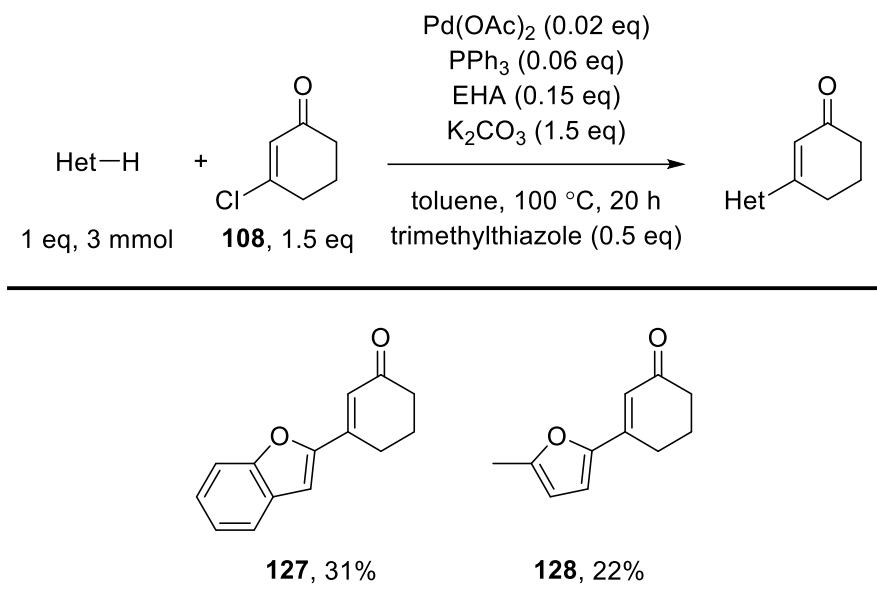
Yields of isolated products are presented based on heteroarene. <sup>a</sup> CyJohnPhos as ligand. <sup>b</sup> PCy<sub>3</sub> as ligand. Catalyst loading 5 mol-%. <sup>c</sup> 2 equivalents of vinyl chloride. <sup>d</sup> 1 equivalent of vinyl chloride. <sup>e</sup> At 120 °C using xylenes as solvent. <sup>f</sup> 0.5 mmol scale.

While the reactions proceeded well with heteroarenes bearing a basic  $sp^2$  nitrogen atom, other electron-rich heteroarenes such as furans and thiophenes gave significantly lower conversions. The dominating reaction was a vinyl chloride homocoupling (Scheme 23). The difference between substrates was proposed to be caused by a ligand effect: a basic nitrogen atom in the heterocycle possibly inhibits the homocoupling reaction. In that case, it was hypothesized that an unreactive blocked thiazole as a co-ligand could allow the reaction to proceed to completion. Indeed, a substoichiometric addition of the inexpensive 2,4,5-trimethylthiazole resulted in increased yields from non-basic heterocycles (Table 12). However, the yields were still far from optimal and vinyl chloride homocoupling remained a moderate side reaction. It is possible that better results could be obtained using a blocked imidazole because the fused imidazoles **109** and **112–115** inhibited homocoupling more efficiently than any of the thiazoles or oxazoles **116–124**. For example, no vinyl chloride homocoupling was observed when a test reaction was run with tenth of the amount of imidazo[1,2-*a*]pyrimidine (corresponding product **114**). Further research could be done in order to discover a convenient and easily removed additive.



**Scheme 23. Homocoupling of 3-chloro-2-cyclohexenone.**

**Table 12. Heteroarylations of 3-chloro-2-cyclohexenone with non-basic substrates.**



Yields of isolated products are presented based on heteroarene.

Selected unsuccessful substrates are presented in Figure 7. Notably, monocyclic imidazoles **129–131** as well as 1,2,4-triazole **133** gave incomplete conversions and complex product mixtures. Nitro-substituted imidazole **132** was completely unreactive, a stark contrast to the cyano-substituted thiazoles **121** and **122**. Benzimidazole **134**, isoxazoles **135** and **136**, aldehyde **137** and pyridine **138** gave no desired products either.

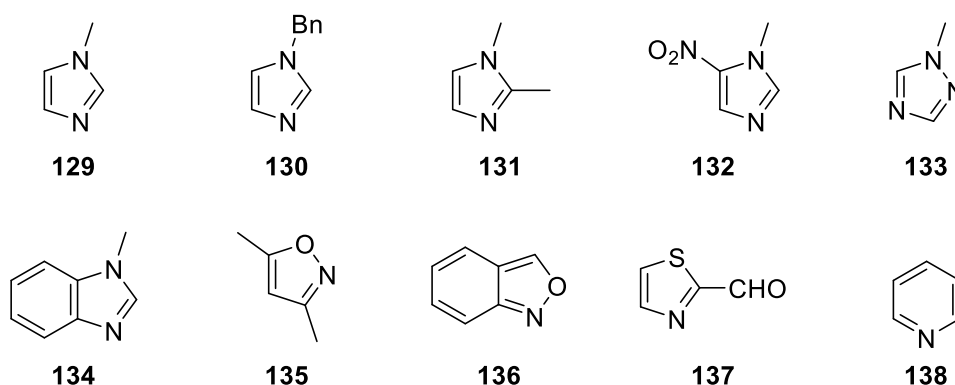
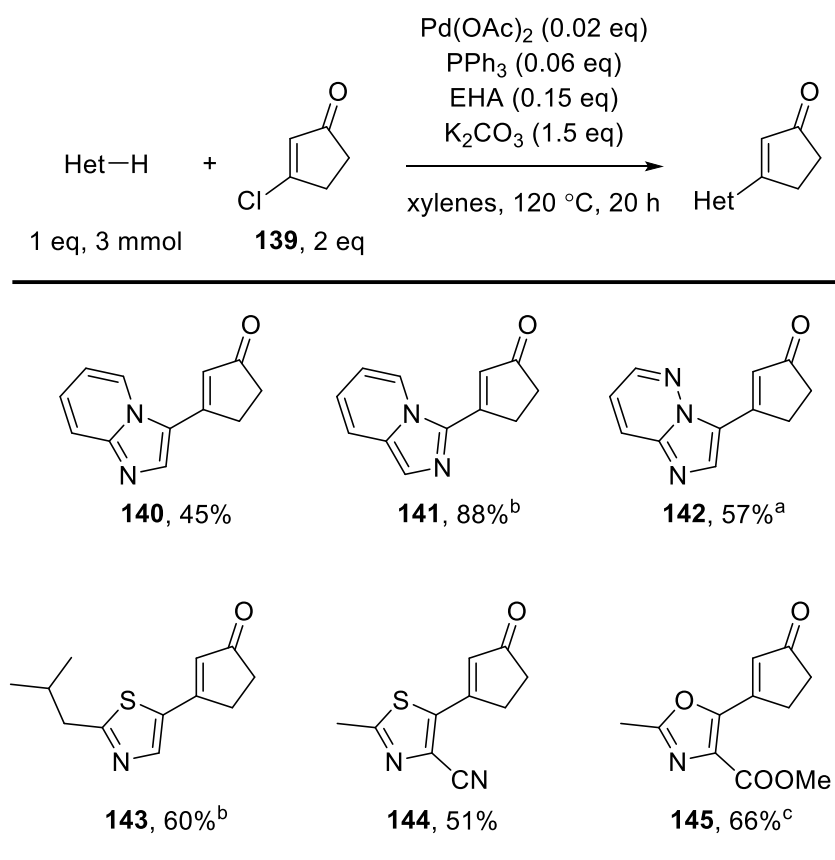


**Figure 7. Representative unsuccessful substrates.**



The performance of the coupling method was also tested on 3-chloro-2-cyclopentenone **139**, a five-membered analogue of 3-chloro-2-cyclohexenone. Some of the same heterocycles were used as coupling partners (Table 13). 3-Chloro-2-cyclopentenone turned out to be a slightly more challenging coupling partner, requiring a temperature of 120 °C and usually a higher ratio of vinyl chloride to heteroarene. Nevertheless, products **140–145** were obtained in fair to very good yields (45–88%). These results show that the developed coupling method is applicable to different heteroarenes as well as different vinyl chlorides.

**Table 13. Heteroarylations of 3-chloro-2-cyclopentenone.**



Yields of isolated products are presented based on heteroarene. <sup>a</sup> 2.5 equivalents of vinyl chloride. <sup>b</sup> 1.5 equivalents of vinyl chloride. <sup>c</sup> 0.5 mmol scale.

## 5 Conclusions and outlook

A palladium-catalyzed coupling reaction to prepare heteroarene-linked cycloalkenones has been developed. Various electron-rich heteroarenes were successfully coupled with vinyl chlorides in fair to excellent yields. The method does not require a pre-activation of the heteroarene and it employs relatively stable vinyl chlorides instead of more reactive halides. Oxazoles and thiazoles were coupled efficiently at the C2 or C5 site provided that one of them had been blocked; coupling at the C4 site did not occur.

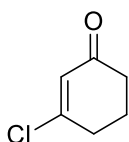
The optimized reagent system consists of a palladium catalyst, phosphine ligand, carbonate base and an acid additive. The reactions were performed in toluene at 100 °C for 20 hours. With some substrates the ligand or temperature were adjusted to give a better yield. As such, the method has potential uses in small-scale medicinal chemistry and other fine chemical industries. Some minor improvements could be made, such as shortening the reaction time.

Some potential topics of further research arose during the experiments. Products obtained using 3-chloro-2-cyclohexenone were oxidized to corresponding phenols when exposed to oxygen under the reaction conditions. This reaction cascade is effectively a regiospecific *meta*-heteroarylation of phenol. It could possibly provide access to phenol substitution patterns that are otherwise unobtainable. Furthermore, while reactions of non-basic heteroarenes such as furans and thiophenes gave poor yields, the addition of a blocked thiazole provided somewhat promising results. More experiments could be run to ascertain the role of the additive and to further improve the results.

## 6 Experimental

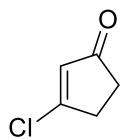
Commercial reagents were used without purification as obtained from various suppliers. Dichloromethane and dimethylformamide were filtered through activated alumina using an MBRAUN SPS-800 solvent drying system. Other reaction solvents were dried over 3 Å molecular sieves. Solid bases were dried overnight in a 120 °C vacuum oven. Products were purified by normal- or reverse-phase flash chromatography on Teledyne Isco CombiFlash R<sub>f</sub> equipment. Normal-phase flash chromatography was performed using a RediSep R<sub>f</sub> silica column and 0–100% heptane/EtOAc solvent system unless otherwise stated. Reverse-phase flash chromatography was performed using a RediSep R<sub>f</sub> C18 column and 10–100% NH<sub>4</sub>OH-water (0.5%) / acetonitrile solvent system. LC-MS data were recorded on a Waters Acquity UPLC and a Waters SQ mass detector. HRMS data were measured on a Waters Micromass Premier Q-TOF. <sup>1</sup>H and <sup>13</sup>C NMR spectra were recorded in CDCl<sub>3</sub> (+0.03% TMS) on a Bruker Avance 400 spectrometer. The chemical shifts are reported in ppm relative to TMS ( $\delta$  = 0.00 ppm). Melting points were determined on a Büchi B-545 apparatus.

### 6.1 Starting materials



**3-Chloro-2-cyclohexenone (108).** To a solution of 1,3-cyclohexanedione (1 eq, 150 mmol, 16.8 g) and dry dichloromethane (125 mL) at 0 °C was added oxalyl chloride (1.2 eq, 180 mmol, 15.4 mL) dropwise over 30 minutes. The mixture was stirred for 15 minutes and allowed to warm up to room temperature. After three hours, 120 mL of cold saturated aqueous NaHCO<sub>3</sub> was added slowly. The layers were separated and the aqueous phase was extracted with dichloromethane (2×50 mL). Combined organic phases were dried with Na<sub>2</sub>SO<sub>4</sub> and concentrated under reduced pressure. Crude product was distilled under reduced pressure. Colorless oil, 15.2 g (78%); <sup>1</sup>H

NMR (400 MHz, CDCl<sub>3</sub>)  $\delta$  ppm 2.06-2.14 (m, 2H), 2.37-2.42 (m, 2H), 2.67-2.72 (m, 2H), 6.21 (t,  $J$  = 1.5 Hz, 1H). The spectral data was identical to previous report.<sup>80</sup>



**3-Chloro-2-cyclopentenone (139).** To a solution of 1,3-cyclopentanedione (1 eq, 150 mmol, 14.7 g) and dry dichloromethane (180 mL) at 0 °C was added a solution of oxalyl chloride (1.3 eq, 195 mmol, 16.7 mL) in dichloromethane (30 mL) dropwise over 30 minutes. The mixture was stirred for 15 minutes and allowed to warm up to room temperature. After three hours, 120 mL of cold saturated aqueous NaHCO<sub>3</sub> was added slowly. The layers were separated and the aqueous phase was extracted with dichloromethane (2×50 mL). Combined organic phases were dried with Na<sub>2</sub>SO<sub>4</sub> and concentrated under reduced pressure. Crude product was distilled under reduced pressure. Colorless oil, 14.9 g (85%); <sup>1</sup>H NMR (400 MHz, CDCl<sub>3</sub>)  $\delta$  ppm 2.57-2.60 (m, 2H), 2.87-2.91 (m, 2H), 6.24 (t,  $J$  = 1.8 Hz, 1H). The spectral data was identical to previous report.<sup>81</sup>

## 6.2 Coupling reactions

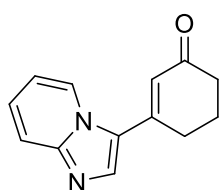
### General procedure for reaction optimization

An oven-dried 5 mL microwave vial was charged with a magnetic stir bar, base (1.5 eq, 0.75 mmol), palladium acetate (0.01–0.05 eq, 0.005–0.025 mmol), acid additive (0.15 eq, 0.075 mmol), 3-chloro-2-cyclohexenone **108** (1–2 eq, 0.5–1 mmol) and a solution of imidazo[1,2-*a*]pyridine **107** (1 eq, 0.5 mmol), mesitylene (1 eq, 0.5 mmol) and sieve-dried solvent (1.5 mL). The vial was flushed with nitrogen flow for 20 seconds while stirring. The ligand (0.03–0.15 eq, 0.015–0.075 mmol) was added. The vial was flushed with nitrogen for a further 20 seconds and sealed. The mixture was stirred at room temperature for 15 minutes and then heated to 100 °C. After 20 hours, the reaction was allowed to cool down to room temperature. 20  $\mu$ L samples taken from the starting material solution and the final reaction mixture were dissolved in 1 mL acetonitrile and analyzed by LC-MS (see Appendix 1).

### General procedure with optimized reaction conditions

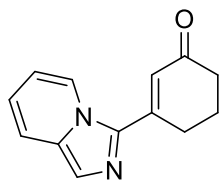
An oven-dried 20 mL microwave vial was charged with a magnetic stir bar, potassium carbonate (1.5 eq, 4.5 mmol, 622 mg), palladium acetate (0.02 eq, 0.06 mmol, 13.5 mg), 2-ethylhexanoic acid (0.15 eq, 0.45 mmol, 72  $\mu$ L), heterocyclic starting material (1 eq, 3 mmol) and sieve-dried toluene (9 mL). The vial was flushed with nitrogen flow for 20 seconds while stirring. Vinyl chloride starting material (1.5 eq, 4.5 mmol) and triphenylphosphine (0.06 eq, 0.18 mmol, 47 mg) were added. The vial was flushed with nitrogen for a further 20 seconds and sealed. The mixture was stirred at room temperature for 15 minutes and then heated to 100 °C. After 20 hours, the reaction was allowed to cool down to room temperature. The reaction mixture was filtered through a Celite filter sheet, flushed with ethyl acetate and dichloromethane (10+20 mL) and evaporated to dryness. The crude product was purified with flash chromatography. The isolated products were analyzed with LC-MS,  $^1\text{H}$  NMR and  $^{13}\text{C}$  NMR. See Appendix 2 for original spectra.

If the reaction was performed on 0.5 mmol scale (see Tables 11 and 13), the following reagent amounts were used: potassium carbonate 0.75 mmol, 104 mg; palladium acetate 0.01 mmol, 2.2 mg; 2-ethylhexanoic acid 0.075 mmol, 12  $\mu$ L; heterocyclic starting material 0.5 mmol; sieve-dried toluene 1.5 mL; vinyl chloride starting material 0.75 mmol; triphenylphosphine 0.03 mmol, 7.9 mg.

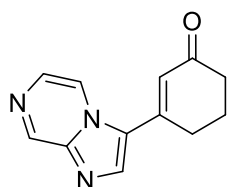


**3-(Imidazo[1,2-a]pyridin-3-yl)cyclohex-2-enone (109)** was prepared according to the general procedure using imidazo[1,2-a]pyridine (3 mmol, 304  $\mu$ L) and 3-chloro-2-cyclohexenone **108** (4.5 mmol, 499  $\mu$ L). Instead of triphenylphosphine, CyJohnPhos (0.18 mmol, 63 mg) was used. Crude product was purified by reverse-phase flash chromatography using a 50 g C18 column. Yellow solid, 549 mg (86%); mp 96–97 °C;  $^1\text{H}$  NMR (400 MHz,  $\text{CDCl}_3$ )  $\delta$  ppm 2.17-2.26 (m, 2H), 2.53-2.59 (m, 2H), 2.86-2.92 (m, 2H), 6.47 (t,  $J$  = 1.3 Hz, 1H), 6.98 (td,  $J$  = 6.9, 1.3 Hz, 1H), 7.31-7.36 (m, 1H), 7.72 (dt,  $J$  = 9.0, 1.1 Hz, 1H), 7.98 (s, 1H), 8.55 (dt,  $J$  = 7.1, 1.1 Hz,

1H);  $^{13}\text{C}$  NMR (100 MHz,  $\text{CDCl}_3$ )  $\delta$  ppm 22.4, 28.7, 37.3, 114.0, 118.7, 120.7, 123.4, 126.1, 126.4, 137.8, 147.8, 149.0, 199.1; HRMS Calculated for  $\text{C}_{13}\text{H}_{13}\text{N}_2\text{O}$  (M+1) 213.1028, found 213.1032.

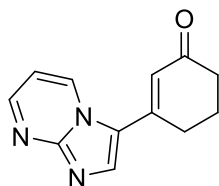


**3-(Imidazo[1,5-*a*]pyridin-3-yl)cyclohex-2-enone (112)** was prepared according to the general procedure using imidazo[1,5-*a*]pyridine (3 mmol, 354 mg) and 3-chloro-2-cyclohexenone **108** (4.5 mmol, 499  $\mu\text{L}$ ). Instead of triphenylphosphine, CyJohnPhos (0.18 mmol, 63 mg) was used. Crude product was purified by reverse-phase flash chromatography using a 30 g C18 column. Orange solid, 572 mg (90%); mp 78–80  $^{\circ}\text{C}$ ;  $^1\text{H}$  NMR (400 MHz,  $\text{CDCl}_3$ )  $\delta$  ppm 2.15–2.24 (m, 2H), 2.54–2.60 (m, 2H), 3.12 (td,  $J$  = 6.0, 1.4 Hz, 2H), 6.55 (t,  $J$  = 1.4 Hz, 1H), 6.74–6.80 (m, 1H), 6.88–6.94 (m, 1H), 7.57 (dt,  $J$  = 9.1, 1.2 Hz, 1H), 7.66 (d,  $J$  = 0.9 Hz, 1H), 8.42–8.46 (m, 1H);  $^{13}\text{C}$  NMR (100 MHz,  $\text{CDCl}_3$ )  $\delta$  ppm 22.4, 28.3, 37.6, 114.7, 119.0, 121.0, 122.6, 123.1, 123.8, 134.1, 135.6, 149.4, 199.9; HRMS Calculated for  $\text{C}_{13}\text{H}_{13}\text{N}_2\text{O}$  (M+1) 213.1028, found 213.1042.

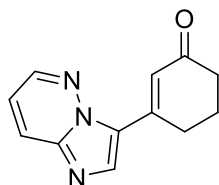


**3-(Imidazo[1,2-*a*]pyrazin-3-yl)cyclohex-2-enone (113)** was prepared according to the general procedure using imidazo[1,2-*a*]pyrazine (3 mmol, 357 mg) and 3-chloro-2-cyclohexenone **108** (6 mmol, 666  $\mu\text{L}$ ). Instead of triphenylphosphine, CyJohnPhos (0.18 mmol, 63 mg) was used. The reaction was performed at 120  $^{\circ}\text{C}$  in xylenes (9 mL). Crude product was purified by reverse-phase flash chromatography using a 30 g C18 column. Orange solid, 417 mg (65%); mp 165–167  $^{\circ}\text{C}$ ;  $^1\text{H}$  NMR (400 MHz,  $\text{CDCl}_3$ )  $\delta$  ppm 2.21–2.30 (m, 2H), 2.56–2.62 (m, 2H), 2.90 (td,  $J$  = 6.0, 1.4 Hz, 2H), 6.48 (t,  $J$  = 1.4 Hz, 1H), 8.06 (d,  $J$  = 5.0 Hz, 1H), 8.09 (s, 1H), 8.40 (dd,  $J$  = 4.8, 1.5 Hz, 1H), 9.20 (d,  $J$  = 1.5 Hz, 1H);  $^{13}\text{C}$  NMR (100 MHz,  $\text{CDCl}_3$ )  $\delta$  ppm 22.4, 28.7,

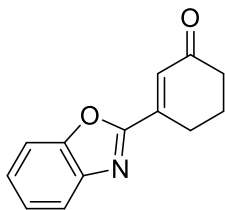
37.3, 118.4, 123.5, 124.5, 131.3, 138.1, 143.1, 145.0, 146.7, 198.6; HRMS Calculated for C<sub>12</sub>H<sub>12</sub>N<sub>3</sub>O (M+1) 214.0980, found 214.0984.



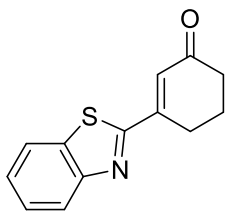
**3-(Imidazo[1,2-*a*]pyrimidin-3-yl)cyclohex-2-enone (114)** was prepared according to the general procedure using imidazo[1,2-*a*]pyrimidine (3 mmol, 357 mg) and 3-chloro-2-cyclohexenone **108** (4.5 mmol, 499  $\mu$ L). Crude product was purified by normal-phase flash chromatography using a 40 g silica column and 40–100% EtOAc/MeOH solvent system and further by reverse-phase flash chromatography using a 50 g C18 column. Orange solid, 392 mg (61%); mp 160–164 °C; <sup>1</sup>H NMR (400 MHz, CDCl<sub>3</sub>)  $\delta$  ppm 2.19–2.28 (m, 2H), 2.54–2.60 (m, 2H), 2.87–2.93 (m, 2H), 6.39 (t, *J* = 1.2 Hz, 1H), 7.08 (dd, *J* = 7.0, 4.1 Hz, 1H), 8.17 (s, 1H), 8.67 (dd, *J* = 4.1, 2.0 Hz, 1H), 8.87 (dd, *J* = 7.1, 2.0 Hz, 1H); <sup>13</sup>C NMR (100 MHz, CDCl<sub>3</sub>)  $\delta$  ppm 22.3, 28.3, 37.3, 110.0, 121.5, 121.9, 133.8, 139.0, 147.1, 151.1, 151.3, 198.8; HRMS Calculated for C<sub>12</sub>H<sub>12</sub>N<sub>3</sub>O (M+1) 214.0980, found 214.0993.



**3-(Imidazo[1,2-*b*]pyridazin-3-yl)cyclohex-2-enone (115)** was prepared according to the general procedure using imidazo[1,2-*b*]pyridazine (3 mmol, 357 mg) and 3-chloro-2-cyclohexenone **108** (6 mmol, 666  $\mu$ L). Instead of triphenylphosphine, CyJohnPhos (0.18 mmol, 63 mg) was used. Crude product was purified by reverse-phase flash chromatography using a 30 g C18 column. Orange solid, 408 mg (64%); mp 181–183 °C; <sup>1</sup>H NMR (400 MHz, CDCl<sub>3</sub>)  $\delta$  ppm 2.18–2.27 (m, 2H), 2.53–2.58 (m, 2H), 2.89–2.96 (m, 2H), 7.20 (dd, *J* = 9.2, 4.5 Hz, 1H), 7.65 (t, *J* = 1.3 Hz, 1H), 8.03–8.07 (dd, *J* = 9.2, 1.7 Hz, 1H), 8.12 (s, 1H), 8.50 (dd, *J* = 4.4, 1.7 Hz, 1H); <sup>13</sup>C NMR (100 MHz, CDCl<sub>3</sub>)  $\delta$  ppm 22.5, 27.0, 37.5, 118.0, 123.3, 126.10, 126.11, 137.1, 142.7, 143.2, 145.4, 200.2; HRMS Calculated for C<sub>12</sub>H<sub>12</sub>N<sub>3</sub>O (M+1) 214.0980, found 214.0985.

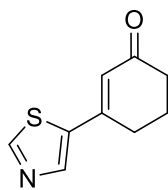


**3-(Benzo[d]oxazol-2-yl)cyclohex-2-enone (116)** was prepared according to the general procedure using benzo[d]oxazole (3 mmol, 357 mg) and 3-chloro-2-cyclohexenone **108** (6 mmol, 666  $\mu$ L). The reaction was performed at 120 °C in xylenes (9 mL). Crude product was purified by normal-phase flash chromatography using a 24 g silica column. Orange solid, 240 mg (38%); mp 105–106 °C;  $^1\text{H}$  NMR (400 MHz,  $\text{CDCl}_3$ )  $\delta$  ppm 2.17-2.25 (m, 2H), 2.38-2.59 (m, 2H), 2.99 (td,  $J$  = 6.1, 1.7 Hz, 2H), 7.00 (t,  $J$  = 1.7 Hz, 1H), 7.35-7.46 (m, 2H), 7.55-7.59 (m, 1H) 7.78-7.81 (m, 1H);  $^{13}\text{C}$  NMR (100 MHz,  $\text{CDCl}_3$ )  $\delta$  ppm 22.3, 25.3, 37.8, 111.0, 120.8, 125.0, 126.9, 129.6, 141.9, 145.1, 150.7, 161.5, 199.2; HRMS Calculated for  $\text{C}_{13}\text{H}_{12}\text{NO}_2$  ( $\text{M}+1$ ) 214.0868, found 214.0881.

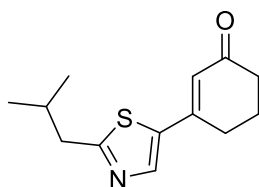


**3-(Benzo[d]thiazol-2-yl)cyclohex-2-enone (117)** was prepared according to the general procedure using benzo[d]thiazole (0.5 mmol, 68 mg) and 3-chloro-2-cyclohexenone **108** (0.75 mmol, 83  $\mu$ L). 5 mol-% palladium acetate was used (5.6 mg). Instead of triphenylphosphine, tricyclohexylphosphine (0.075 mmol, 21 mg) was used. Crude product was purified by normal-phase flash chromatography using a 12 g silica column. Light brown solid, 35 mg (31%); mp 145–147 °C;  $^1\text{H}$  NMR (400 MHz,  $\text{CDCl}_3$ )  $\delta$  ppm 2.16-2.26 (m, 2H), 2.53-2.60 (m, 2H), 3.08 (td,  $J$  = 6.1, 1.6 Hz, 2H), 6.77 (t,  $J$  = 1.6 Hz, 1H), 7.42-7.55 (m, 2H), 7.88-7.93 (m, 1H) 8.06-8.10 (m, 1H);  $^{13}\text{C}$  NMR (100 MHz,  $\text{CDCl}_3$ )  $\delta$  ppm 22.3, 26.7, 37.8, 121.8, 124.1, 126.6, 126.7, 129.1, 135.1, 152.6, 153.8, 166.6, 199.5; HRMS Calculated for  $\text{C}_{13}\text{H}_{12}\text{NOS}$  ( $\text{M}+1$ ) 230.0640, found 230.0654.

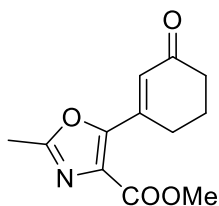




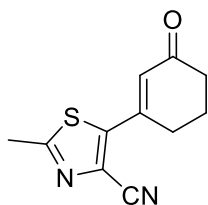
**3-(Thiazol-5-yl)cyclohex-2-enone (118)** was prepared according to the general procedure using thiazole (3 mmol, 213  $\mu$ L) and 3-chloro-2-cyclohexenone **108** (3 mmol, 333  $\mu$ L). Crude product was purified by reverse-phase flash chromatography using a 50 g C18 column. Brown solid, 157 mg (29%); mp 50–55  $^{\circ}$ C;  $^1\text{H}$  NMR (400 MHz,  $\text{CDCl}_3$ )  $\delta$  ppm 2.14–2.23 (m, 2H), 2.47–2.53 (m, 2H), 2.82 (td,  $J$  = 6.1, 1.4 Hz, 2H), 6.37 (t,  $J$  = 1.4 Hz, 1H), 8.13 (s, 1H), 8.86 (s, 1H);  $^{13}\text{C}$  NMR (100 MHz,  $\text{CDCl}_3$ )  $\delta$  ppm 22.3, 28.1, 37.2, 125.8, 138.3, 142.8, 149.6, 155.0, 198.8; HRMS Calculated for  $\text{C}_9\text{H}_{10}\text{NOS}$  ( $\text{M}+1$ ) 180.0483, found 180.0493.



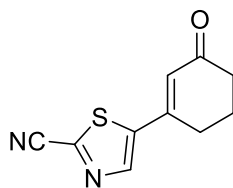
**3-(2-Isobutylthiazol-5-yl)cyclohex-2-enone (119)** was prepared according to the general procedure using 2-isobutylthiazole (3 mmol, 426  $\mu$ L) and 3-chloro-2-cyclohexenone **108** (4.5 mmol, 499  $\mu$ L). Crude product was purified by reverse-phase flash chromatography using a 50 g C18 column and further by normal-phase flash chromatography using a 12 g silica column. Yellow oil, 537 mg (76%);  $^1\text{H}$  NMR (400 MHz,  $\text{CDCl}_3$ )  $\delta$  ppm 1.00 (d,  $J$  = 6.7 Hz, 6H), 2.07–2.20 (m, 3H), 2.45–2.51 (m, 2H), 2.77 (td,  $J$  = 6.1, 1.4 Hz, 2H), 2.87 (d,  $J$  = 7.2 Hz, 2H), 6.27 (t,  $J$  = 1.4 Hz, 1H), 7.88 (s, 1H);  $^{13}\text{C}$  NMR (100 MHz,  $\text{CDCl}_3$ )  $\delta$  ppm 22.3, 22.4, 27.7, 29.8, 37.3, 42.7, 125.0, 137.5, 142.1, 150.2, 173.3, 198.9; HRMS Calculated for  $\text{C}_{13}\text{H}_{18}\text{NOS}$  ( $\text{M}+1$ ) 236.1109, found 236.1110.



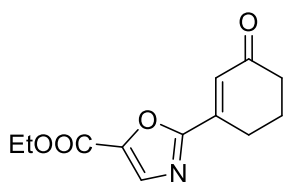
**Methyl 2-methyl-5-(3-oxocyclohex-1-en-1-yl)oxazole-4-carboxylate (120)** was prepared according to the general procedure using methyl 2-methyloxazole-4-carboxylate (3 mmol, 423 mg) and 3-chloro-2-cyclohexenone **108** (4.5 mmol, 499  $\mu$ L). Crude product was purified by normal-phase flash chromatography using a 40 g silica column. Yellow solid, 611 mg (87%); mp 54–55  $^{\circ}$ C;  $^1\text{H}$  NMR (400 MHz,  $\text{CDCl}_3$ )  $\delta$  ppm 2.10–2.18 (m, 2H), 2.48–2.53 (m, 2H), 2.54 (s, 3H), 2.84 (td,  $J = 6.1$ , 1.7 Hz, 2H), 3.94 (s, 3H), 6.87 (t,  $J = 1.7$  Hz, 1H);  $^{13}\text{C}$  NMR (100 MHz,  $\text{CDCl}_3$ )  $\delta$  ppm 13.9, 22.6, 26.6, 37.5, 52.6, 129.0, 130.8, 144.8, 152.7, 161.4, 161.9, 199.2; HRMS Calculated for  $\text{C}_{12}\text{H}_{14}\text{NO}_4$  ( $\text{M}+1$ ) 236.0923, found 236.0945.



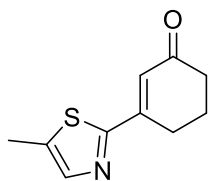
**2-Methyl-5-(3-oxocyclohex-1-en-1-yl)thiazole-4-carbonitrile (121)** was prepared according to the general procedure using 2-methylthiazole-4-carbonitrile (3 mmol, 372 mg) and 3-chloro-2-cyclohexenone **108** (4.5 mmol, 499  $\mu$ L). Crude product was purified by reverse-phase flash chromatography using a 30 g C18 column and further by normal-phase flash chromatography using a 12 g silica column. White solid, 581 mg (89%); mp 111–113  $^{\circ}$ C;  $^1\text{H}$  NMR (400 MHz,  $\text{CDCl}_3$ )  $\delta$  ppm 2.16–2.25 (m, 2H), 2.49–2.54 (m, 2H), 2.74 (s, 3H), 2.93 (td,  $J = 3.1$ , 1.5 Hz, 2H), 6.47 (t,  $J = 1.5$  Hz, 1H);  $^{13}\text{C}$  NMR (100 MHz,  $\text{CDCl}_3$ )  $\delta$  ppm 19.6, 22.5, 28.9, 37.0, 114.3, 123.1, 129.2, 147.1, 147.6, 167.9, 198.2; HRMS Calculated for  $\text{C}_{11}\text{H}_{11}\text{N}_2\text{OS}$  ( $\text{M}+1$ ) 219.0592, found 219.0606.



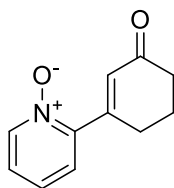
**5-(3-Oxocyclohex-1-en-1-yl)thiazole-2-carbonitrile (122)** was prepared according to the general procedure using thiazole-2-carbonitrile (3 mmol, 330 mg) and 3-chloro-2-cyclohexenone **108** (6 mmol, 666  $\mu$ L). The reaction was performed at 120  $^{\circ}$ C in xylenes (9 mL). Crude product was purified by reverse-phase flash chromatography using a 50 g C18 column and further by normal-phase flash chromatography using a 24 g silica column. Yellow solid, 160 mg (26%); mp 134–135  $^{\circ}$ C;  $^1\text{H}$  NMR (400 MHz,  $\text{CDCl}_3$ )  $\delta$  ppm 2.18–2.27 (m, 2H), 2.50–2.57 (m, 2H), 2.81 (td,  $J$  = 6.1, 1.5 Hz, 2H), 6.43 (t,  $J$  = 1.5 Hz, 1H), 8.20 (s, 1H);  $^{13}\text{C}$  NMR (100 MHz,  $\text{CDCl}_3$ )  $\delta$  ppm 22.2, 28.3, 37.1, 112.3, 127.9, 137.2, 143.3, 144.0, 147.2, 198.0; HRMS Calculated for  $\text{C}_{10}\text{H}_9\text{N}_2\text{OS}$  ( $\text{M}+1$ ) 205.0436, found 205.0450.



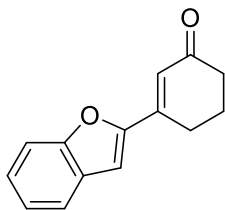
**Ethyl 2-(3-oxocyclohex-1-en-1-yl)oxazole-5-carboxylate (123)** was prepared according to the general procedure using ethyl 5-oxazolecarboxylate (0.5 mmol, 61  $\mu$ L) and 3-chloro-2-cyclohexenone **108** (0.75 mmol, 83  $\mu$ L). Crude product was purified by reverse-phase flash chromatography using a 15.5 g C18 column. White solid, 61 mg (52%); mp 75–76  $^{\circ}$ C;  $^1\text{H}$  NMR (400 MHz,  $\text{CDCl}_3$ )  $\delta$  ppm 1.41 (t,  $J$  = 7.1 Hz, 3H), 2.14–2.22 (m, 2H), 2.51–2.56 (m, 2H), 2.88 (td,  $J$  = 6.1, 1.7 Hz, 2H), 4.41 (q,  $J$  = 7.1 Hz, 2H), 6.93 (t,  $J$  = 1.7, 1H), 7.86 (s, 1H);  $^{13}\text{C}$  NMR (100 MHz,  $\text{CDCl}_3$ )  $\delta$  ppm 14.2, 22.2, 25.0, 37.6, 61.9, 129.3, 135.4, 143.4, 143.8, 157.4, 162.5, 198.9; HRMS Calculated for  $\text{C}_{12}\text{H}_{14}\text{NO}_4$  ( $\text{M}+1$ ) 236.0923, found 236.0930.



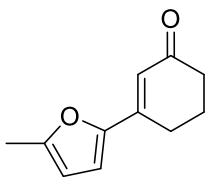
**3-(5-Methylthiazol-2-yl)cyclohex-2-enone (124)** was prepared according to the general procedure using 5-methylthiazole (3 mmol, 266  $\mu$ L) and 3-chloro-2-cyclohexenone **108** (4.5 mmol, 499  $\mu$ L). Crude product was purified by reverse-phase flash chromatography using a 50 g C18 column. Orange solid, 253 mg (44%); mp 48–55  $^{\circ}$ C;  $^1\text{H}$  NMR (400 MHz,  $\text{CDCl}_3$ )  $\delta$  ppm 2.10-2.18 (m, 2H), 2.48-2.52 (m, 2H), 2.53 (d,  $J$  = 1.1 Hz, 3H), 2.92 (td,  $J$  = 6.1, 1.6 Hz, 2H), 6.58 (t,  $J$  = 1.6 Hz, 1H), 7.59 (q,  $J$  = 1.1 Hz, 1H);  $^{13}\text{C}$  NMR (100 MHz,  $\text{CDCl}_3$ )  $\delta$  ppm 12.3, 22.3, 26.5, 37.7, 125.8, 137.2, 142.7, 152.3, 164.9, 199.6; HRMS Calculated for  $\text{C}_{10}\text{H}_{12}\text{NOS}$  ( $\text{M}+1$ ) 194.0640, found 194.0643.



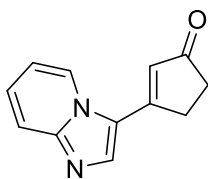
**2-(3-Oxocyclohex-1-en-1-yl)pyridine 1-oxide (125)** was prepared according to the general procedure using pyridine *N*-oxide (0.5 mmol, 48 mg) and 3-chloro-2-cyclohexenone **108** (0.75 mmol, 83  $\mu$ L). Crude product was purified by reverse-phase flash chromatography using a 15.5 g C18 column. Yellow solid, 19 mg (20%); mp 107–108  $^{\circ}$ C;  $^1\text{H}$  NMR (400 MHz,  $\text{CDCl}_3$ )  $\delta$  ppm 2.13-2.22 (m, 2H), 2.53-2.58 (m, 2H), 2.91 (td,  $J$  = 6.0, 1.5 Hz, 2H), 6.23 (t,  $J$  = 1.5 Hz, 1H), 7.26-7.33 (m, 3H), 8.22-8.27 (m, 1H);  $^{13}\text{C}$  NMR (100 MHz,  $\text{CDCl}_3$ )  $\delta$  ppm 23.1, 27.0, 37.9, 125.86, 125.92, 125.97, 130.3, 140.4, 149.3, 155.7, 199.4; HRMS Calculated for  $\text{C}_{11}\text{H}_{12}\text{NO}_2$  ( $\text{M}+1$ ) 190.0868, found 190.0882.



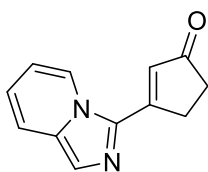
**3-(Benzofuran-2-yl)cyclohex-2-enone (127)** was prepared according to the general procedure using 2,3-benzofuran (3 mmol, 331  $\mu$ L) and 3-chloro-2-cyclohexenone **108** (4.5 mmol, 499  $\mu$ L). 2,4,5-Trimethylthiazole (1.5 mmol, 188  $\mu$ L) was finally added. Crude product was purified by normal-phase flash chromatography using a 50 g silica column. Yellow solid, 197 mg (31%); mp 100–101  $^{\circ}$ C;  $^1\text{H}$  NMR (400 MHz,  $\text{CDCl}_3$ )  $\delta$  ppm 2.12–2.21 (m, 2H), 2.49–2.54 (m, 2H), 2.75 (td,  $J = 6.1, 1.4$  Hz, 2H), 6.71 (t,  $J = 1.4$  Hz, 1H), 7.06 (s, 1H), 7.22–7.27 (m, 1H), 7.34–7.39 (m, 1H), 7.47–7.51 (m, 1H), 7.58–7.61 (m, 1H);  $^{13}\text{C}$  NMR (100 MHz,  $\text{CDCl}_3$ )  $\delta$  ppm 22.4, 25.4, 37.6, 108.6, 111.5, 121.7, 123.3, 123.4, 126.6, 128.2, 147.0, 153.7, 155.5, 199.3; HRMS Calculated for  $\text{C}_{14}\text{H}_{13}\text{O}_2$  ( $\text{M}+1$ ) 213.0916, found 213.0911.



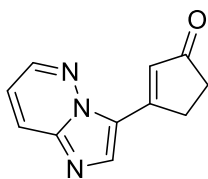
**3-(5-Methylfuran-2-yl)cyclohex-2-enone (128)** was prepared according to the general procedure using 2-methylfuran (3 mmol, 266  $\mu$ L) and 3-chloro-2-cyclohexenone **108** (4.5 mmol, 499  $\mu$ L). 2,4,5-Trimethylthiazole (1.5 mmol, 188  $\mu$ L) was finally added. Crude product was purified by reverse-phase flash chromatography using a 40 g silica column. Orange solid, 115 mg (22%); mp 55–60  $^{\circ}$ C;  $^1\text{H}$  NMR (400 MHz,  $\text{CDCl}_3$ )  $\delta$  ppm 2.05–2.14 (m, 2H), 2.35–2.36 (m, 3H), 2.43–2.48 (m, 2H), 2.62 (td,  $J = 6.1, 1.3$  Hz, 2H), 6.10–6.13 (m, 1H), 6.41–6.43 (m, 1H), 6.65 (d,  $J = 3.4$  Hz, 1H);  $^{13}\text{C}$  NMR (100 MHz,  $\text{CDCl}_3$ )  $\delta$  ppm 13.9, 22.5, 25.2, 37.5, 108.9, 114.2, 119.7, 147.2, 150.6, 155.8, 199.5; HRMS Calculated for  $\text{C}_{11}\text{H}_{13}\text{O}_2$  ( $\text{M}+1$ ) 177.0916, found 177.0910.



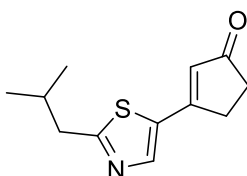
**3-(Imidazo[1,2-*a*]pyridin-3-yl)cyclopent-2-enone (140)** was prepared according to the general procedure using imidazo[1,2-*a*]pyridine (3 mmol, 304  $\mu$ L) and 3-chloro-2-cyclopentenone **139** (6 mmol, 580  $\mu$ L). The reaction was performed at 120 °C in xylenes (9 mL). Crude product was purified by reverse-phase flash chromatography using a 30 g C18 column. Beige solid, 266 mg (45%); mp 239–241 °C;  $^1\text{H}$  NMR (400 MHz,  $\text{CDCl}_3$ )  $\delta$  ppm 2.55–2.60 (m, 2H), 3.22–3.27 (m, 2H), 6.48 (t,  $J$  = 1.4 Hz, 1H), 7.11 (td,  $J$  = 6.9, 1.2 Hz, 1H), 7.41–7.46 (m, 1H), 7.79 (dt,  $J$  = 9.0, 1.1 Hz, 1H), 8.12 (s, 1H), 8.45 (dt,  $J$  = 7.0, 1.1 Hz, 1H);  $^{13}\text{C}$  NMR (100 MHz,  $\text{CDCl}_3$ )  $\delta$  ppm 29.6, 33.3, 114.7, 118.8, 121.3, 121.5, 126.1, 127.1, 138.9, 149.4, 159.2, 208.6; HRMS Calculated for  $\text{C}_{12}\text{H}_{11}\text{N}_2\text{O}$  ( $M+1$ ) 199.0871, found 199.0881.



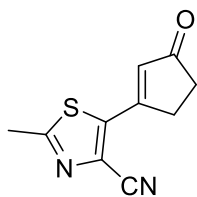
**3-(Imidazo[1,5-*a*]pyridin-3-yl)cyclopent-2-enone (141)** was prepared according to the general procedure using imidazo[1,5-*a*]pyridine (3 mmol, 354 mg) and 3-chloro-2-cyclopentenone **139** (4.5 mmol, 435  $\mu$ L). The reaction was performed at 120 °C in xylenes (9 mL). Crude product was purified by reverse-phase flash chromatography using a 30 g C18 column. Yellow solid, 521 mg (88%); mp 166–170 °C;  $^1\text{H}$  NMR (400 MHz,  $\text{CDCl}_3$ )  $\delta$  ppm 2.55–2.59 (m, 2H), 3.39–3.43 (m, 2H), 6.56 (t,  $J$  = 1.6 Hz, 1H), 6.91–6.96 (m, 1 H), 7.01–7.06 (m, 1 H), 7.66 (dt,  $J$  = 9.0, 1.2 Hz, 1H), 7.76 (d,  $J$  = 0.9 Hz, 1H), 8.33–8.37 (m, 1 H);  $^{13}\text{C}$  NMR (100 MHz,  $\text{CDCl}_3$ )  $\delta$  ppm 30.2, 33.7, 115.6, 119.1, 121.7, 123.4, 123.7, 124.2, 133.6, 134.5, 160.8, 209.5; HRMS Calculated for  $\text{C}_{12}\text{H}_{11}\text{N}_2\text{O}$  ( $M+1$ ) 199.0871, found 199.0878.



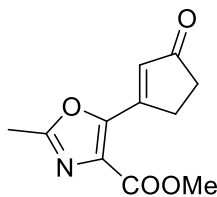
**3-(Imidazo[1,2-*b*]pyridazin-3-yl)cyclopent-2-enone (142)** was prepared according to the general procedure using imidazo[1,2-*b*]pyridazine (3 mmol, 357 mg) and 3-chloro-2-cyclopentenone **139** (7.5 mmol, 725  $\mu$ L). The reaction was performed at 120 °C in xylenes (9 mL). Crude product was purified by reverse-phase flash chromatography using a 30 g C18 column. Light brown solid, 339 mg (57%); mp 225–226 °C;  $^1\text{H}$  NMR (400 MHz,  $\text{CDCl}_3$ )  $\delta$  ppm 2.55–2.60 (m, 2H), 3.18–3.23 (m, 2H), 7.26 (dd,  $J$  = 9.2, 4.5 Hz, 1H), 7.32 (t,  $J$  = 1.7 Hz, 1H), 8.09 (dd,  $J$  = 9.2, 1.7 Hz, 1H), 8.18 (s, 1H), 8.56 (dd,  $J$  = 4.5, 1.7 Hz, 1H);  $^{13}\text{C}$  NMR (100 MHz,  $\text{CDCl}_3$ )  $\delta$  ppm 28.6, 33.6, 118.6, 124.8, 126.1, 126.3, 136.9, 142.8, 143.8, 158.1, 209.5; HRMS Calculated for  $\text{C}_{11}\text{H}_{10}\text{N}_3\text{O}$  ( $M+1$ ) 200.0824, found 200.0835.



**3-(2-Isobutylthiazol-5-yl)cyclopent-2-enone (143)** was prepared according to the general procedure using 2-isobutylthiazole 3 mmol, 426  $\mu$ L) and 3-chloro-2-cyclopentenone **139** (4.5 mmol, 435  $\mu$ L). The reaction was performed at 120 °C in xylenes (9 mL). Crude product was purified by normal-phase flash chromatography using a 40 g silica column. Yellow oil, 395 mg (60%);  $^1\text{H}$  NMR (400 MHz,  $\text{CDCl}_3$ )  $\delta$  ppm 1.02 (d,  $J$  = 6.7 Hz, 6H), 2.08–2.22 (m, 1H), 2.56–2.60 (m, 2H), 2.91 (d,  $J$  = 7.2 Hz, 2H), 3.02–3.07 (m, 2H), 6.28 (t,  $J$  = 1.6 Hz, 1H), 7.95 (s, 1H);  $^{13}\text{C}$  NMR (100 MHz,  $\text{CDCl}_3$ )  $\delta$  ppm 22.3, 29.1, 29.9, 34.8, 42.8, 128.1, 133.3, 143.0, 163.8, 174.8, 207.9; HRMS Calculated for  $\text{C}_{12}\text{H}_{16}\text{NOS}$  ( $M+1$ ) 222.0953, found 222.0912.



**2-Methyl-5-(3-oxocyclopent-1-en-1-yl)thiazole-4-carbonitrile (144)** was prepared according to the general procedure using 2-methylthiazole-4-carbonitrile (3 mmol, 372 mg) and 3-chloro-2-cyclopentenone **139** (6 mmol, 580  $\mu$ L). The reaction was performed at 120 °C in xylenes (9 mL). Crude product was purified by reverse-phase flash chromatography using a 30 g C18 column. Light brown solid, 311 mg (51%); mp 141–142 °C;  $^1\text{H}$  NMR (400 MHz,  $\text{CDCl}_3$ )  $\delta$  ppm 2.60–2.65 (m, 2H), 2.78 (s, 3H), 3.17–3.22 (m, 2H), 6.68 (t,  $J$  = 1.8 Hz, 1H);  $^{13}\text{C}$  NMR (100 MHz,  $\text{CDCl}_3$ )  $\delta$  ppm 19.7, 30.3, 35.0, 114.1, 124.3, 132.1, 142.9, 159.6, 169.3, 207.2; HRMS Calculated for  $\text{C}_{10}\text{H}_9\text{N}_2\text{OS}$  ( $\text{M}+1$ ) 205.0436, found 205.0457.



**Methyl 2-methyl-5-(3-oxocyclopent-1-en-1-yl)oxazole-4-carboxylate (145)** was prepared according to the general procedure using methyl 2-methyloxazole-4-carboxylate (0.5 mmol, 71 mg) and 3-chloro-2-cyclopentenone **139** (1 mmol, 97  $\mu$ L). The reaction was performed at 120 °C in xylenes (9 mL). Crude product was purified by reverse-phase flash chromatography using a 15.5 g C18 column. Light brown solid, 73 mg (66%); mp 96–98 °C;  $^1\text{H}$  NMR (400 MHz,  $\text{CDCl}_3$ )  $\delta$  ppm 2.53–2.57 (m, 2H), 2.59 (s, 3H), 3.12–3.17 (m, 2H), 3.96 (s, 3H), 7.12 (t,  $J$  = 1.9 Hz, 1H);  $^{13}\text{C}$  NMR (100 MHz,  $\text{CDCl}_3$ )  $\delta$  ppm 14.0, 28.8, 34.5, 52.7, 132.0, 132.9, 150.5, 157.4, 161.5, 162.4, 208.9; HRMS Calculated for  $\text{C}_{11}\text{H}_{12}\text{NO}_4$  ( $\text{M}+1$ ) 222.0766, found 222.0785.



## 7 References

1. Yamaguchi, J.; Yamaguchi, A. D.; Itami, K. *Angew. Chem. Int. Ed.* **2012**, *51*, 8960-9009.
2. Fujiwara, Y.; Moritani, I.; Danno, S.; Asano, R.; Teranishi, S. *J. Am. Chem. Soc.* **1969**, *91*, 7166-7169.
3. Low, J. A.; Wedam, S. B.; Lee, J. J.; Berman, A. W.; Brufsky, A.; Yang, S. X.; Poruchynsky, M. S.; Steinberg, S. M.; Mannan, N.; Fojo, T.; Swain, S. M. *J. Clin. Oncol.* **2005**, *23*, 2726-2734.
4. Austin, W. C.; Courtney, W.; Danilewicz, J. C.; Morgan, D. H.; Conover, L. H.; Howes Jr., H. L.; Lynch, J. E.; McFarland, J. W.; Cornwell, R. L.; Theodorides, V. J. *Nature* **1966**, *212*, 1273-1274.
5. Edwards, R. M.; Trizna, W.; Stack, E. J.; Weinstock, J. *J. Pharmacol. Exp. Ther.* **1996**, *276*, 125-129.
6. Jones, T. R.; Labelle, M.; Belley, M.; Champion, E.; Charette, L.; Evans, J.; Ford-Hutchinson, A. W.; Gauthier, J.-Y.; Lord, A.; Masson, P.; McAuliffe, M.; McFarlane, C. S.; Metters, K. M.; Pickett, C.; Piechuta, H.; Rochette, C.; Rodger, I. W.; Sawyer, N.; Young, R. N. *Can. J. Physiol. Pharmacol.* **1995**, *73*, 191-201.
7. Faivre, S.; Delbaldo, C.; Vera, K.; Robert, C.; Lozahic, S.; Lassau, N.; Bello, C.; Deprimo, S.; Brega, N.; Massimini, G.; Armand, J.-P.; Scigalla, P.; Raymond, E. *J. Clin. Oncol.* **2006**, *24*, 25-35.
8. Jarman, M.; Barrie, E.; Llera, J. M. *J. Med. Chem.* **1998**, *41*, 5375-5381.
9. Tse, F. L. S.; Smith, H. T.; Ballard, F. H.; Nicoletti, J. *Biopharm. Drug Dispos.* **1990**, *11*, 519-531.
10. McTaggart, F.; Buckett, L.; Davidson, R.; Holdgate, G.; McCormick, A.; Schneck, D.; Smith, G.; Warwick, M. *Am. J. Cardiol.* **2001**, *87* (5A), 28-32.
11. Harrold, M. In *Antihyperlipoproteinemics and Inhibitors of Cholesterol Biosynthesis*; Lemke, T. L., Williams, D. A., Roche, V. F. and Zito, S. W., Eds.; Foye's Principles of Medicinal Chemistry; LWW: Philadelphia, 2012; Vol. 7, pp 815-840.
12. Jimenez, M. E.; Bush, K.; Pawlik, J.; Sower, L.; Peterson, J. W.; Gilbertson, S. R. *Bioorg. Med. Chem. Lett.* **2008**, *18*, 4215-4218.

13. Fitzner, R.; Mena-Osteritz, E.; Walzer, K.; Pfeiffer, M.; Bäuerle, P. *Adv. Funct. Mater.* **2015**, *25*, 1845-1856.
14. Zhao, Y.; He, G.; Nack, W. A.; Chen, G. *Org. Lett.* **2012**, *14*, 2948-2951.
15. Zaitsev, V. G.; Daugulis, O. *J. Am. Chem. Soc.* **2005**, *127*, 4156-4157.
16. Das, B.; Reddy, G. C.; Balasubramanyam, P.; Salvanna, N. *Tetrahedron* **2012**, *68*, 300-305.
17. Grigorjeva, L.; Daugulis, O. *Angew. Chem. Int. Ed.* **2014**, *53*, 10209-10212.
18. Vabre, R.; Chevot, F.; Legraverend, M.; Piguel, S. *J. Org. Chem.* **2011**, *76*, 9542-9547.
19. Sahnoun, S.; Messaoudi, S.; Brion, J.-D.; Alami, M. *Eur. J. Org. Chem.* **2010**, 6097-6102.
20. Raux, E.; Klenc, J.; Blake, A.; Sączewski, J.; Strekowski, L. *Molecules* **2010**, *15*, 1973-1984.
21. Tanaka, S.; Fukui, Y.; Nakagawa, N.; Murakami, K.; Murakami, T. N.; Koumura, N.; Mori, A. *Org. Lett.* **2016**, *18*, 650-653.
22. Besselièvre, F.; Lebrequier, S.; Mahuteau-Betzer, F.; Piguel, S. *Synthesis* **2009**, 3511-3518.
23. Liégault, B.; Lapointe, D.; Caron, L.; Vlassova, A.; Fagnou, K. *J. Org. Chem.* **2009**, *74*, 1826-1834.
24. Hughes, C. C.; Trauner, D. *Tetrahedron* **2004**, *60*, 9675-9686.
25. Pivsa-Art, S.; Satoh, T.; Kawamura, Y.; Miura, M.; Nomura, M. *Bull. Chem. Soc. Jpn.* **1998**, *71*, 467-473.
26. Koubachi, J.; El Kazzouli, S.; Berteina-Raboin, S.; Mouaddib, A.; Guillaumet, G. *Synthesis* **2008**, 2537-2542.
27. Chai, D. I.; Lautens, M. *J. Org. Chem.* **2009**, *74*, 3054-3061.
28. Albicker, M. R.; Cramer, N. *Angew. Chem. Int. Ed.* **2009**, *48*, 9139-9142.
29. Peng, J.; Shang, G.; Chen, C.; Miao, Z.; Li, B. *J. Org. Chem.* **2013**, *78*, 1242-1248.
30. Tang, F.; Chen, C.; Zhou, Y.; Lin, C.; Zhang, J. *RSC Adv.* **2014**, *4*, 51298-51301.
31. Yu, Y.; Wang, Z.; Zhang, X. *Sci. China Chem.* **2014**, *57*, 276-281.
32. Hao, W.; Wang, H.; Ye, Q.; Zhang, W.-X.; Xi, Z. *Org. Lett.* **2015**, *17*, 5674-5677.

33. Jutand, A. In *Mechanisms of the Mizoroki-Heck Reaction*; Oestreich, M., Ed.; The Mizoroki-Heck Reaction; Wiley: 2009; pp 1-50.
34. Dieck, H. A.; Heck, R. F. *J. Am. Chem. Soc.* **1974**, *96*, 1133-1136.
35. Zhao, Q.; Besset, T.; Poisson, T.; Bouillon, J.-P.; Pannecoucke, X. *Eur. J. Org. Chem.* **2016**, *2016*, 76-82.
36. Liu, M.; Niu, Y.; Wu, Y.-F.; Ye, X.-S. *Org. Lett.* **2016**, *18*, 1836-1839.
37. Gorelsky, S. I.; Lapointe, D.; Fagnou, K. *J. Org. Chem.* **2012**, *77*, 658-668.
38. Gorelsky, S. I.; Lapointe, D.; Fagnou, K. *J. Am. Chem. Soc.* **2008**, *130*, 10848-10849.
39. Larhed, M.; Hallberg, A. In *The Heck Reaction (Alkene Substitution via Carbopalladation–Dehydropalladation) and Related Carbopalladation Reactions*; Negishi, E., Ed.; Handbook of Organopalladium Chemistry for Organic Synthesis; Wiley-Interscience: New York, 2002; Vol. 1, pp 1133-1178.
40. Koubachi, J.; Berteina-Raboin, S.; Mouaddib, A.; Guillaumet, G. *Synthesis* **2009**, 271-276.
41. Heck, R. F. *J. Am. Chem. Soc.* **1971**, *93*, 6896-6901.
42. Wu, X.; Zhou, J. *Chem. Commun.* **2013**, *49*, 4794-4796.
43. Izawa, Y.; Zheng, C.; Stahl, S. S. *Angew. Chem. Int. Ed.* **2013**, *52*, 3672-3675.
44. Zhu, G.; Lu, X. *Organometallics* **1995**, *14*, 4899-4904.
45. Zhao, H.; Ariafield, A.; Lin, Z. *Organometallics* **2006**, *25*, 812-819.
46. Portnoy, M.; Ben-David, Y.; Milstein, D. *Organometallics* **1993**, *12*, 4734-4735.
47. Verrier, C.; Hoarau, C.; Marsais, F. *Org. Biomol. Chem.* **2009**, *7*, 647-650.
48. Nilsson, P.; Olofsson, K.; Larhed, M. In *Focus on Regioselectivity and Product Outcome in Organic Synthesis*; Oestreich, M., Ed.; The Mizoroki-Heck Reaction; Wiley: 2009; pp 133-162.
49. Blanksby, S. J.; Ellison, G. B. *Acc. Chem. Res.* **2003**, *36*, 255-263.
50. Grushin, V. V.; Alper, H. *Chem. Rev.* **1994**, *94*, 1047-1062.
51. Willis, M. C.; Claverie, C. K.; Mahon, M. F. *Chem. Commun.* **2002**, 832-833.
52. Karabelas, K.; Westerlund, C.; Hallberg, A. *J. Org. Chem.* **1985**, *50*, 3896-3900.
53. Campeau, L.-C.; Parisien, M.; Jean, A.; Fagnou, K. *J. Am. Chem. Soc.* **2006**, *128*, 581-590.

54. Petit, A.; Flygare, J.; Miller, A. T.; Winkel, G.; Ess, D. H. *Org. Lett.* **2012**, *14*, 3680-3683.
55. Leclerc, J.-P.; Fagnou, K. *Angew. Chem. Int. Ed.* **2006**, *45*, 7781-7786.
56. Strotman, N. A.; Chobanian, H. R.; Guo, Y.; He, J.; Wilson, J. E. *Org. Lett.* **2010**, *12*, 3578-3581.
57. Roger, J.; Gottumukkala, A. L.; Doucet, H. *ChemCatChem* **2010**, *2*, 20-40.
58. Lane, B. S.; Brown, M. A.; Sames, D. *J. Am. Chem. Soc.* **2005**, *127*, 8050-8057.
59. Kuhl, N.; Hopkinson, M. N.; Wencel-Delord, J.; Glorius, F. *Angew. Chem. Int. Ed.* **2012**, *51*, 10236-10254.
60. Lafrance, M.; Rowley, C. N.; Woo, T. K.; Fagnou, K. *J. Am. Chem. Soc.* **2006**, *128*, 8754-8756.
61. Gembus, V.; Bonfanti, J.-F.; Querolle, O.; Jubault, P.; Levacher, V.; Hoarau, C. *Org. Lett.* **2012**, *14*, 6012-6015.
62. Ahlers, A.; De Haro, T.; Gabor, B.; Fürstner, A. *Angew. Chem. Int. Ed.* **2016**, *55*, 1406-1411.
63. Gottumukkala, A. L.; Derridj, F.; Djebbar, S.; Doucet, H. *Tetrahedron Lett.* **2008**, *49*, 2926-2930.
64. Chen, W.; Su, C.; Huang, X. *Synlett* **2006**, 1446-1448.
65. Ye, S.; Liu, J.; Wu, J. *Chem. Commun.* **2012**, *48*, 5028-5030.
66. Martino, E.; Della Volpe, S.; Terribile, E.; Benetti, E.; Sakaj, M.; Centamore, A.; Sala, A.; Collina, S. *Bioorg. Med. Chem. Lett.* **2017**, *27*, 701-707.
67. Yamagishi, M.; Nishigai, K.; Ishii, A.; Hata, T.; Urabe, H. *Angew. Chem. Int. Ed.* **2012**, *51*, 6471-6474.
68. Yamagishi, M.; Ishii, A.; Hata, T.; Urabe, H. *Heterocycles* **2015**, *90*, 847-856.
69. Beydoun, K.; Roger, J.; Boixel, J.; Bozec, H. L.; Guerchais, V.; Doucet, H. *Chem. Commun.* **2012**, *48*, 11951-11953.
70. Yuen, O. Y.; Charoensak, M.; So, C. M.; Kuhakarn, C.; Kwong, F. Y. *Chem. Asian J.* **2015**, *10*, 857-861.
71. Gao, D.-W.; Gu, Y.; Wang, S.-B.; Gu, Q.; You, S.-L. *Organometallics* **2016**, *35*, 3227-3233.
72. Fishwick, C. W. G.; Grigg, R.; Sridharan, V.; Virica, J. *Tetrahedron* **2003**, *59*, 4451-4468.

73. Cruz, A. C. F.; Miller, N. D.; Willis, M. C. *Org. Lett.* **2007**, *9*, 4391-4393.
74. Karaki, F.; Ohgane, K.; Fukuda, H.; Nakamura, M.; Dodo, K.; Hashimoto, Y. *Bioorg. Med. Chem.* **2014**, *22*, 3587-3609.
75. Kumpulainen, E. T. T.; Pohjakallio, A. *Adv. Synth. Catal.* **2014**, *356*, 1555-1561.
76. Ihanainen, N. E.; Kumpulainen, E. T. T.; Koskinen, A. M. P. *Eur. J. Org. Chem.* **2015**, *2015*, 3226-3229.
77. Harris, R. M.; Andrews, B. I.; Clark, S.; Cooke, J. W. B.; Gray, J. C. S.; Ng, S. Q. Q. *Org. Process Res. Dev.* **2013**, *17*, 1239-1246.
78. Prat, D.; Wells, A.; Hayler, J.; Sneddon, H.; McElroy, C. R.; Abou-Shehada, S.; Dunn, P. J. *Green Chem.* **2015**, *18*, 288-296.
79. Fiebig, L.; Schlörer, N.; Schmalz, H.-G.; Schäfer, M. *Chem. Eur. J.* **2014**, *20*, 4906-4910.
80. Gomes Constantino, M.; Lacerda Jr., V.; Da Silva, G. V. J. *Molecules* **2002**, *7*, 456-464.
81. Eckelbarger, J. D.; Wilmot, J. T.; Epperson, M. T.; Thakur, C. S.; Shum, D.; Antczak, C.; Tarassishin, L.; Djaballah, H.; Gin, D. Y. *Chem. Eur. J.* **2008**, *14*, 4293-4306.

## **Appendices**

**Appendix 1:** Chromatographic analysis

**Appendix 2:** NMR spectra of products

## Appendix 1: Chromatographic analysis

The LC-MS measurements were calibrated using a combination of an external and internal standard. The external standard, a mixture of 0.2 mg/mL each expected component (see Table 1 below), was used to relate the UV responses of the components to actual molar concentrations. An inert component (mesitylene) was added in the reaction to normalize the concentrations in the blank sample and the reaction sample. All results were collected using wavelength 230 nm.

The samples were analyzed with a 3-minute method using acetonitrile and 0.1% ammonia solution as solvents. The standard sample was run with a shallower gradient and smaller injection volume to better resolve the product and phenol peaks (Figure 1). In the reaction samples amounts of phenol were lower so the samples could be run with the default method which gave narrower peaks (Figure 2).

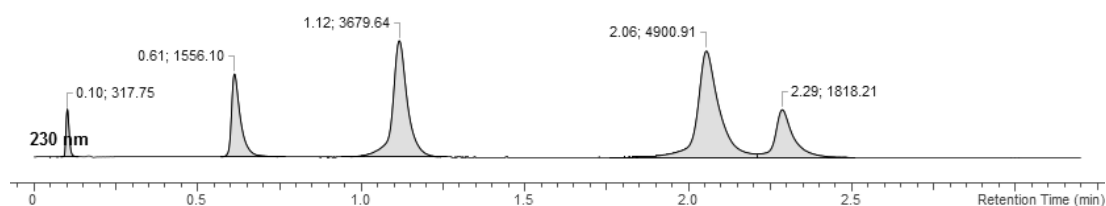


**Figure 1.** UV chromatogram of the standard sample. Identified components: 1,3-cyclohexanedione 0.10 min; imidazo[1,2-*a*]pyridine 0.61 min; 3-chloro-2-cyclohexenone 1.12 min; phenol product 2.06 min; product 2.29 min.

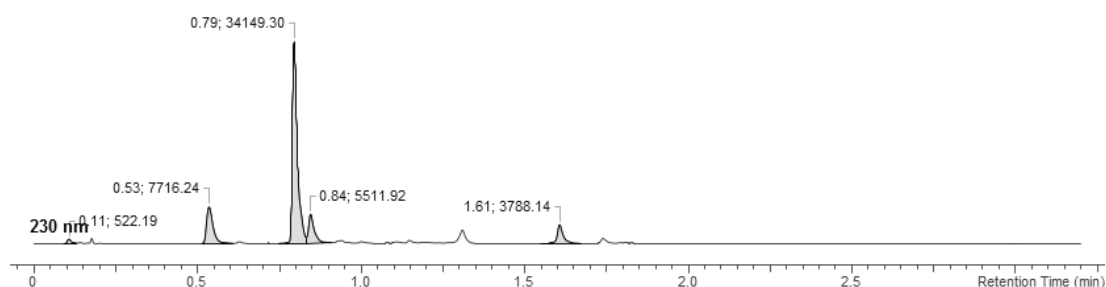


**Figure 2.** UV chromatogram of the reaction sample of Entry 1 (Table 9 in the text). Identified components: 1,3-cyclohexanedione 0.11 min; imidazo[1,2-*a*]pyridine 0.53 min; product 0.79 min; phenol product 0.84 min; mesitylene 1.61 min.

The areas in the standard sample chromatogram (Figure 1) were divided by the molar concentration to obtain the UV correlation factors  $\varepsilon$  (Table 1). The values are multiplied by 5 to account for the difference in injection volumes. Example calculation for imidazo[1,2-*a*]pyridine (ipy) below.

$$\varepsilon_{\text{ipy}} = 5 \cdot \frac{A_{\text{ipy}}}{c_{\text{ipy}}} = 5 \cdot \frac{1556.10 \text{ cts}}{\frac{0.2 \text{ mol}}{118.136 \text{ L}}} = 4595786 \frac{\text{cts L}}{\text{mol}}$$

**Table 1. UV correlation factors for each component.**

Component	$\varepsilon$ (cts L/mol)
1,3-cyclohexanedione	890709
3-chloro-2-cyclohexenone	12011449
imidazo[1,2- <i>a</i> ]pyridine	4595786
product <b>109</b>	9647740
phenol product <b>110</b>	25758080

Chromatographic yields of the desired product compared to imidazo[1,2-*a*]pyridine were calculated using the following equation. Yields of the phenol product were calculated similarly. Results are presented in the text. Example calculation for Entry 1 (Table 9 in the text) is shown.

$$Y_{\text{prod}} = \frac{[\text{product}]_1}{[\text{ipy}]_0} = \frac{A_{\text{mes},0} A_{\text{prod},1} \varepsilon_{\text{ipy}}}{A_{\text{mes},1} A_{\text{ipy},0} \varepsilon_{\text{prod}}} = \frac{5304.12 \cdot 34149.30 \cdot 4595786}{3788.14 \cdot 39468.27 \cdot 9647740} = 58\%$$

Starting material conversions were calculated using the following equation. Results are presented in the text. Example calculation for Entry 1 (Table 9 in the text) is shown.

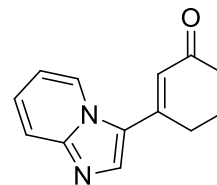
$$X_{\text{ipy}} = 1 - \frac{[\text{ipy}]_1}{[\text{ipy}]_0} = 1 - \frac{A_{\text{ipy},1} A_{\text{mes},0}}{A_{\text{ipy},0} A_{\text{mes},1}} = 1 - \frac{7716.24 \cdot 5304.12}{39468.27 \cdot 3788.14} = 73\%$$



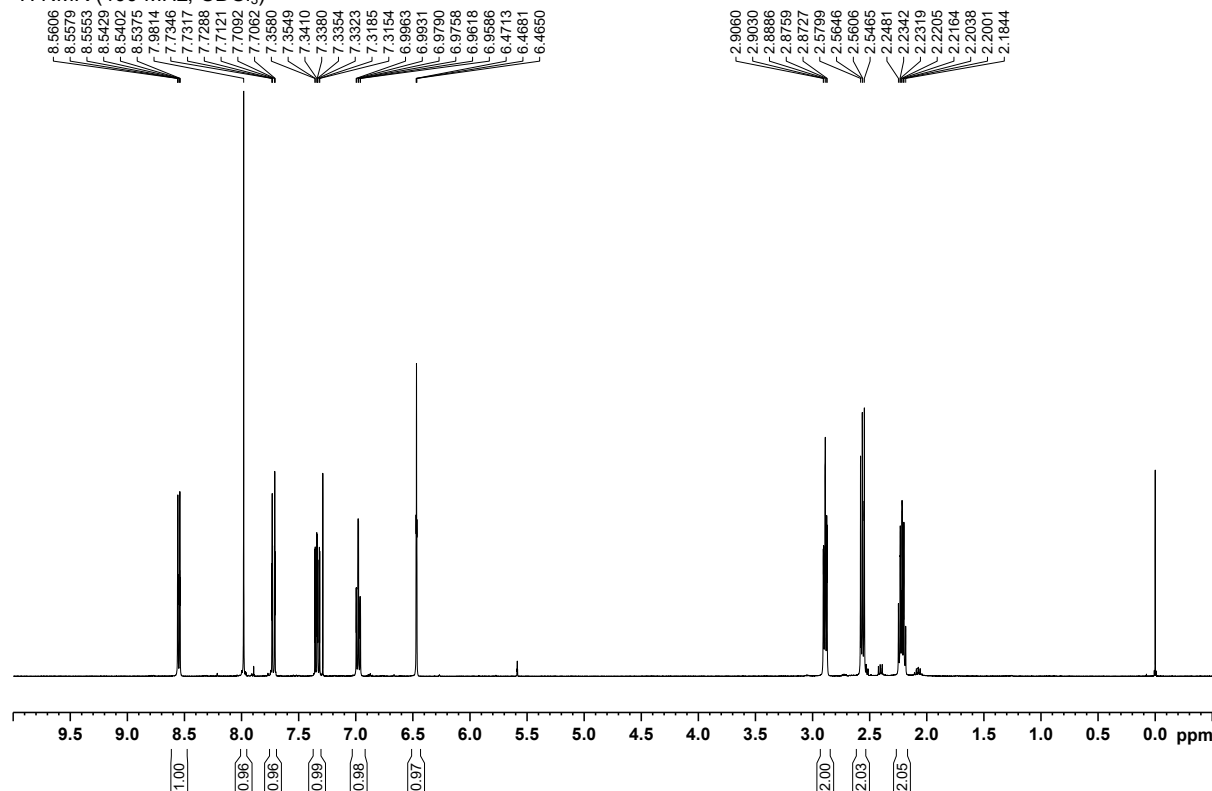
## Appendix 2: NMR spectra of products

3-(Imidazo[1,2-*a*]pyridin-3-yl)cyclohex-2-enone **109**:  $^1\text{H}$ ,  $^{13}\text{C}$ , NOESY  
3-(Imidazo[1,5-*a*]pyridin-3-yl)cyclohex-2-enone **112**:  $^1\text{H}$ ,  $^{13}\text{C}$   
3-(Imidazo[1,2-*a*]pyrazin-3-yl)cyclohex-2-enone **113**:  $^1\text{H}$ ,  $^{13}\text{C}$   
3-(Imidazo[1,2-*a*]pyrimidin-3-yl)cyclohex-2-enone **114**:  $^1\text{H}$ ,  $^{13}\text{C}$   
3-(Imidazo[1,2-*b*]pyridazin-3-yl)cyclohex-2-enone **115**:  $^1\text{H}$ ,  $^{13}\text{C}$   
3-(Benzo[*d*]oxazol-2-yl)cyclohex-2-enone **116**:  $^1\text{H}$ ,  $^{13}\text{C}$   
3-(Benzo[*d*]thiazol-2-yl)cyclohex-2-enone **117**:  $^1\text{H}$ ,  $^{13}\text{C}$   
3-(Thiazol-5-yl)cyclohex-2-enone **118**:  $^1\text{H}$ ,  $^{13}\text{C}$   
3-(2-Isobutylthiazol-5-yl)cyclohex-2-enone **119**:  $^1\text{H}$ ,  $^{13}\text{C}$   
Methyl 2-methyl-5-(3-oxocyclohex-1-en-1-yl)oxazole-4-carboxylate **120**:  $^1\text{H}$ ,  $^{13}\text{C}$   
2-Methyl-5-(3-oxocyclohex-1-en-1-yl)thiazole-4-carbonitrile **121**:  $^1\text{H}$ ,  $^{13}\text{C}$   
5-(3-Oxocyclohex-1-en-1-yl)thiazole-2-carbonitrile **122**:  $^1\text{H}$ ,  $^{13}\text{C}$   
Ethyl 2-(3-oxocyclohex-1-en-1-yl)oxazole-5-carboxylate **123**:  $^1\text{H}$ ,  $^{13}\text{C}$   
3-(5-Methylthiazol-2-yl)cyclohex-2-enone **124**:  $^1\text{H}$ ,  $^{13}\text{C}$   
2-(3-Oxocyclohex-1-en-1-yl)pyridine 1-oxide **125**:  $^1\text{H}$ ,  $^{13}\text{C}$   
3-(Benzofuran-2-yl)cyclohex-2-enone **127**:  $^1\text{H}$ ,  $^{13}\text{C}$   
3-(5-Methylfuran-2-yl)cyclohex-2-enone **128**:  $^1\text{H}$ ,  $^{13}\text{C}$   
3-(Imidazo[1,2-*a*]pyridin-3-yl)cyclopent-2-enone **140**:  $^1\text{H}$ ,  $^{13}\text{C}$   
3-(Imidazo[1,5-*a*]pyridin-3-yl)cyclopent-2-enone **141**:  $^1\text{H}$ ,  $^{13}\text{C}$   
3-(Imidazo[1,2-*b*]pyridazin-3-yl)cyclopent-2-enone **142**:  $^1\text{H}$ ,  $^{13}\text{C}$   
3-(2-Isobutylthiazol-5-yl)cyclopent-2-enone **143**:  $^1\text{H}$ ,  $^{13}\text{C}$   
2-Methyl-5-(3-oxocyclopent-1-en-1-yl)thiazole-4-carbonitrile **144**:  $^1\text{H}$ ,  $^{13}\text{C}$   
Methyl 2-methyl-5-(3-oxocyclopent-1-en-1-yl)oxazole-4-carboxylate **145**:  $^1\text{H}$ ,  $^{13}\text{C}$

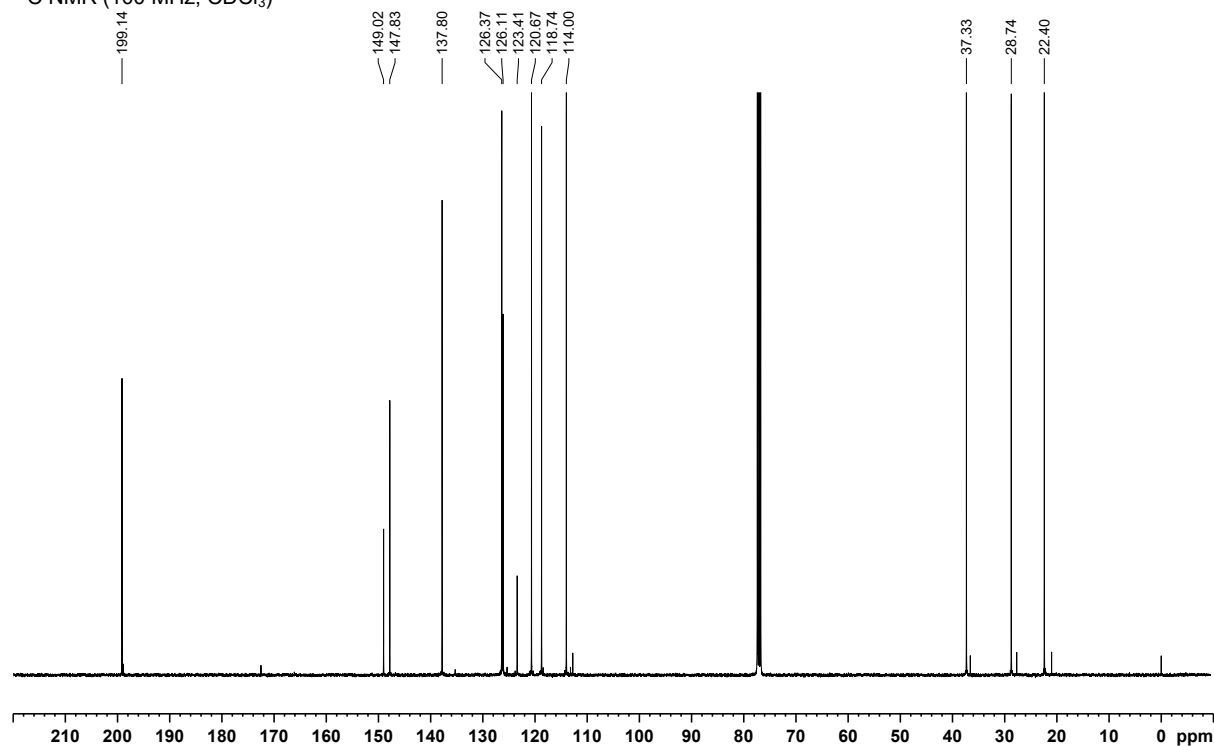
# 3-(Imidazo[1,2-a]pyridin-3-yl)cyclohex-2-enone 109



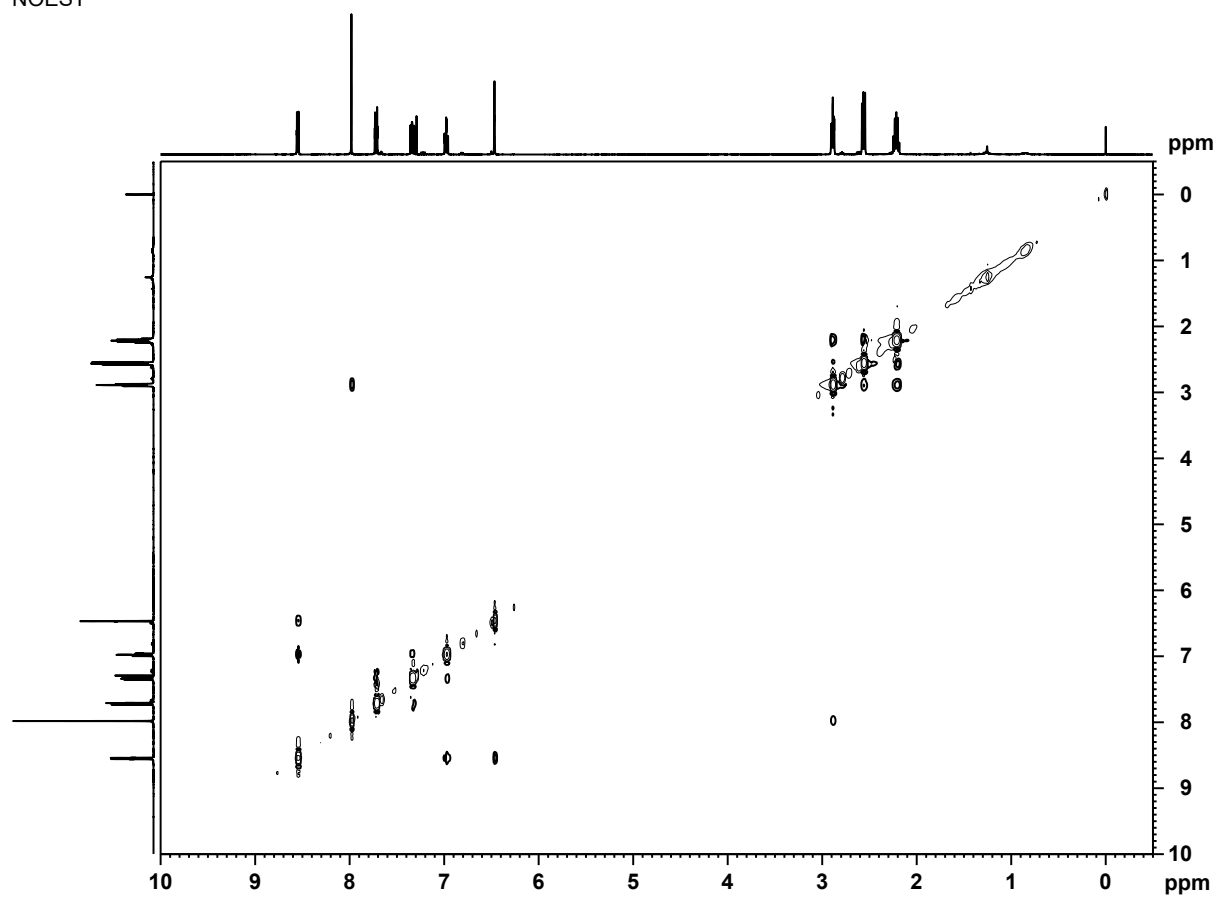
<sup>1</sup>H NMR (400 MHz, CDCl<sub>3</sub>)



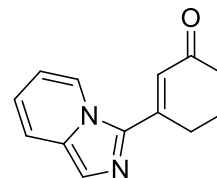
<sup>13</sup>C NMR (100 MHz, CDCl<sub>3</sub>)



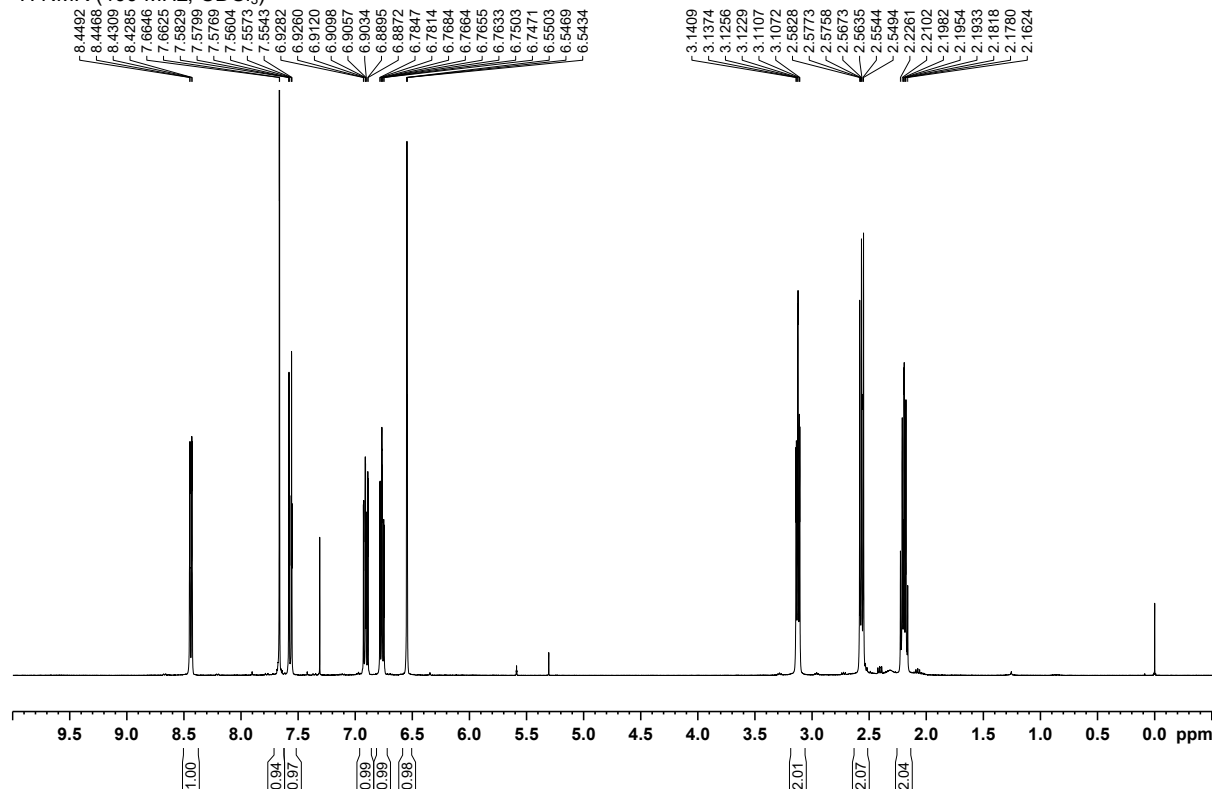
NOESY



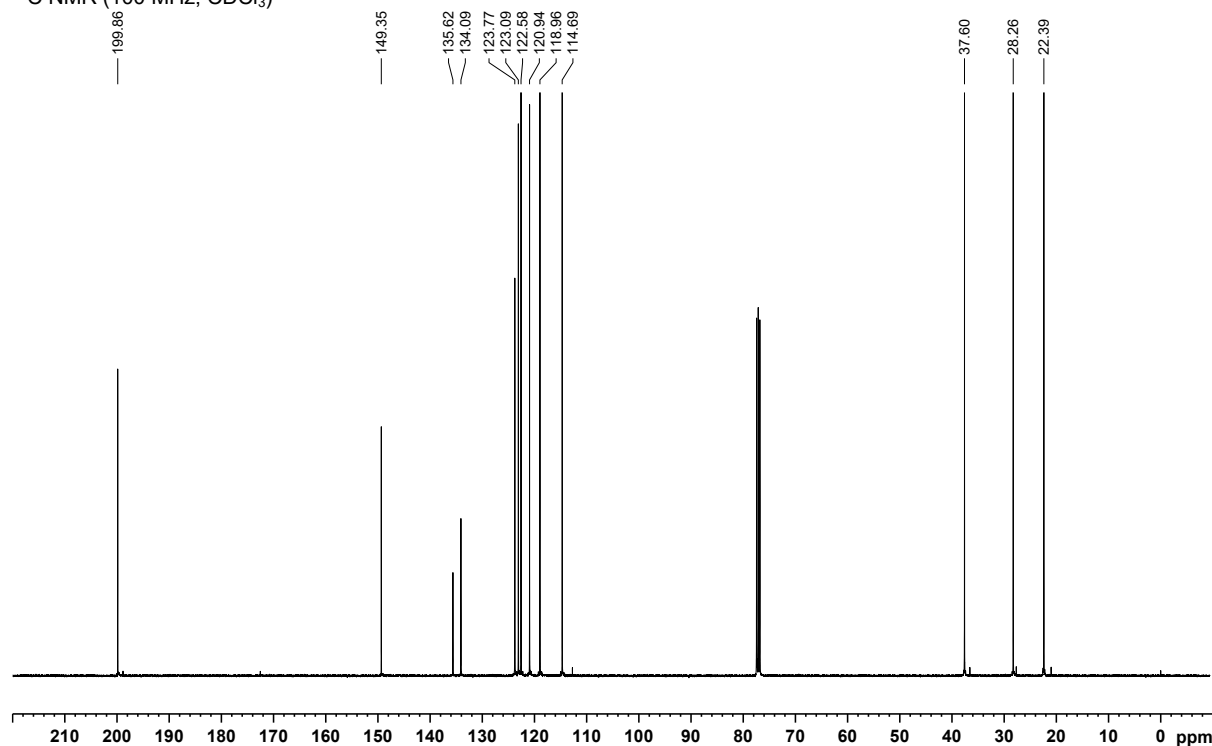
# 3-(Imidazo[1,5-*a*]pyridin-3-yl)cyclohex-2-enone 112



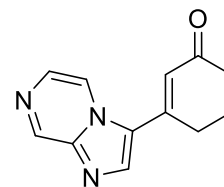
<sup>1</sup>H NMR (400 MHz, CDCl<sub>3</sub>)



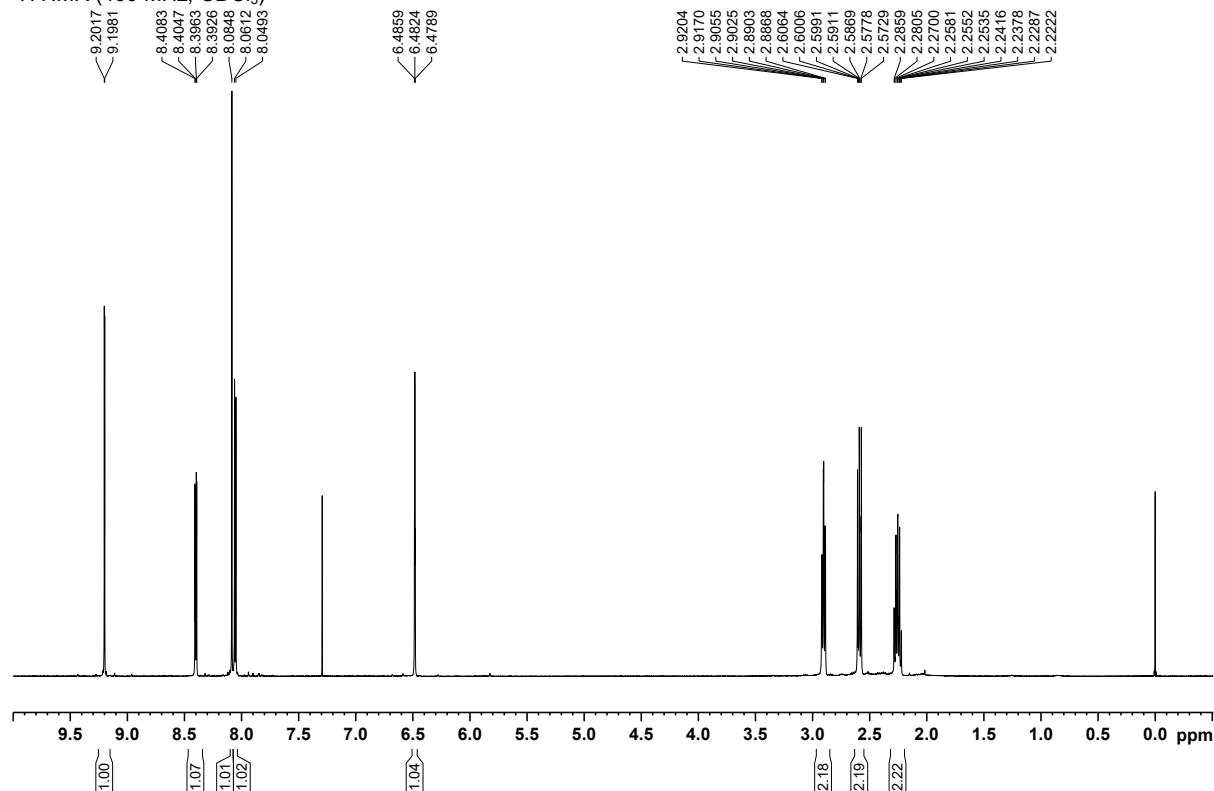
<sup>13</sup>C NMR (100 MHz, CDCl<sub>3</sub>)



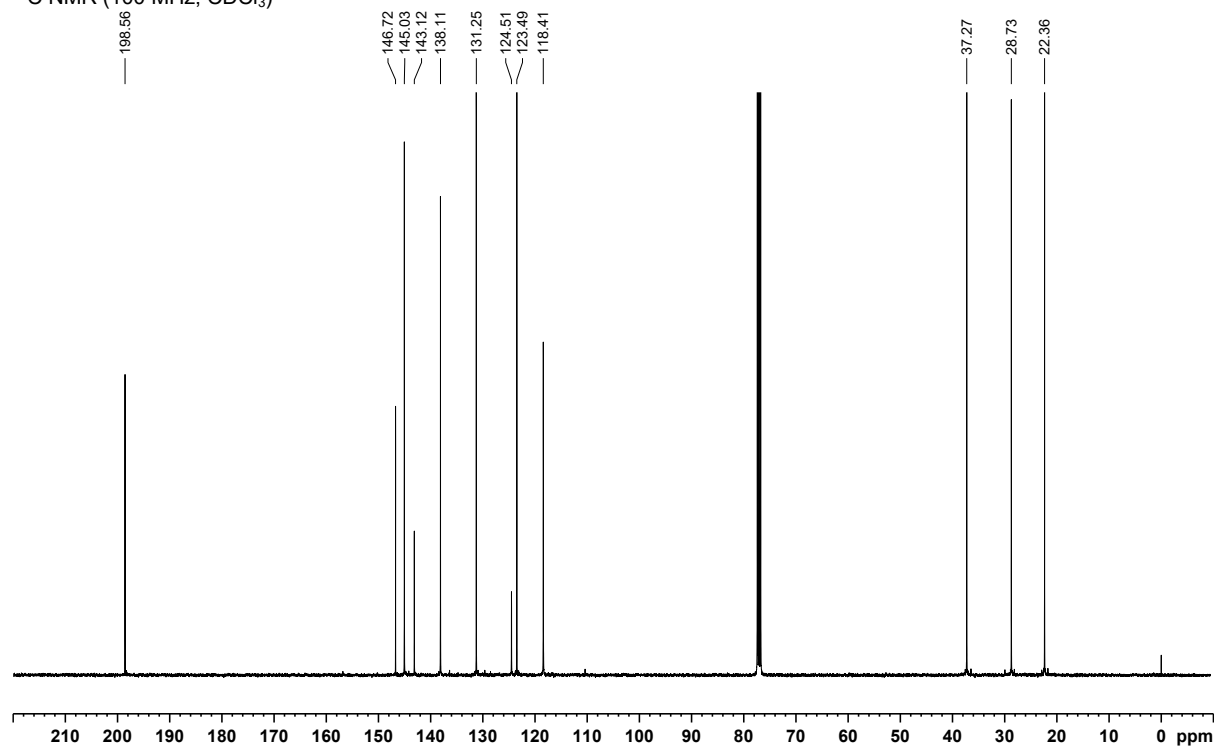
### 3-(Imidazo[1,2-*a*]pyrazin-3-yl)cyclohex-2-enone 113



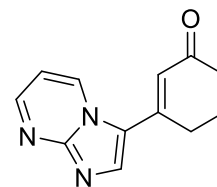
$^1\text{H}$  NMR (400 MHz,  $\text{CDCl}_3$ )



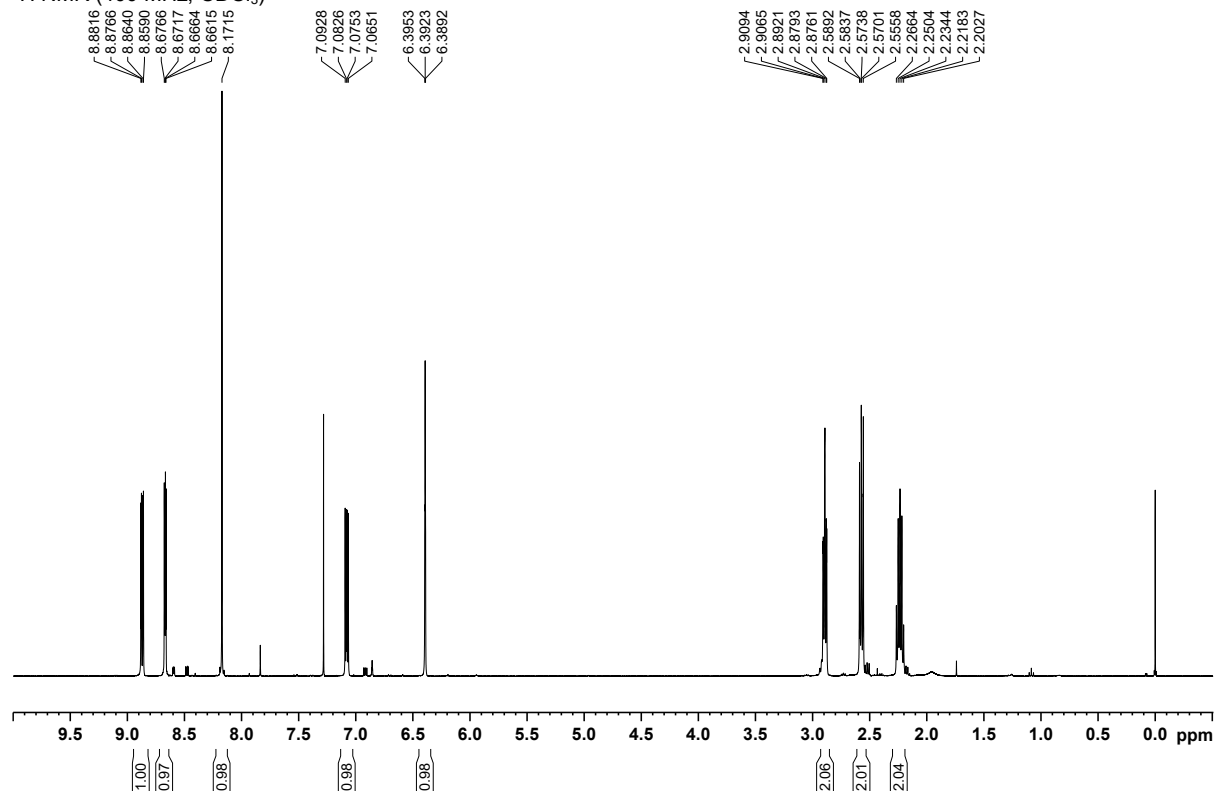
$^{13}\text{C}$  NMR (100 MHz,  $\text{CDCl}_3$ )



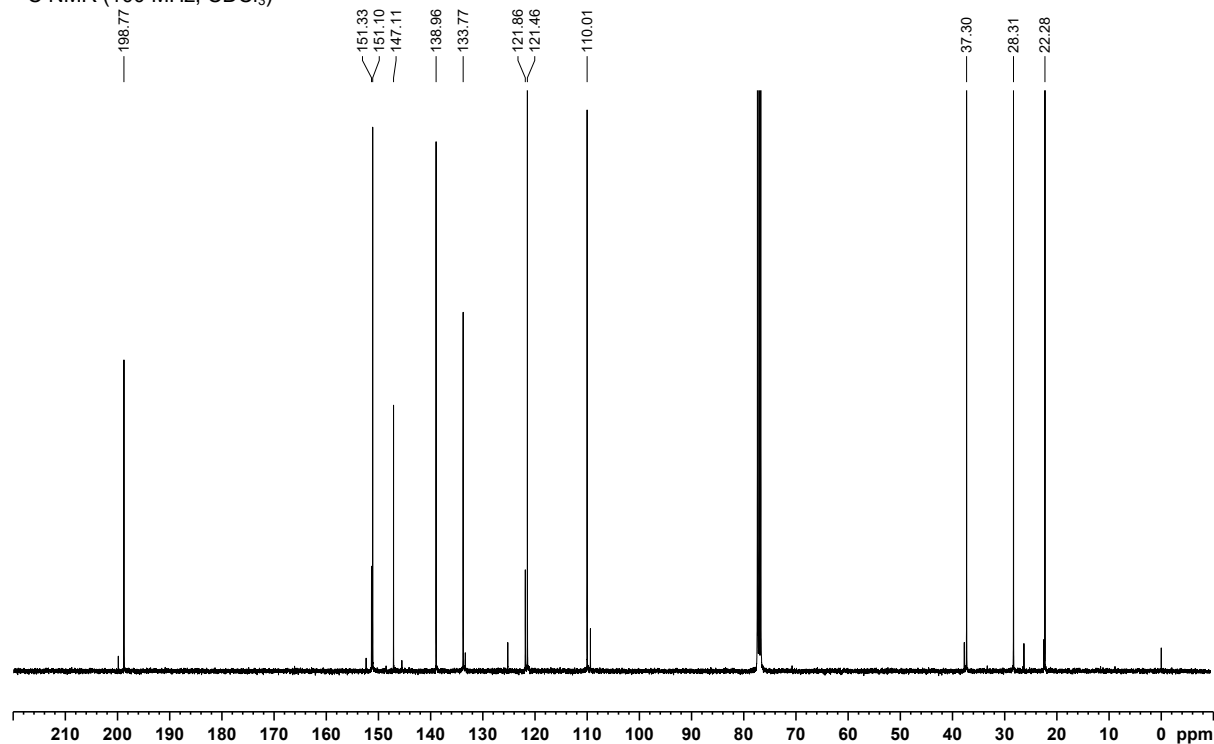
### 3-(Imidazo[1,2-*a*]pyrimidin-3-yl)cyclohex-2-enone 114



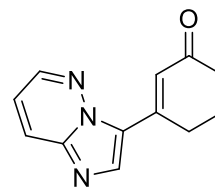
<sup>1</sup>H NMR (400 MHz, CDCl<sub>3</sub>)



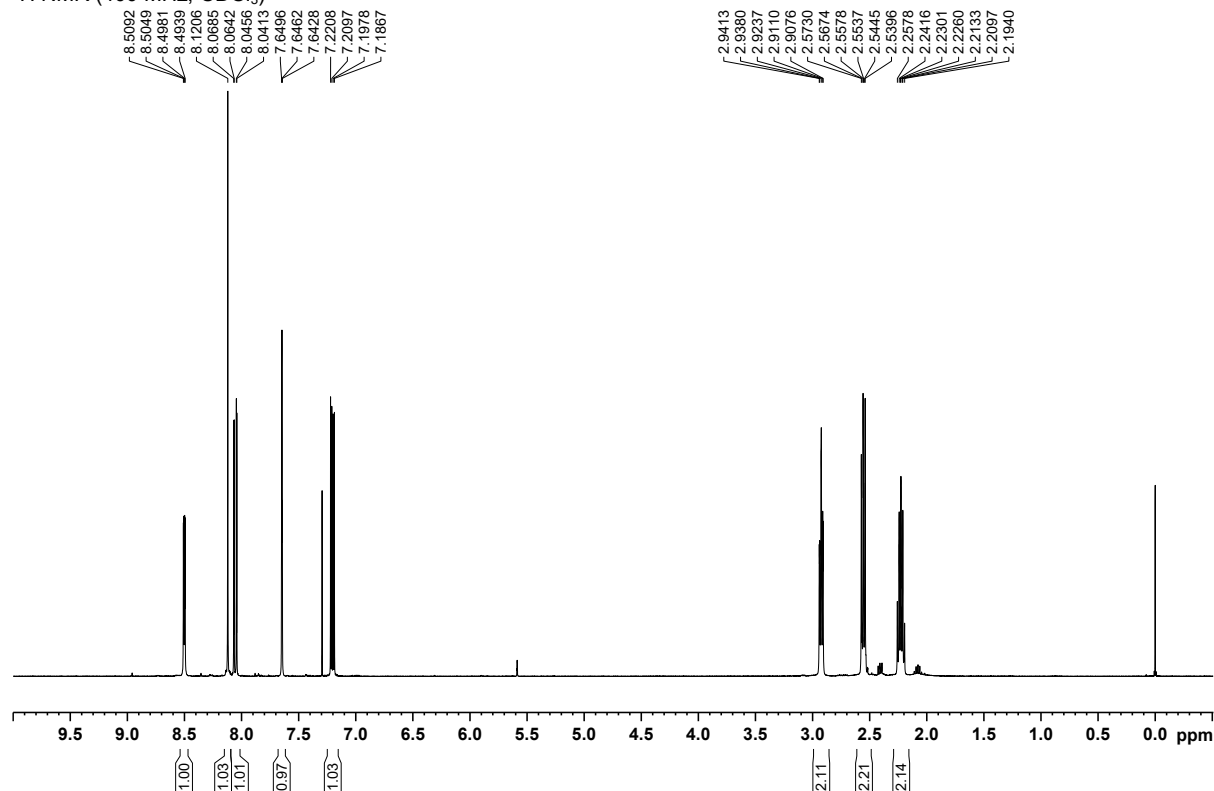
<sup>13</sup>C NMR (100 MHz, CDCl<sub>3</sub>)



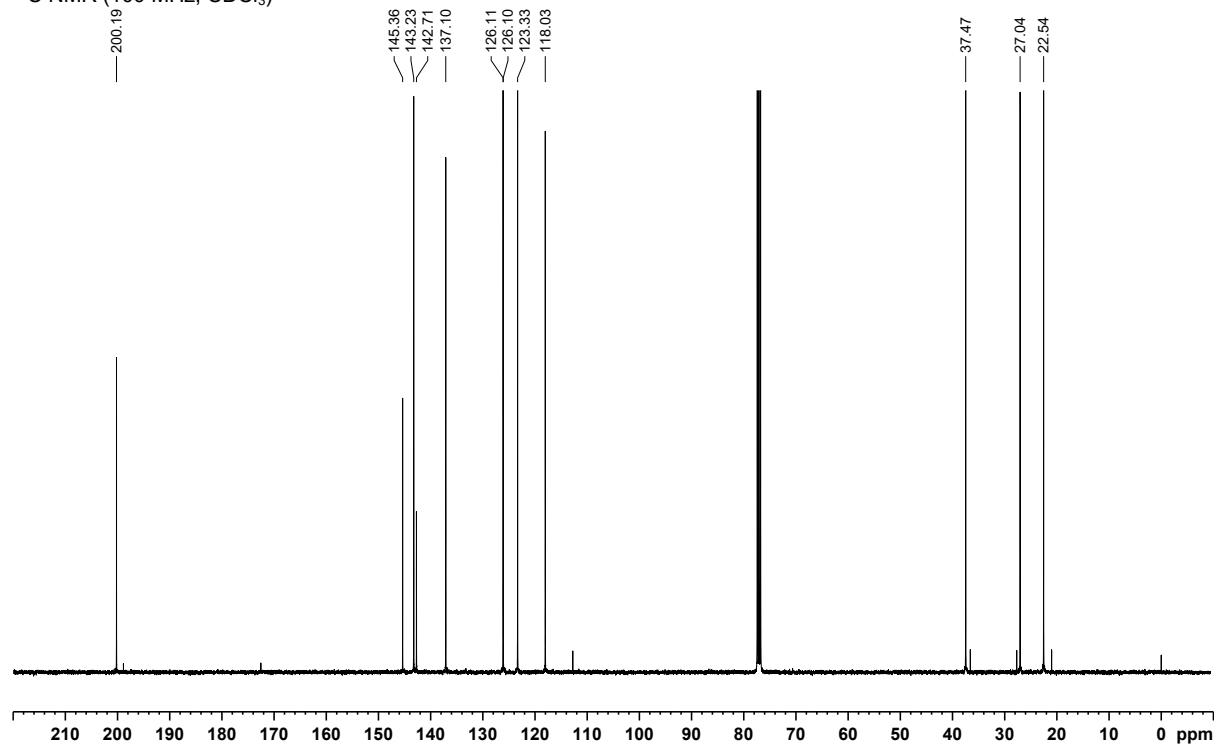
### 3-(Imidazo[1,2-*b*]pyridazin-3-yl)cyclohex-2-enone 115



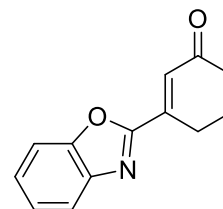
<sup>1</sup>H NMR (400 MHz, CDCl<sub>3</sub>)



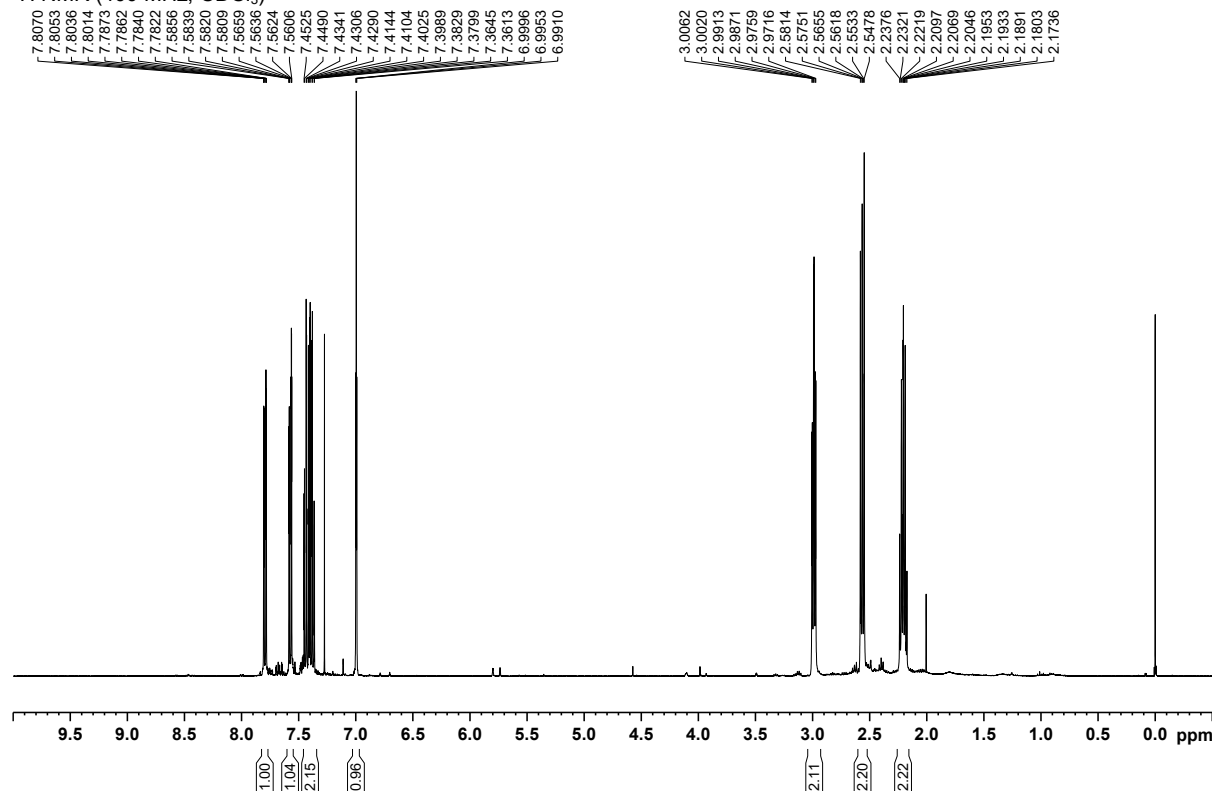
<sup>13</sup>C NMR (100 MHz, CDCl<sub>3</sub>)



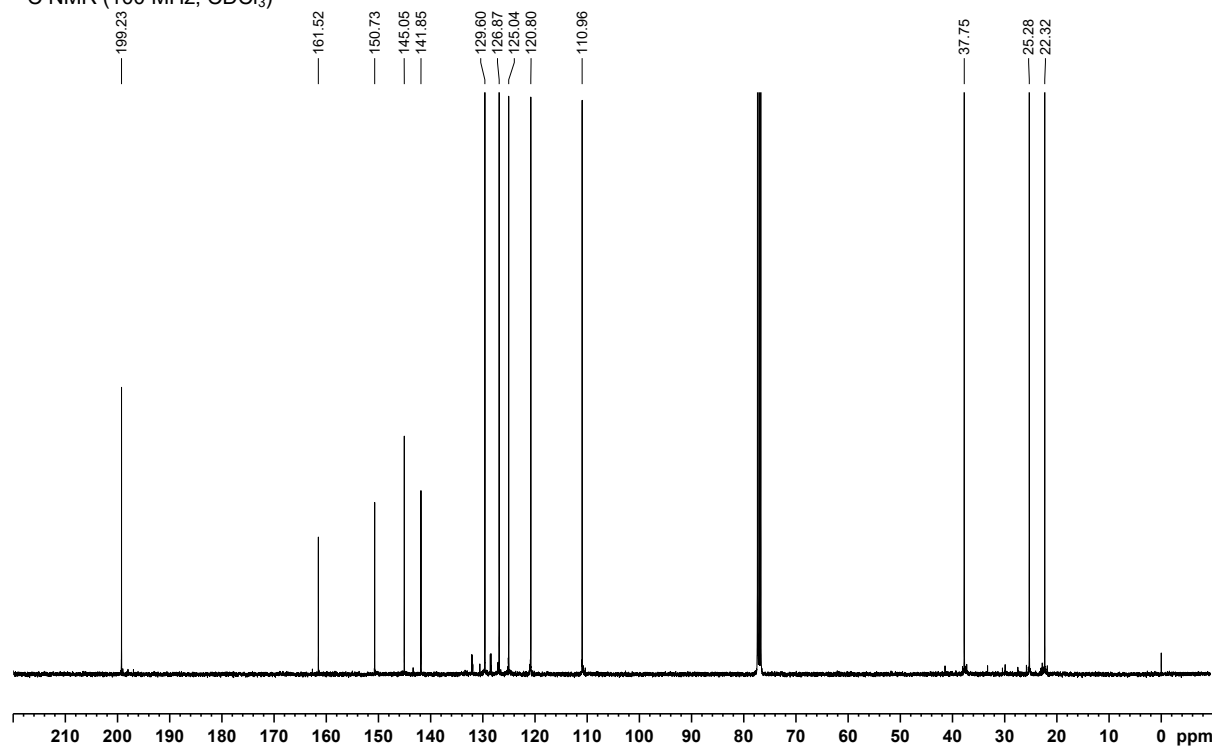
# 3-(Benzo[d]oxazol-2-yl)cyclohex-2-enone 116



<sup>1</sup>H NMR (400 MHz, CDCl<sub>3</sub>)

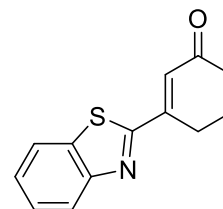


<sup>13</sup>C NMR (100 MHz, CDCl<sub>3</sub>)

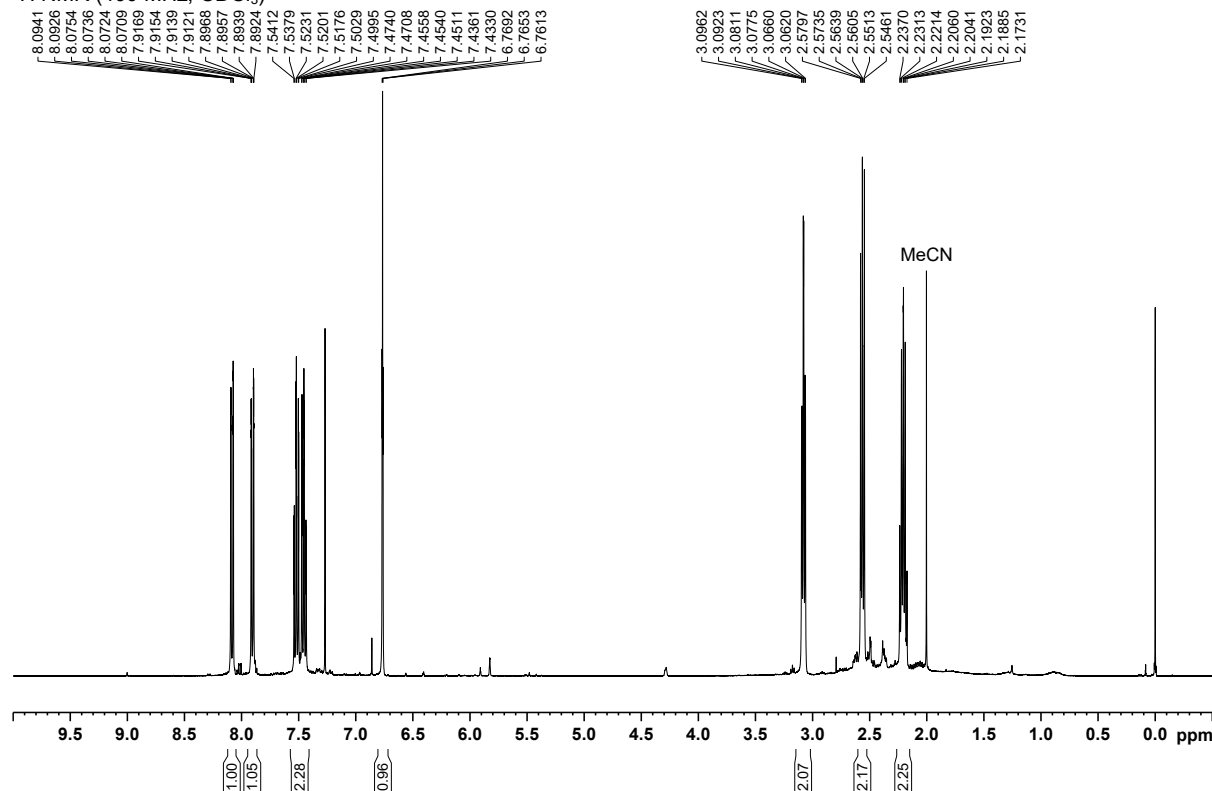




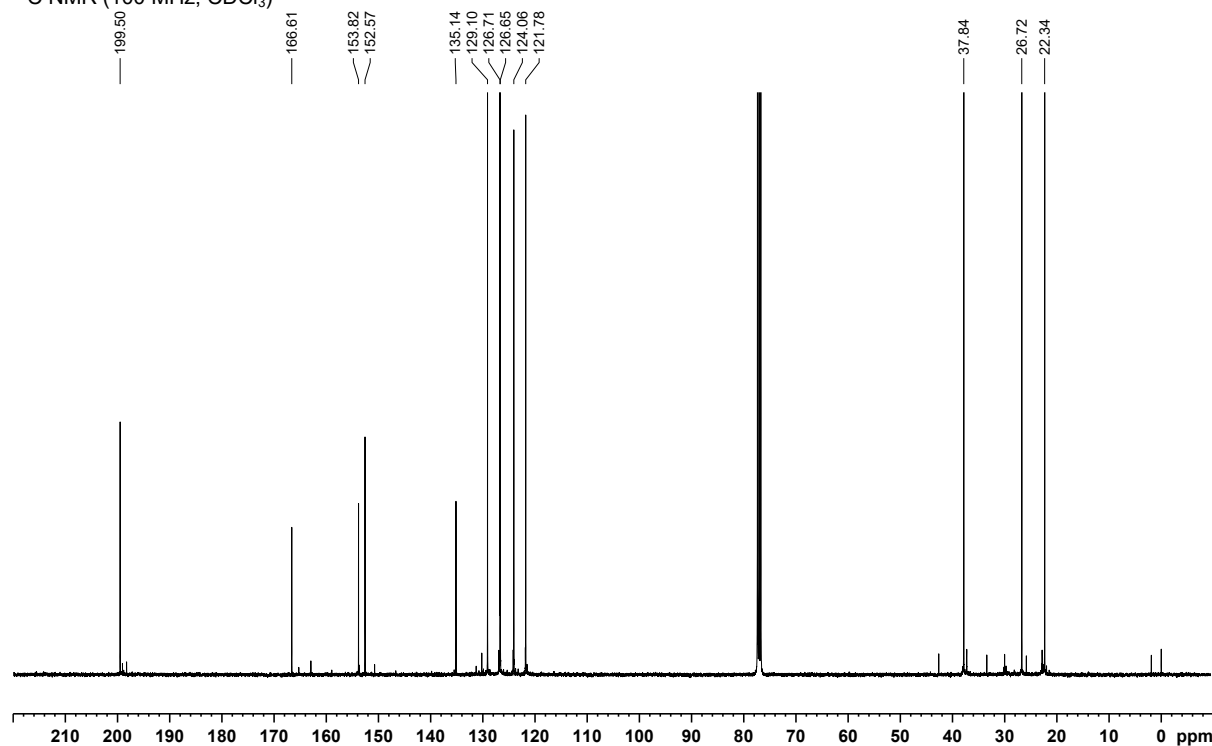
# 3-(Benzo[d]thiazol-2-yl)cyclohex-2-enone 117



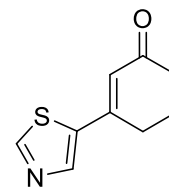
<sup>1</sup>H NMR (400 MHz, CDCl<sub>3</sub>)



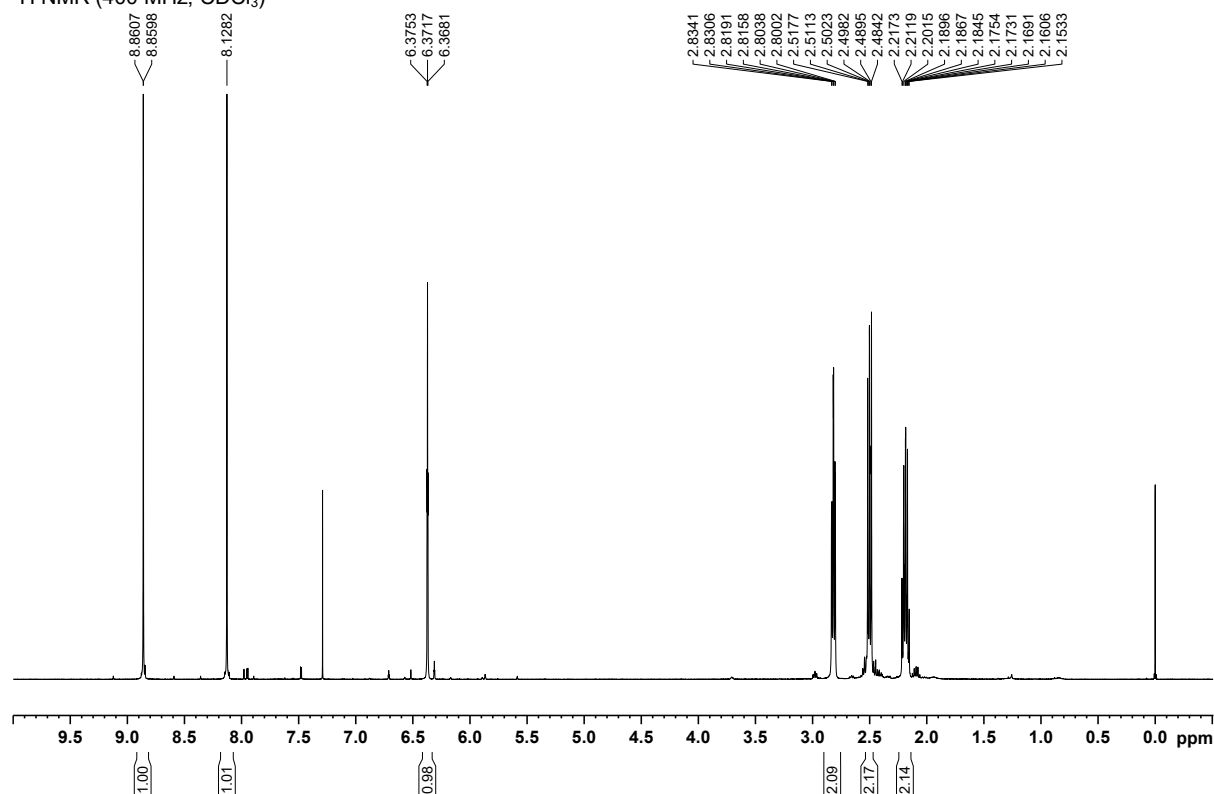
<sup>13</sup>C NMR (100 MHz, CDCl<sub>3</sub>)



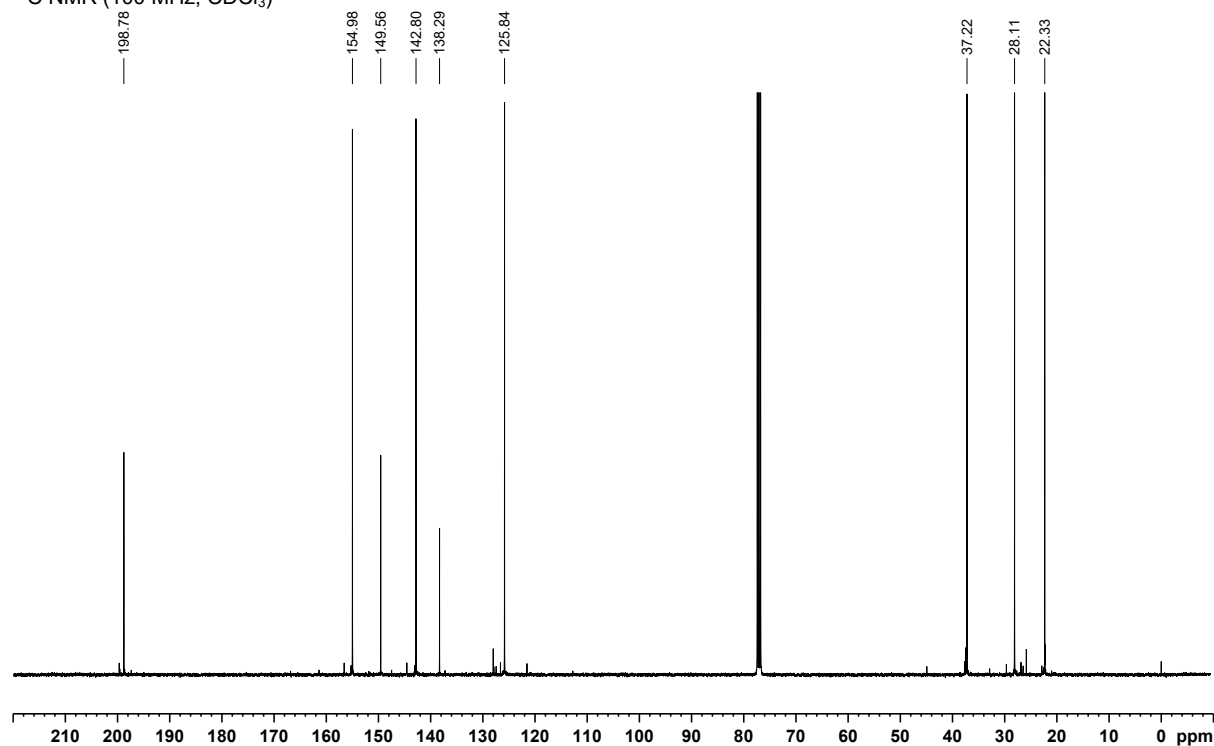
### 3-(Thiazol-5-yl)cyclohex-2-enone 118



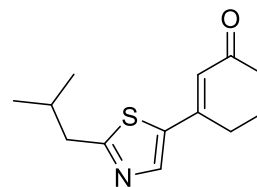
$^1\text{H}$  NMR (400 MHz,  $\text{CDCl}_3$ )



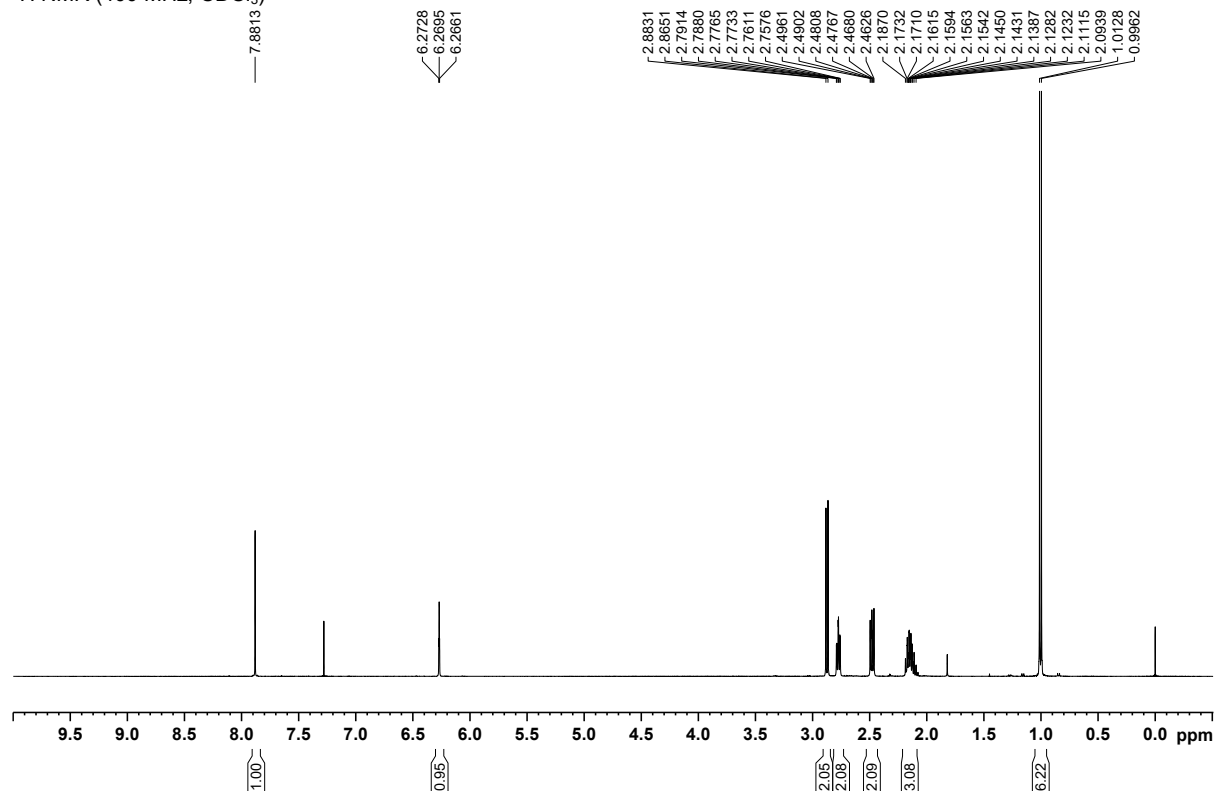
$^{13}\text{C}$  NMR (100 MHz,  $\text{CDCl}_3$ )



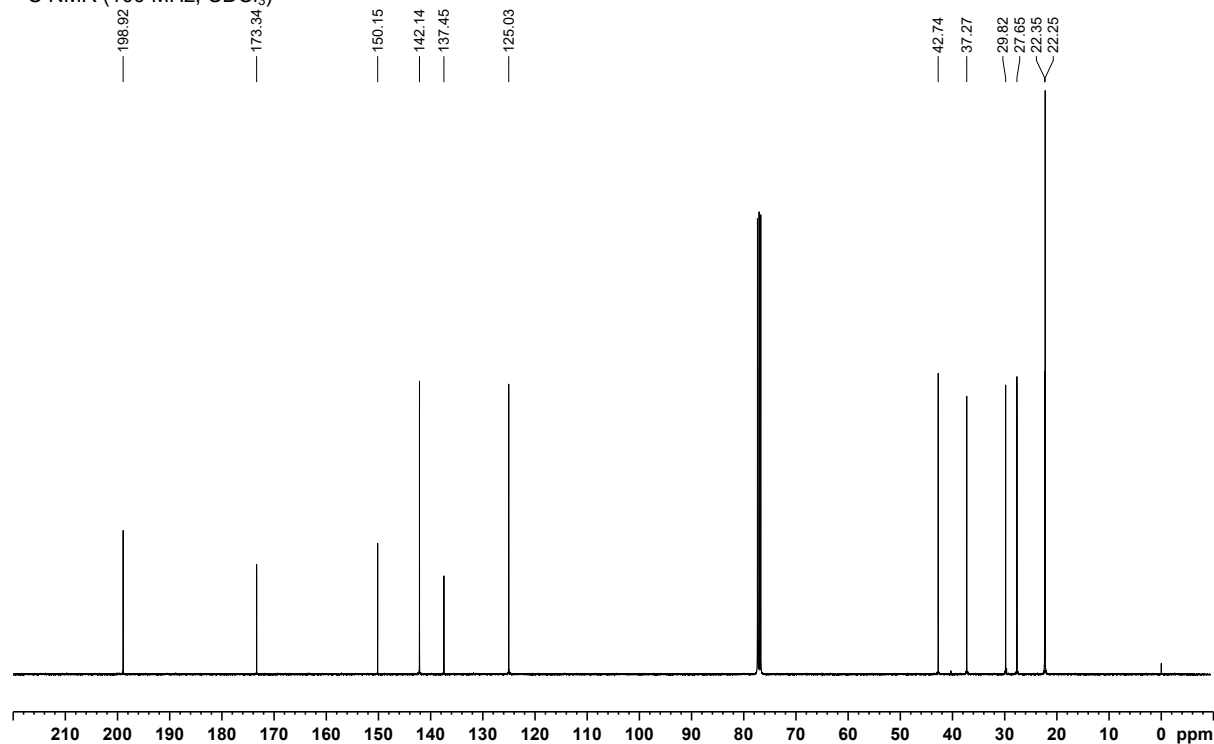
# 3-(2-Isobutylthiazol-5-yl)cyclohex-2-enone 119



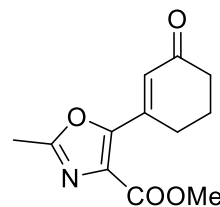
$^1\text{H}$  NMR (400 MHz,  $\text{CDCl}_3$ )



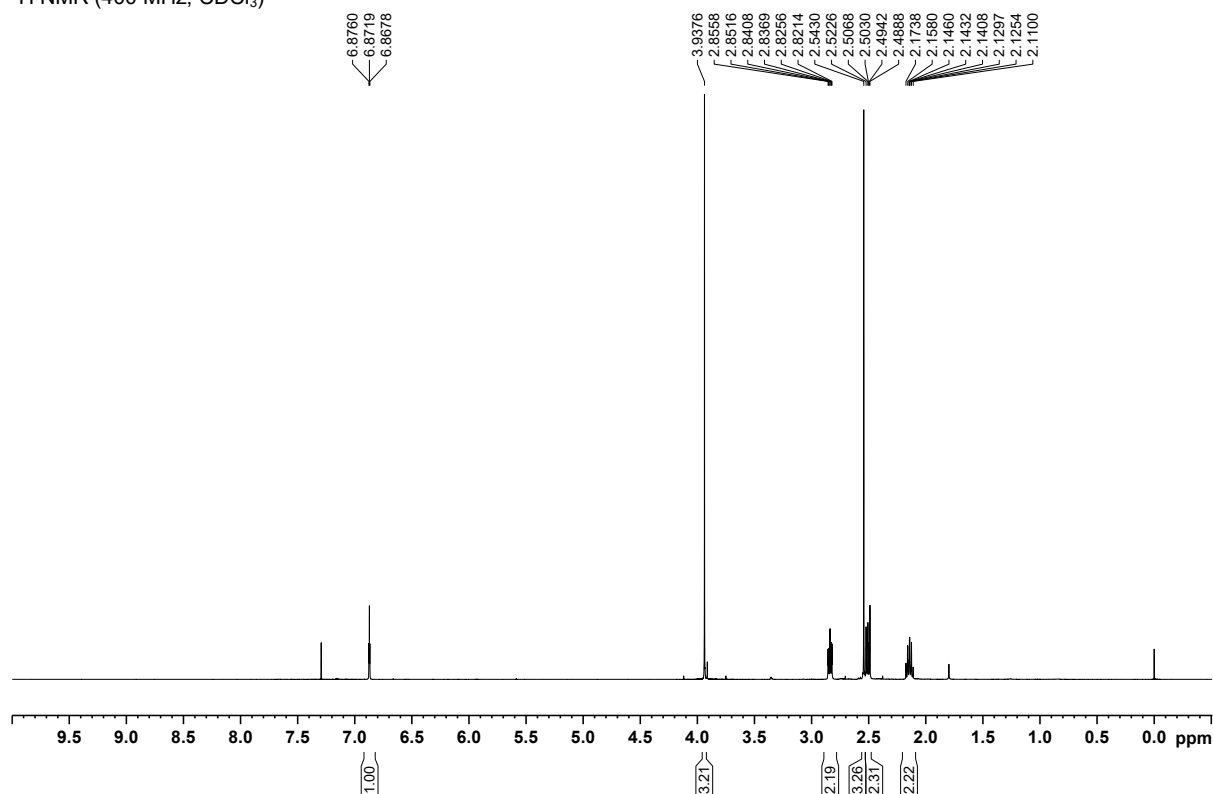
$^{13}\text{C}$  NMR (100 MHz,  $\text{CDCl}_3$ )



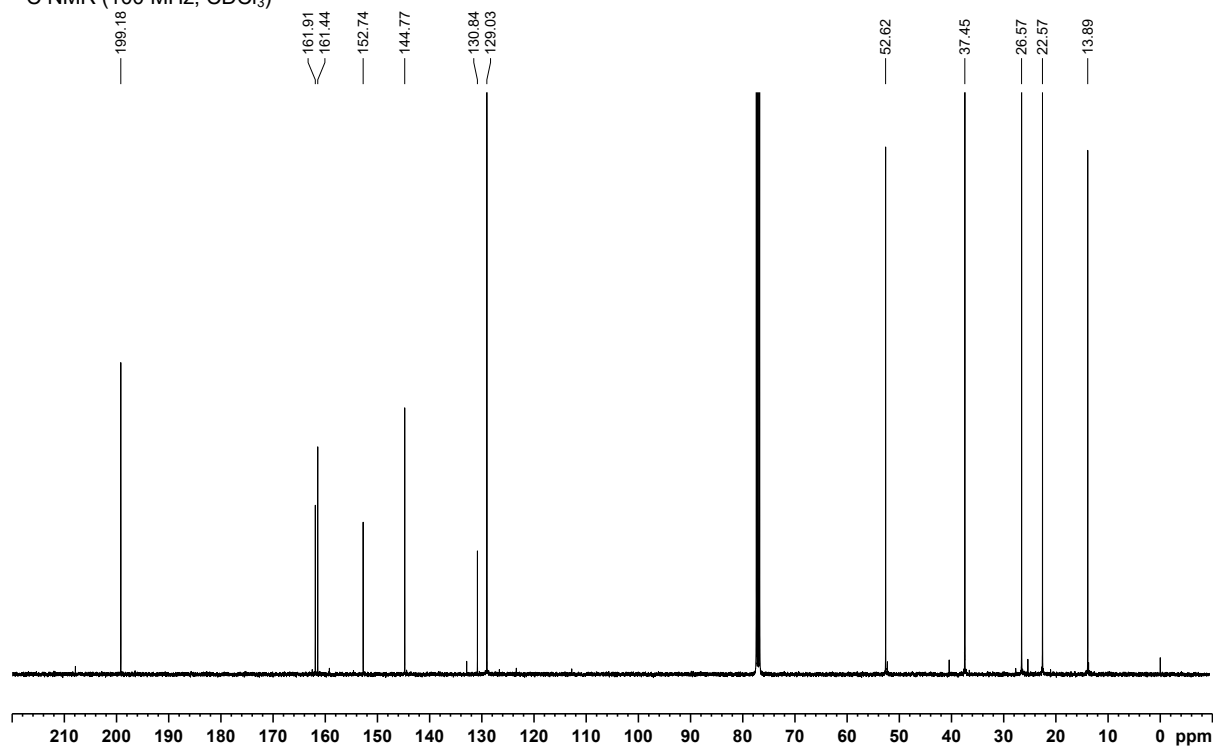
# Methyl 2-methyl-5-(3-oxocyclohex-1-en-1-yl)oxazole-4-carboxylate 120



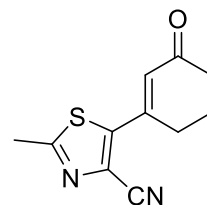
$^1\text{H}$  NMR (400 MHz,  $\text{CDCl}_3$ )



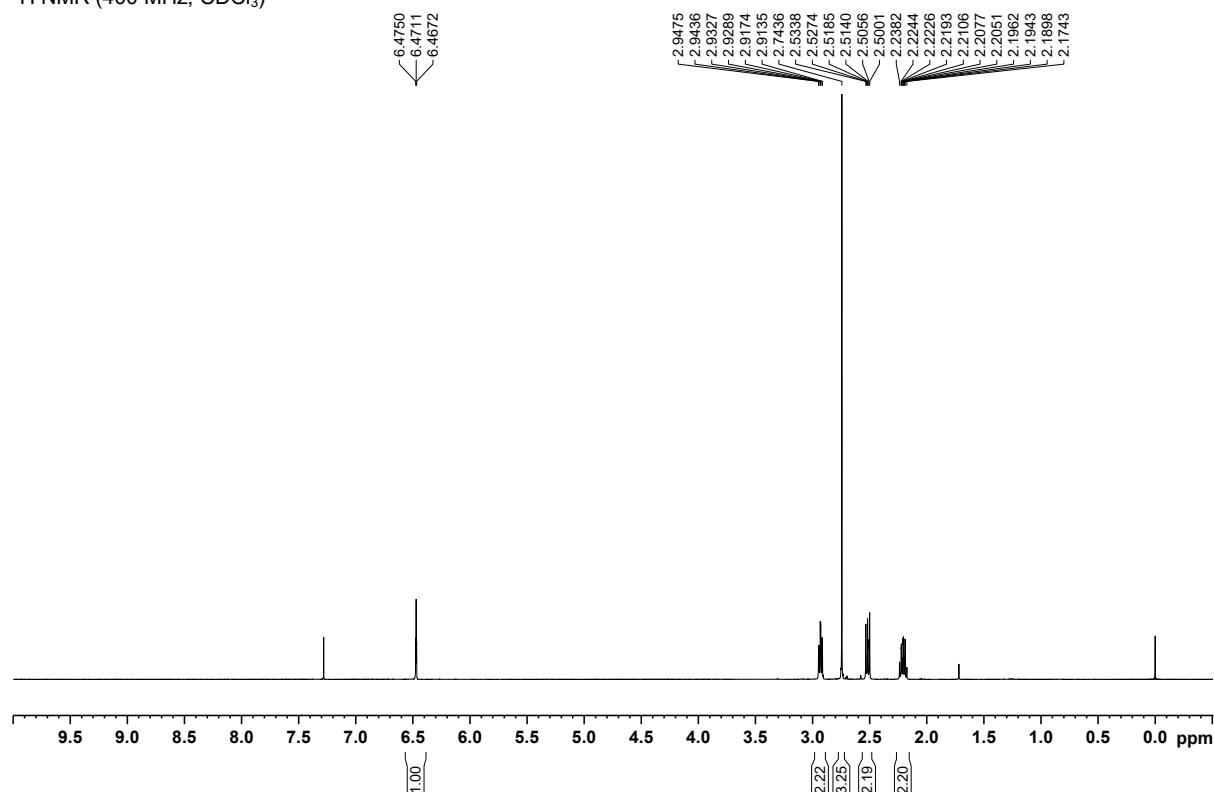
$^{13}\text{C}$  NMR (100 MHz,  $\text{CDCl}_3$ )



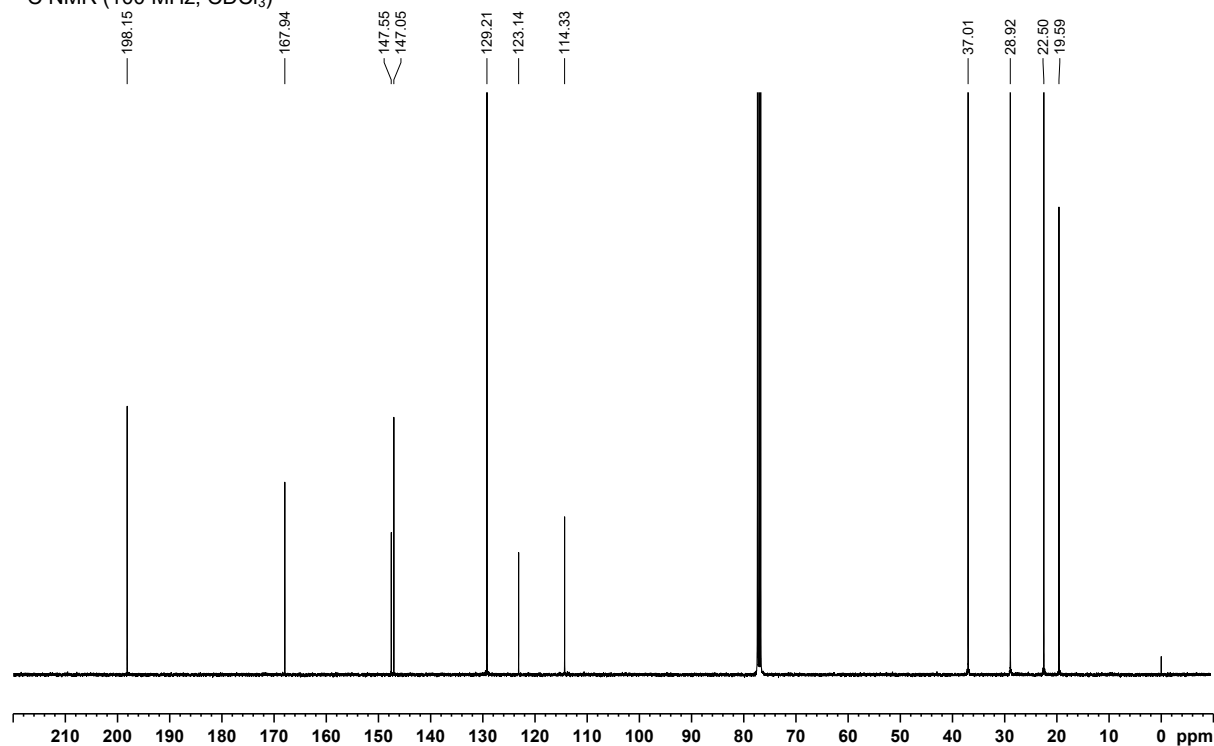
# 2-Methyl-5-(3-oxocyclohex-1-en-1-yl)thiazole-4-carbonitrile 121



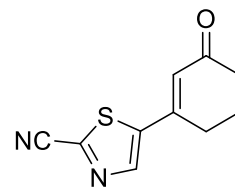
$^1\text{H}$  NMR (400 MHz,  $\text{CDCl}_3$ )



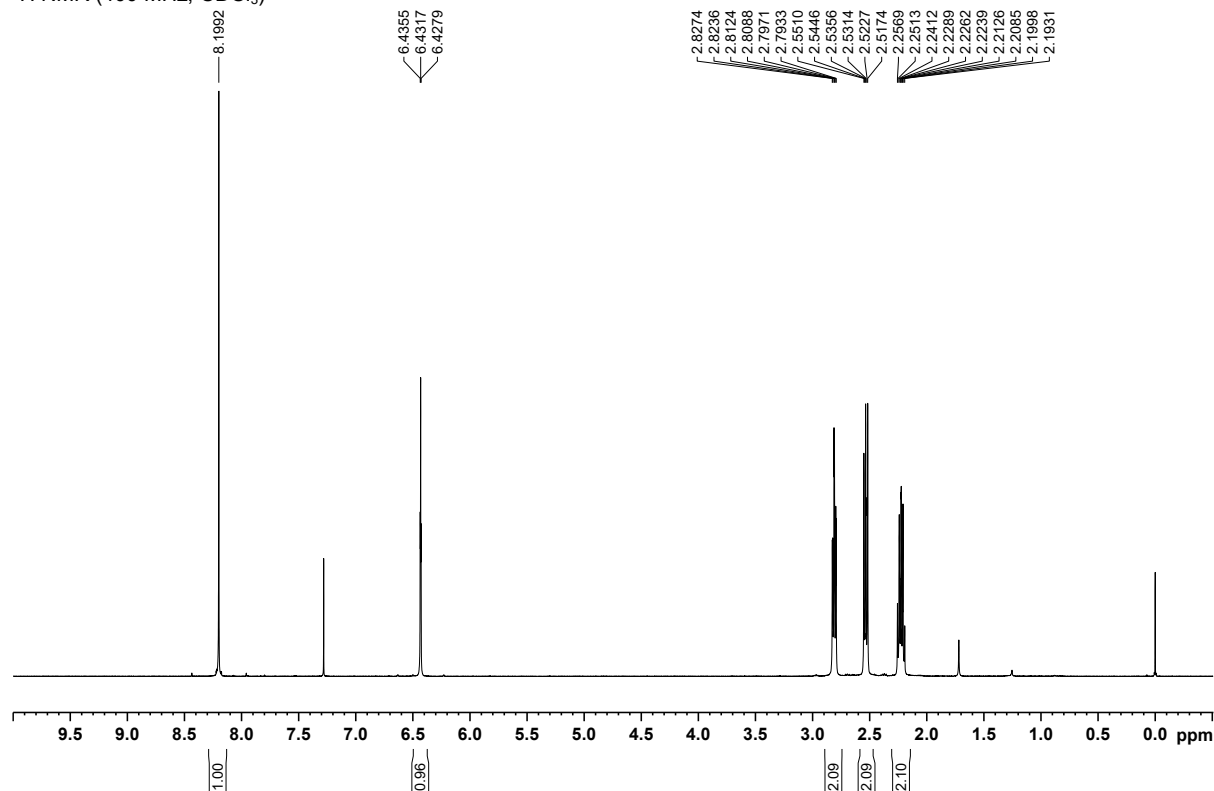
$^{13}\text{C}$  NMR (100 MHz,  $\text{CDCl}_3$ )



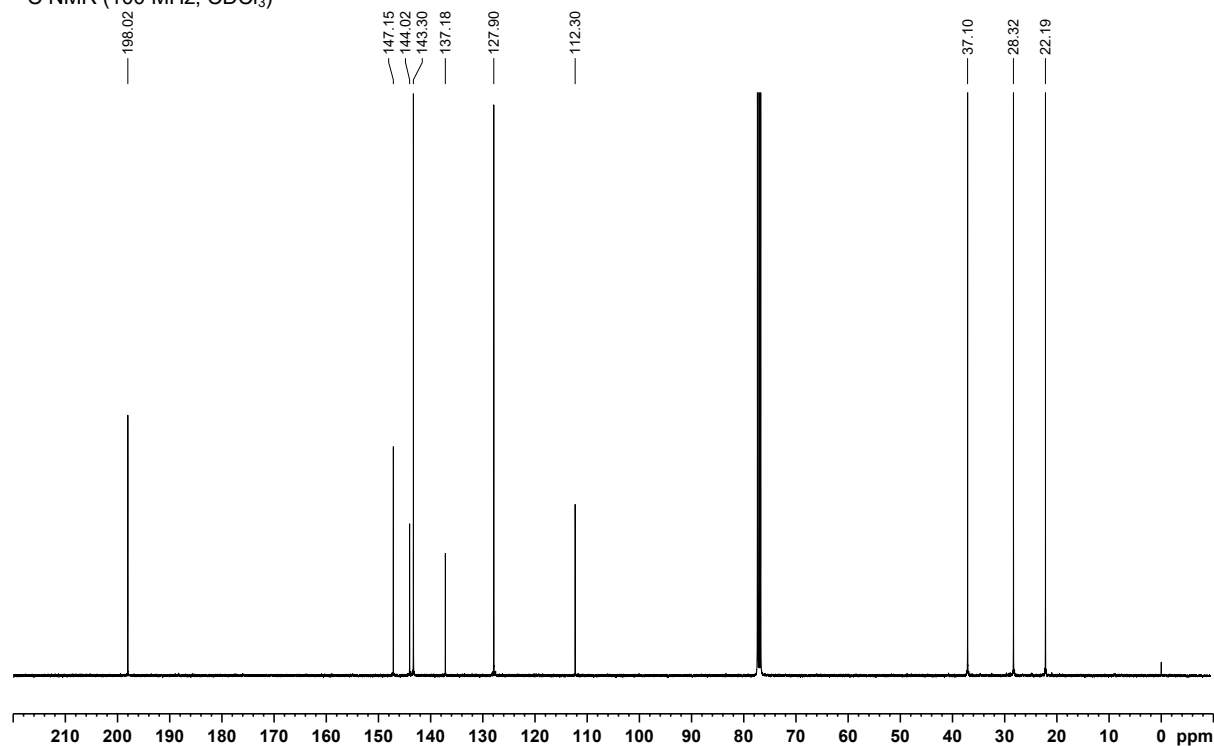
# 5-(3-Oxocyclohex-1-en-1-yl)thiazole-2-carbonitrile 122



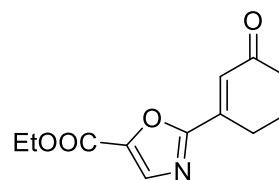
$^1\text{H}$  NMR (400 MHz,  $\text{CDCl}_3$ )



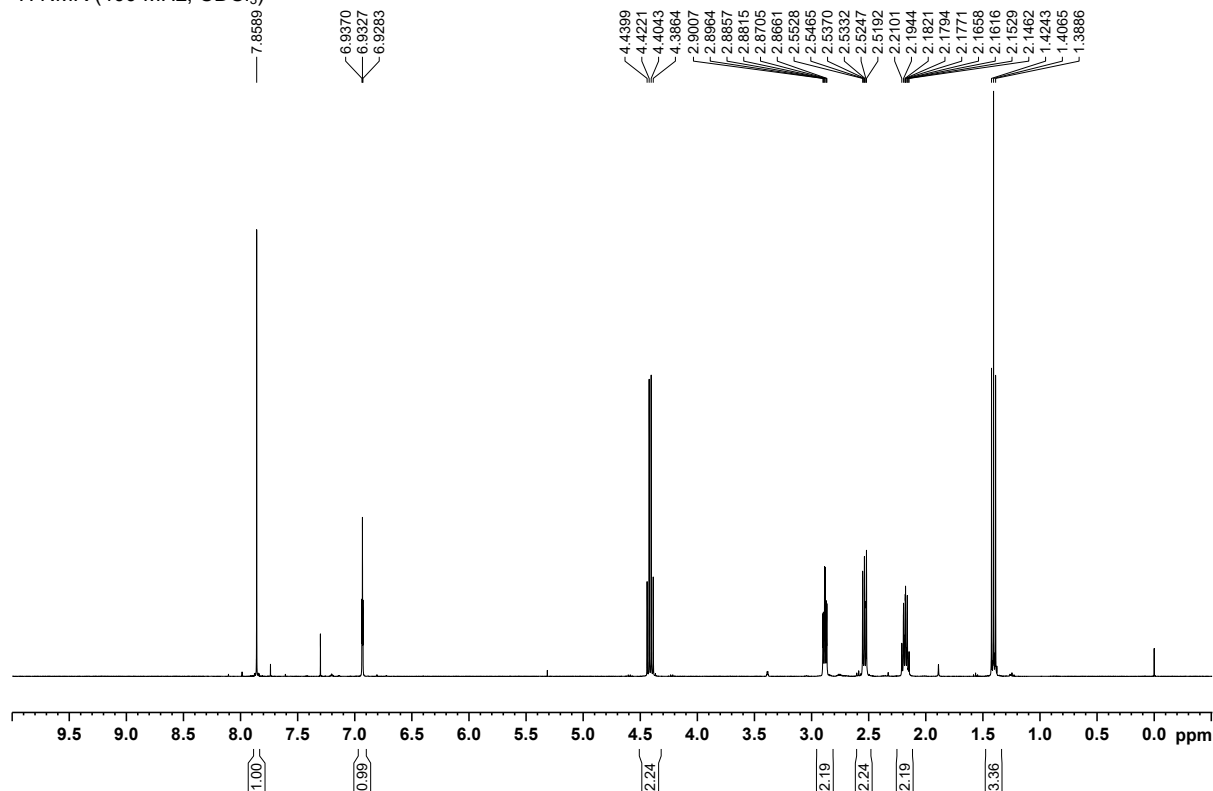
$^{13}\text{C}$  NMR (100 MHz,  $\text{CDCl}_3$ )



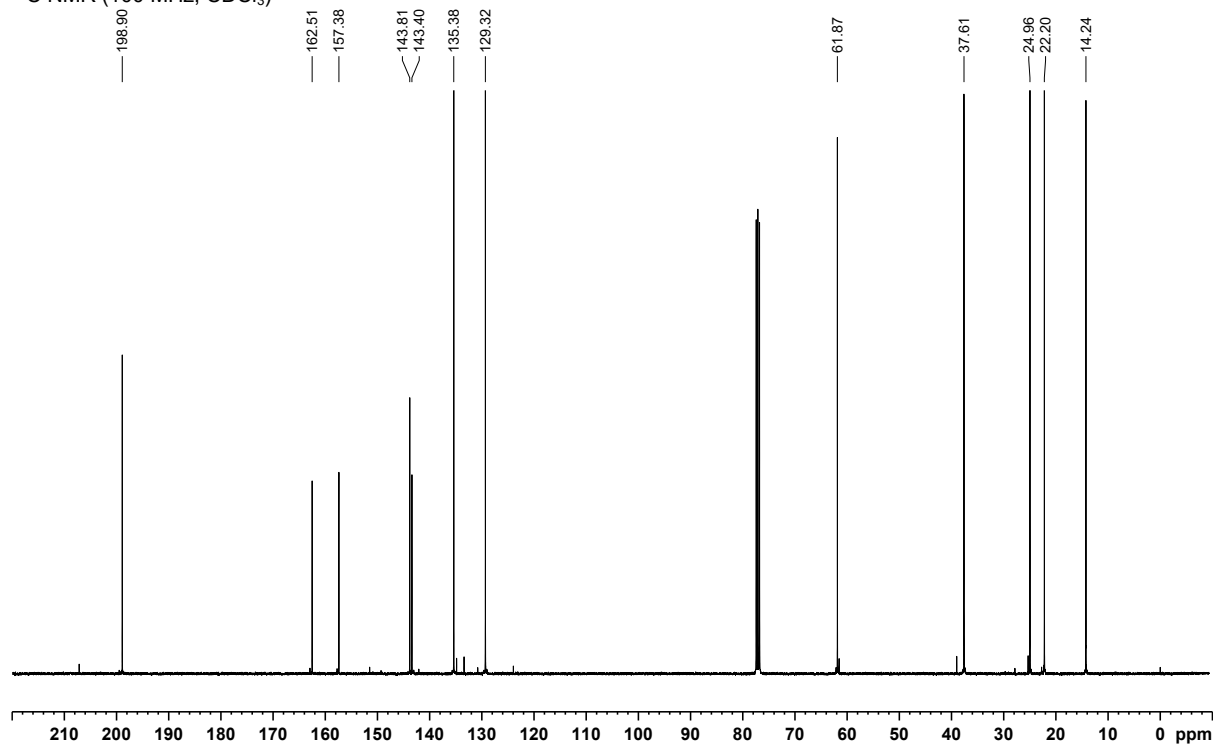
# **Ethyl 2-(3-oxocyclohex-1-en-1-yl)oxazole-5-carboxylate 123**



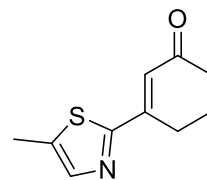
<sup>1</sup>H NMR (400 MHz, CDCl<sub>3</sub>)



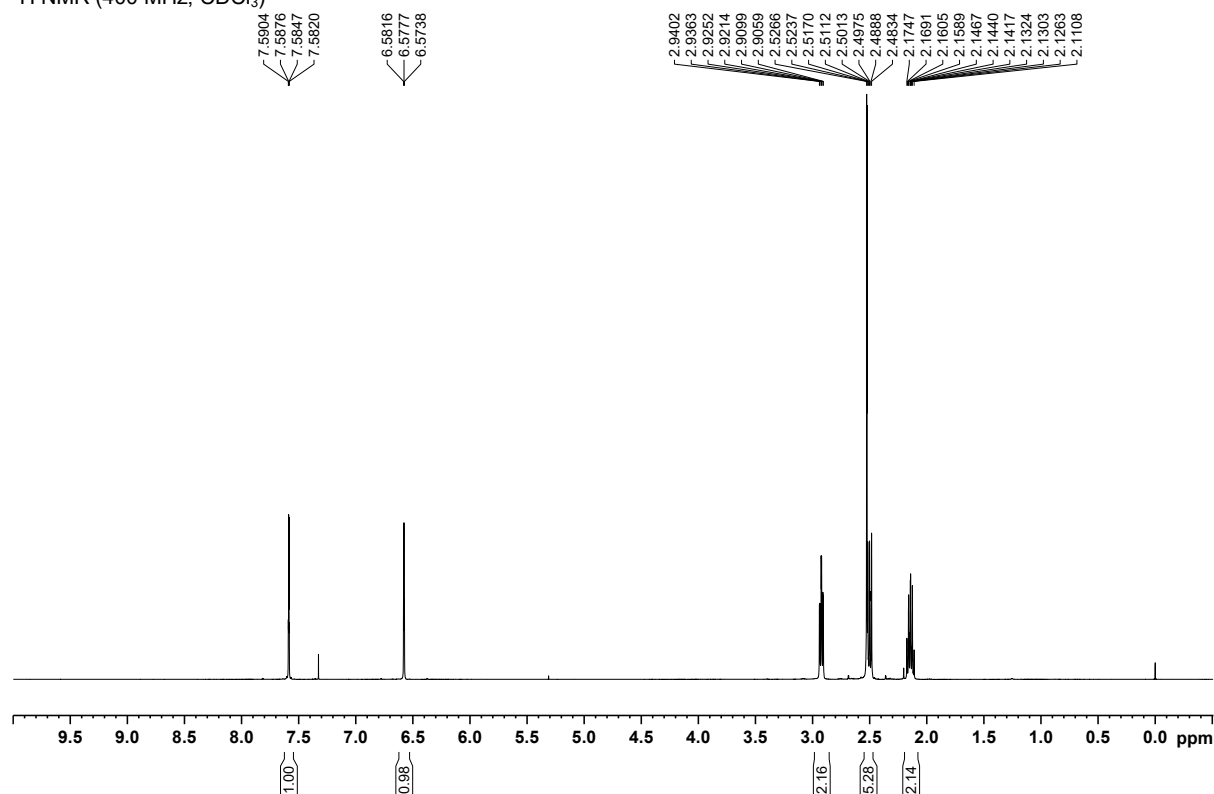
<sup>13</sup>C NMR (100 MHz, CDCl<sub>3</sub>)



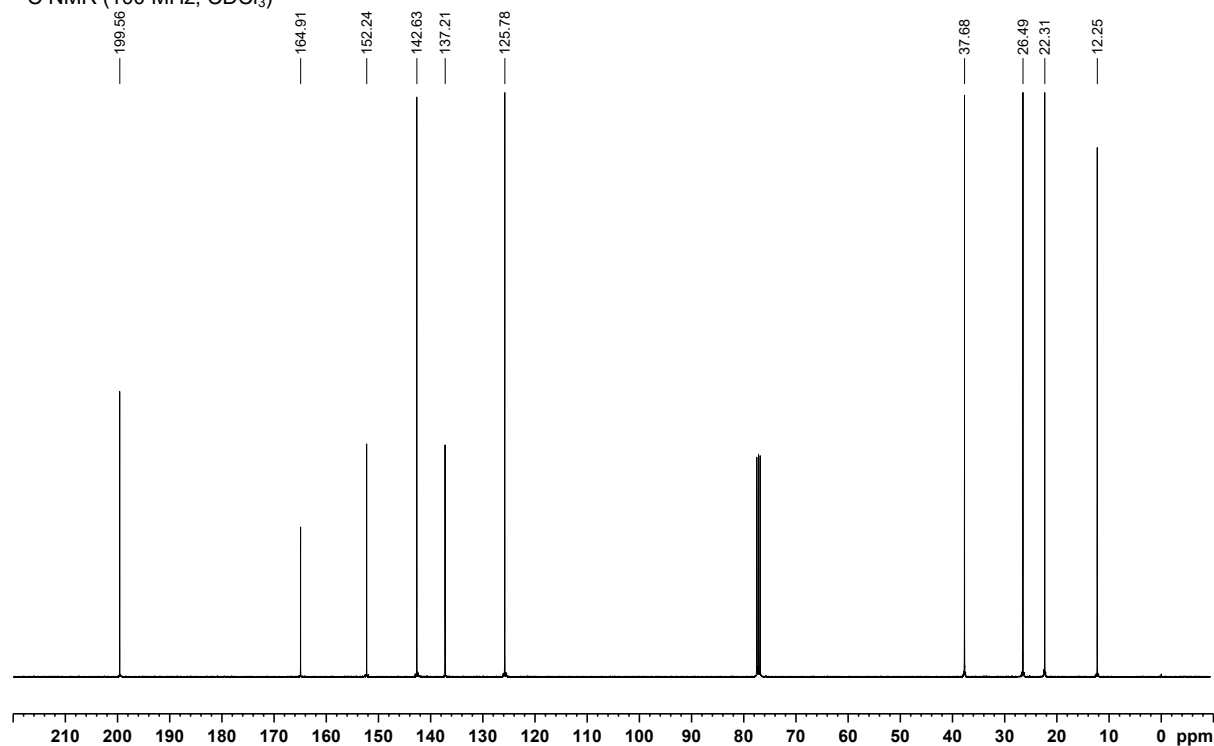
### 3-(5-Methylthiazol-2-yl)cyclohex-2-enone 124



$^1\text{H}$  NMR (400 MHz,  $\text{CDCl}_3$ )

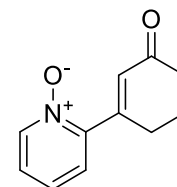


$^{13}\text{C}$  NMR (100 MHz,  $\text{CDCl}_3$ )

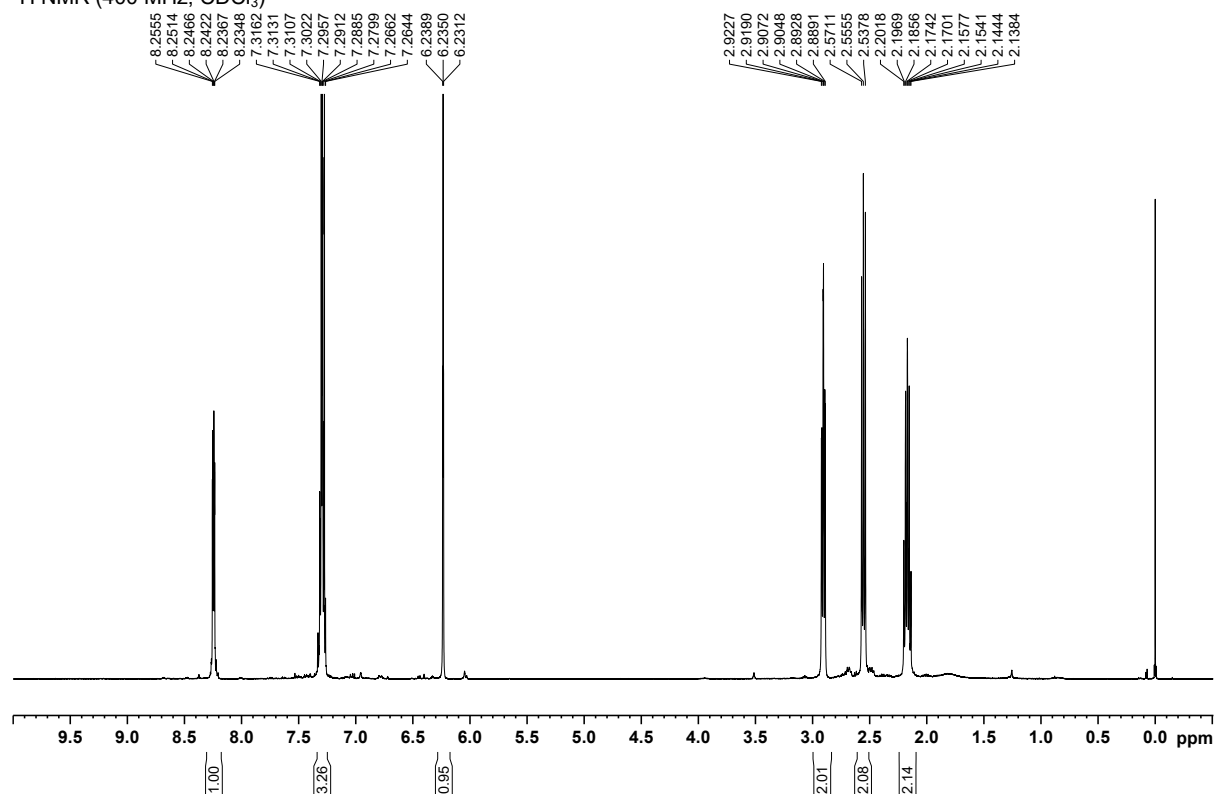




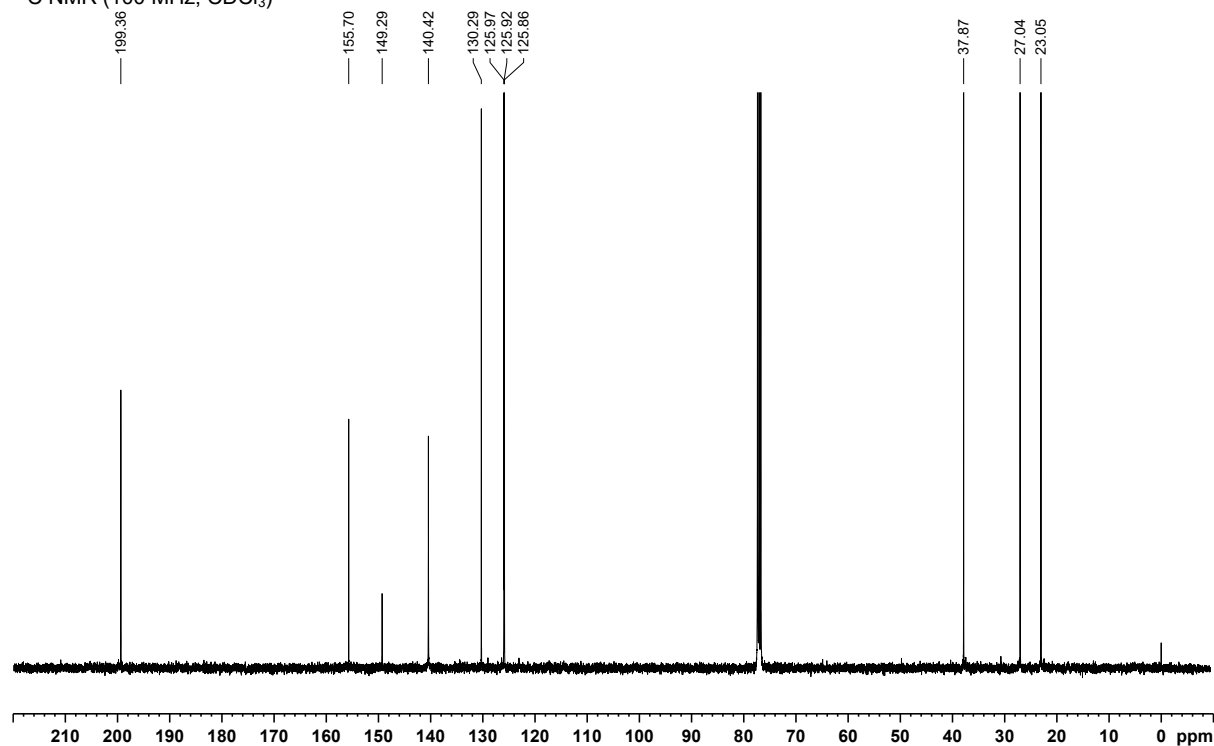
# 2-(3-Oxocyclohex-1-en-1-yl)pyridine 1-oxide 125



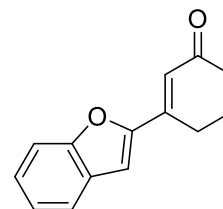
$^1\text{H}$  NMR (400 MHz,  $\text{CDCl}_3$ )



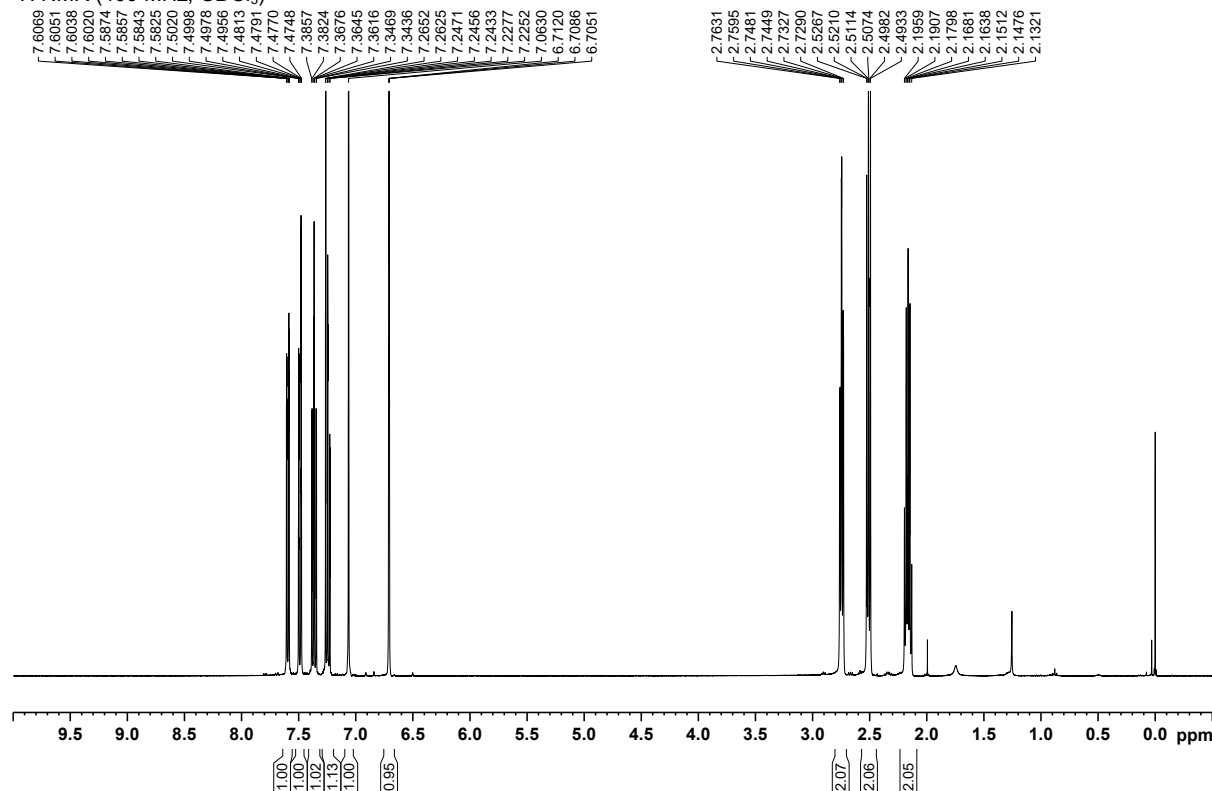
$^{13}\text{C}$  NMR (100 MHz,  $\text{CDCl}_3$ )



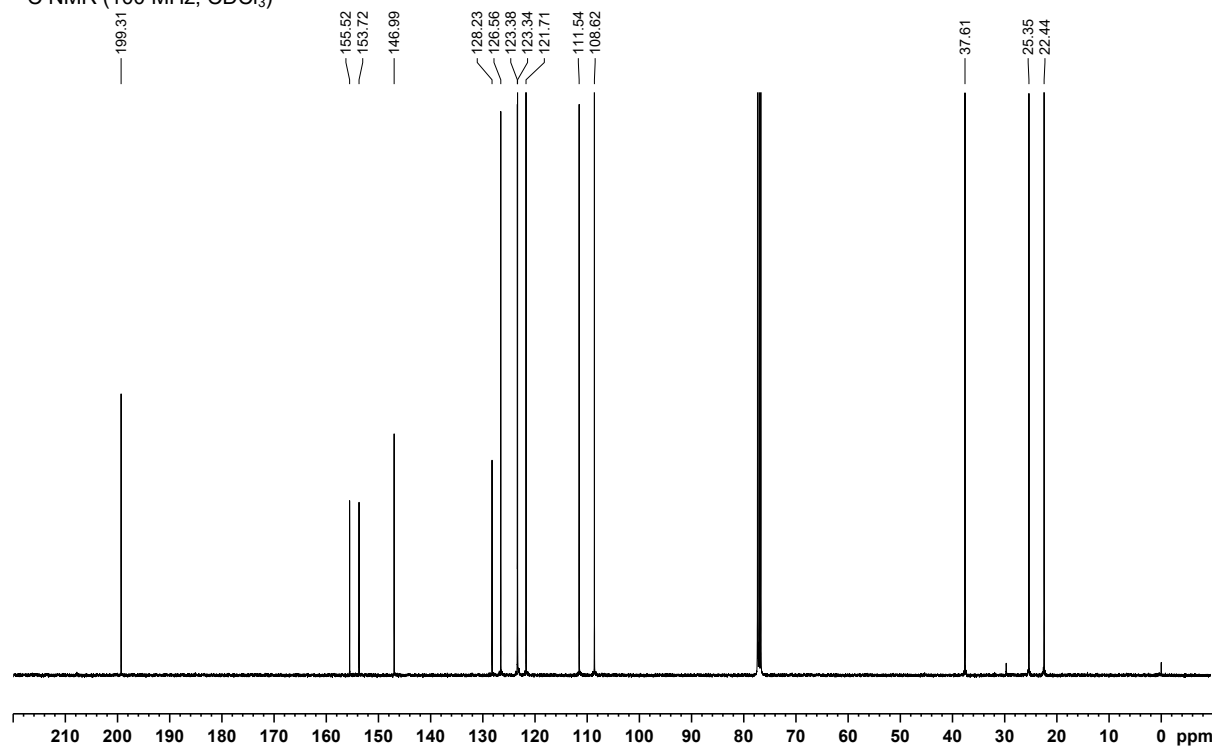
# 3-(Benzofuran-2-yl)cyclohex-2-enone 127



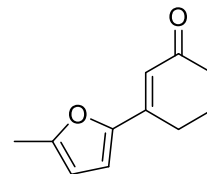
<sup>1</sup>H NMR (400 MHz, CDCl<sub>3</sub>)



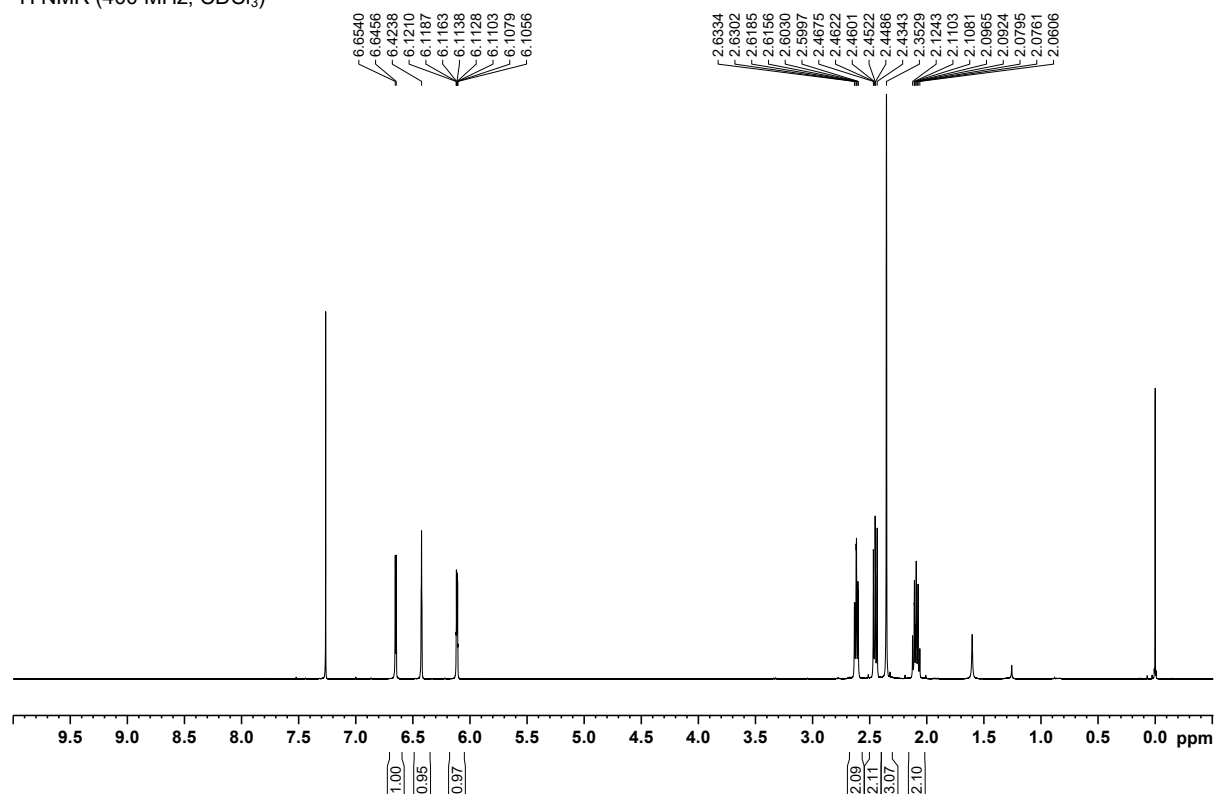
<sup>13</sup>C NMR (100 MHz, CDCl<sub>3</sub>)



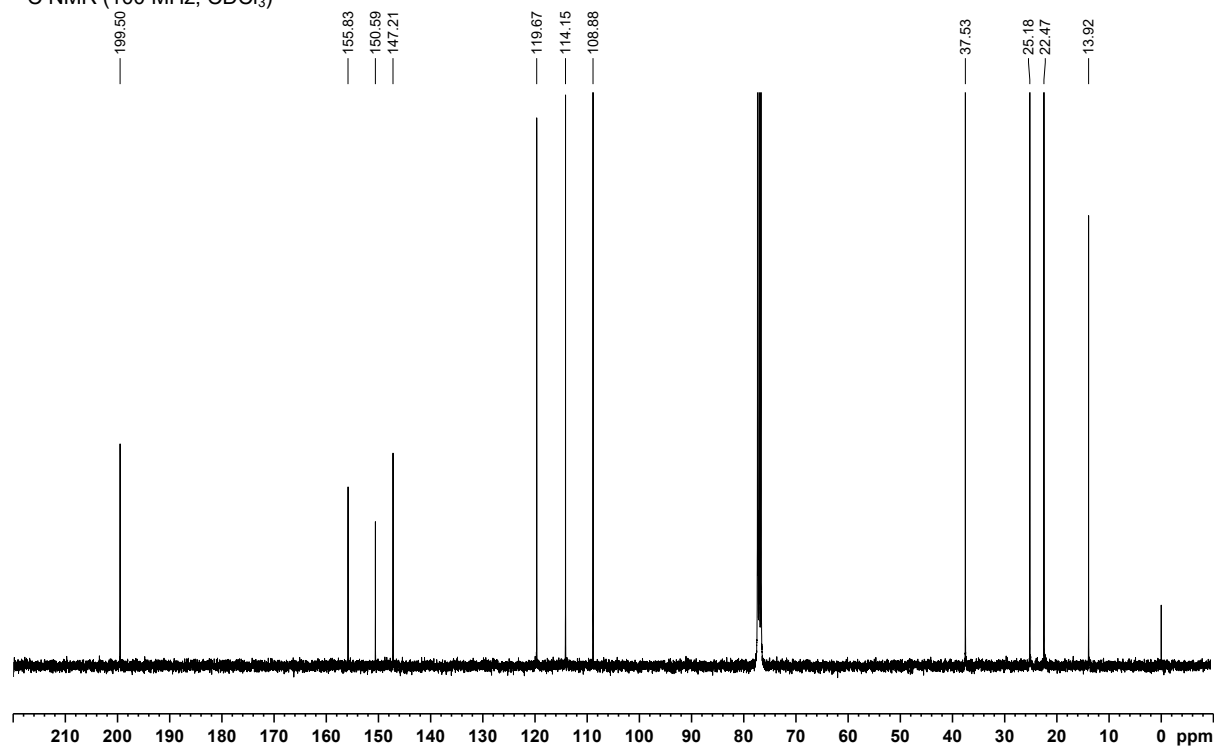
# 3-(5-Methylfuran-2-yl)cyclohex-2-enone 128



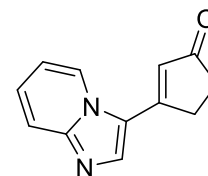
$^1\text{H}$  NMR (400 MHz,  $\text{CDCl}_3$ )



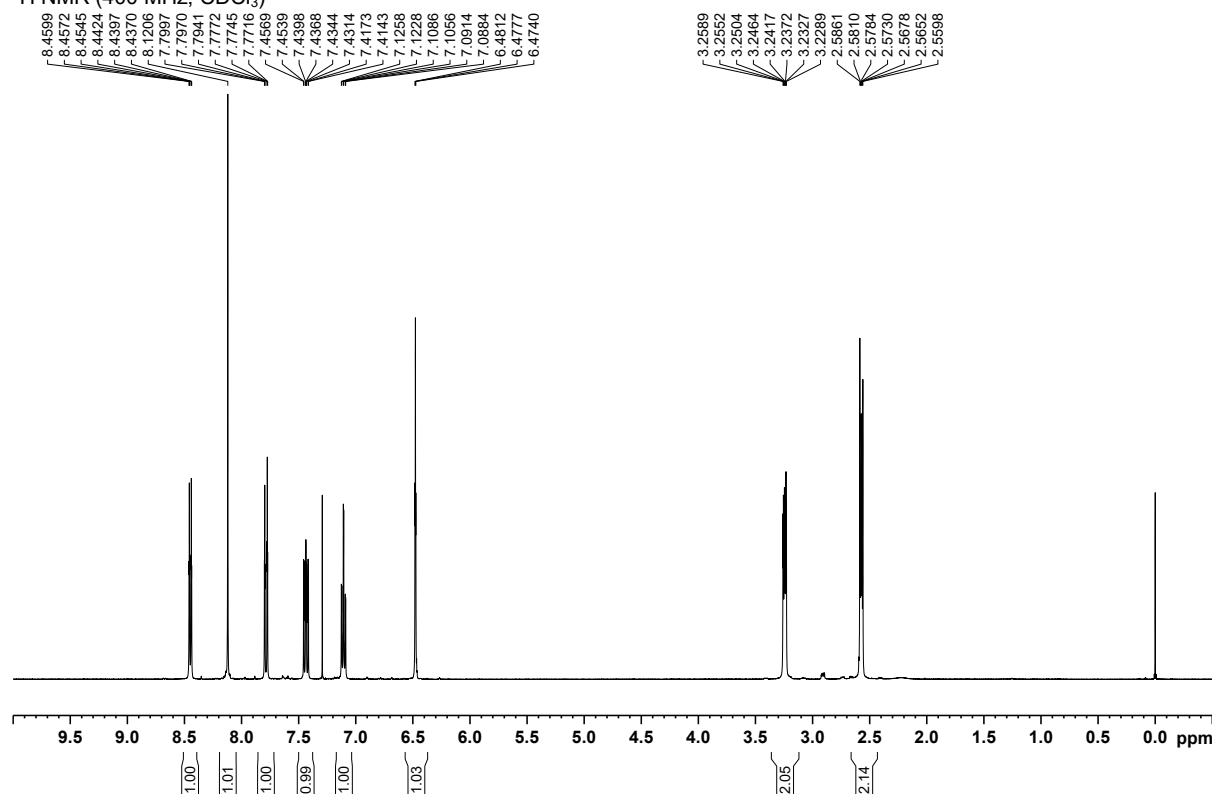
$^{13}\text{C}$  NMR (100 MHz,  $\text{CDCl}_3$ )



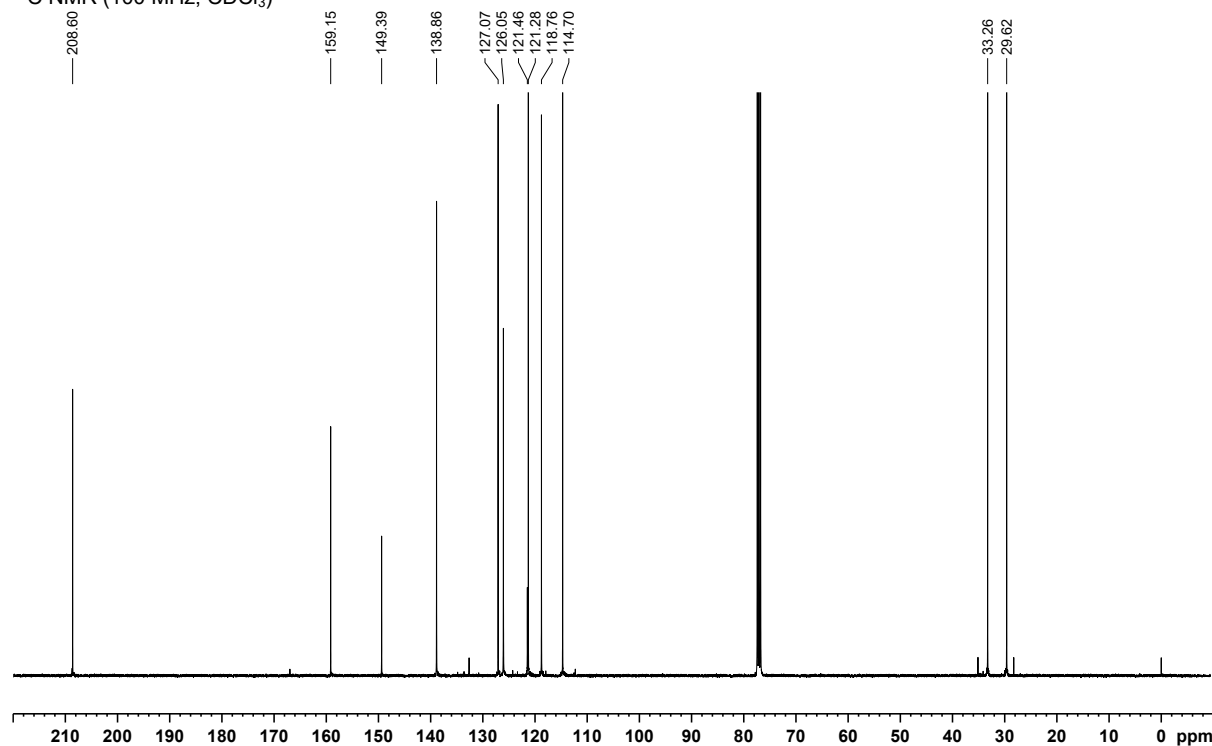
# 3-(Imidazo[1,2-a]pyridin-3-yl)cyclopent-2-enone 140



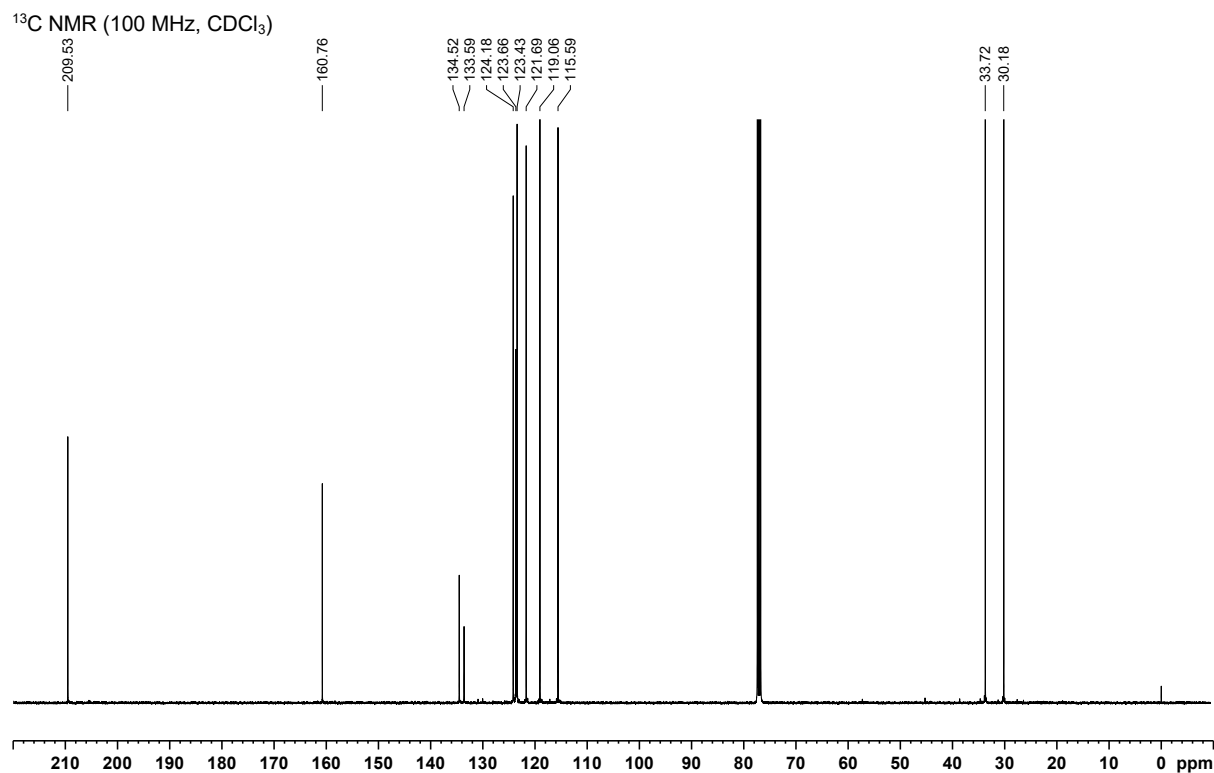
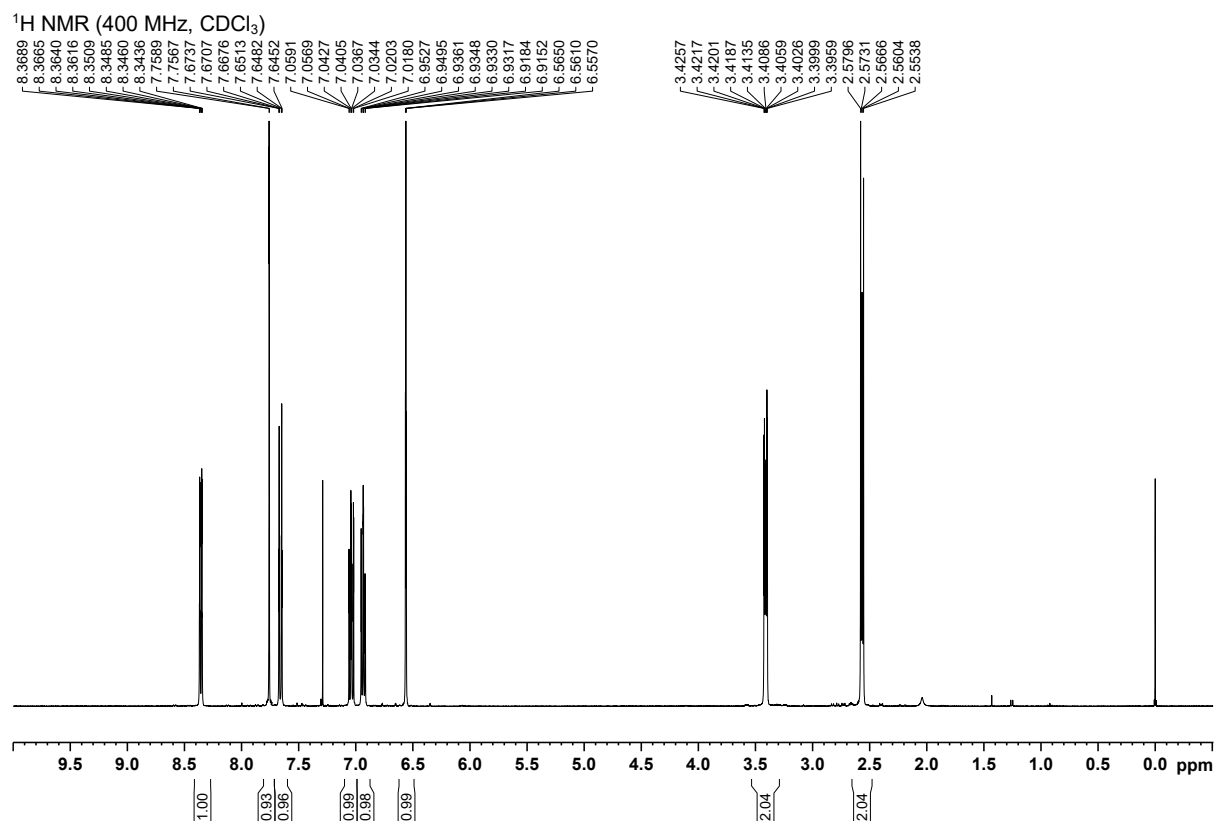
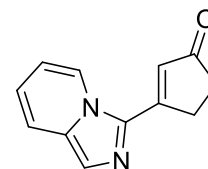
<sup>1</sup>H NMR (400 MHz, CDCl<sub>3</sub>)



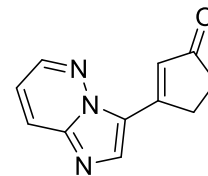
<sup>13</sup>C NMR (100 MHz, CDCl<sub>3</sub>)



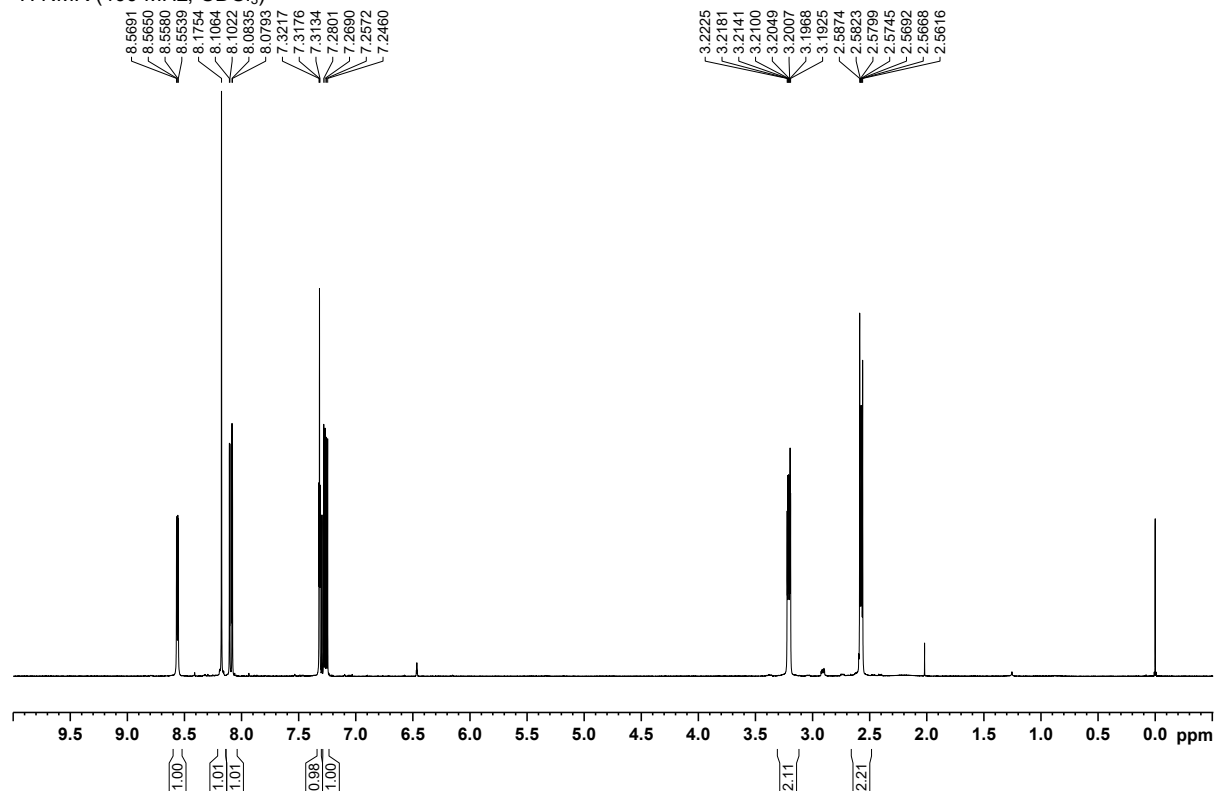
# 3-(Imidazo[1,5-*a*]pyridin-3-yl)cyclopent-2-enone 141



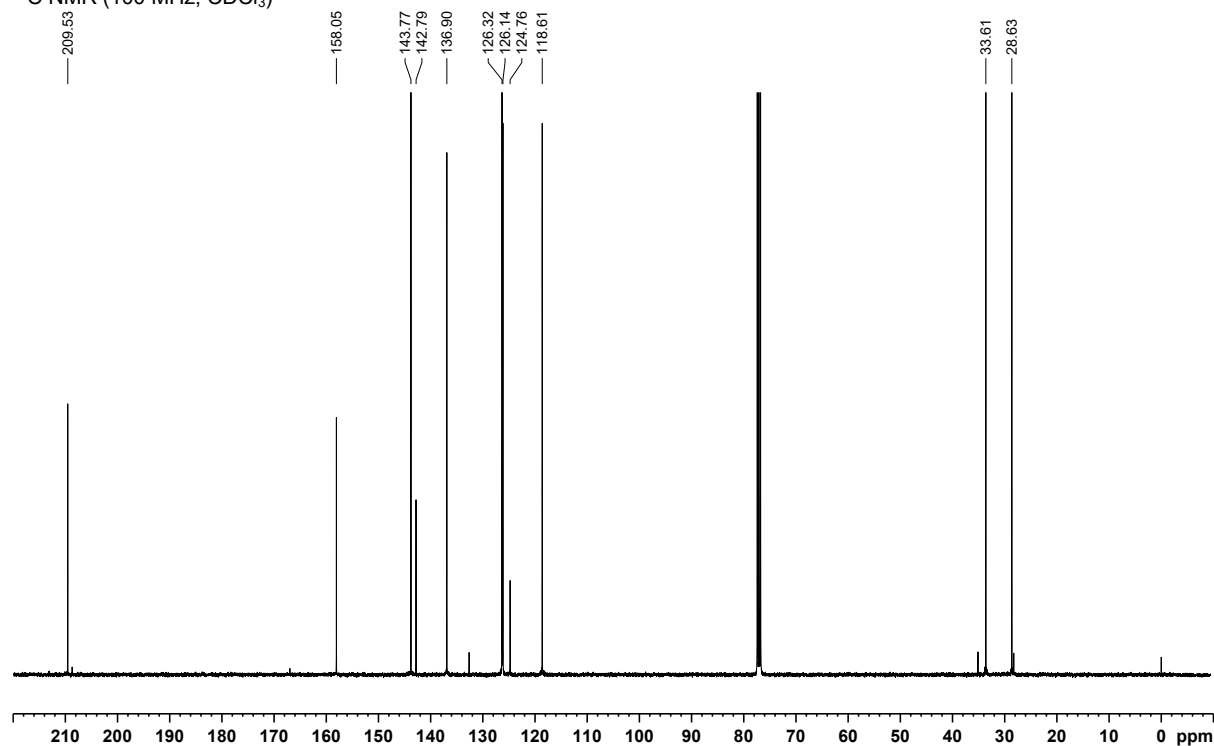
### 3-(Imidazo[1,2-*b*]pyridazin-3-yl)cyclopent-2-enone 142



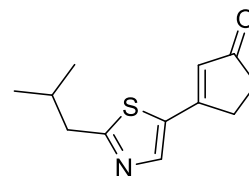
<sup>1</sup>H NMR (400 MHz, CDCl<sub>3</sub>)



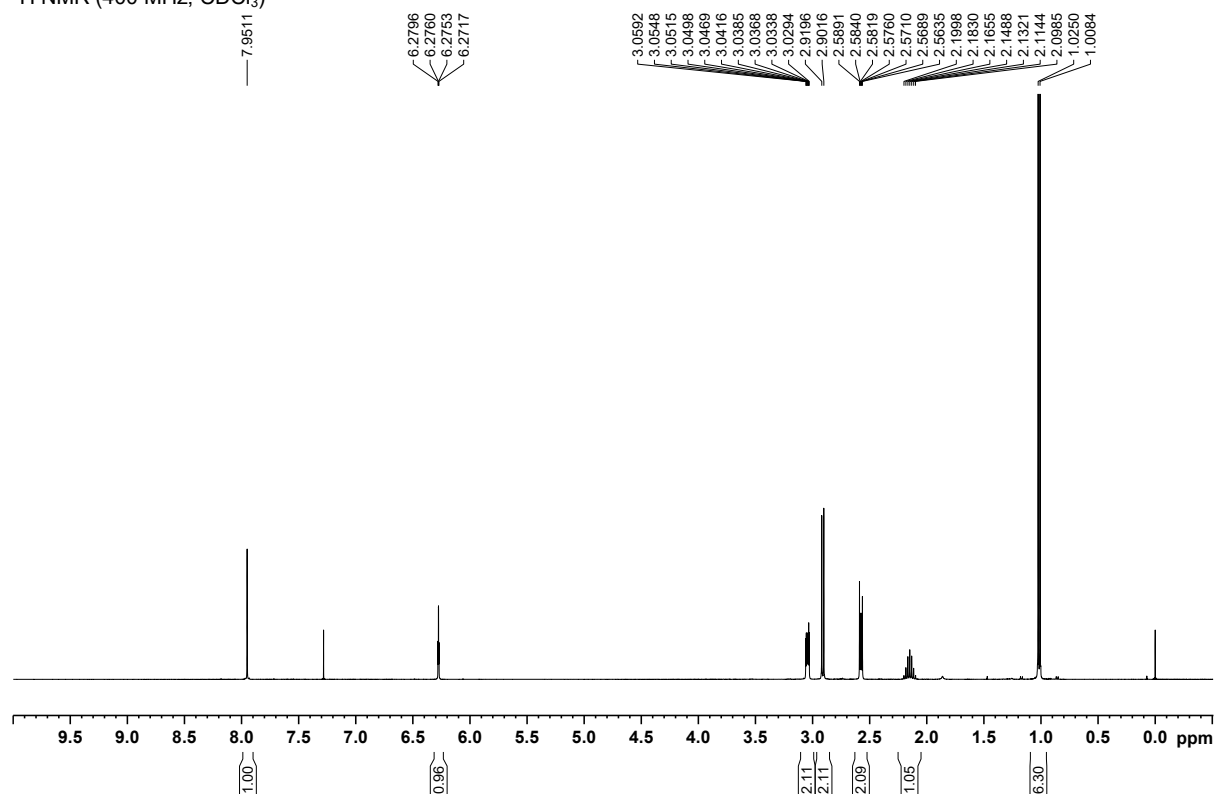
<sup>13</sup>C NMR (100 MHz, CDCl<sub>3</sub>)



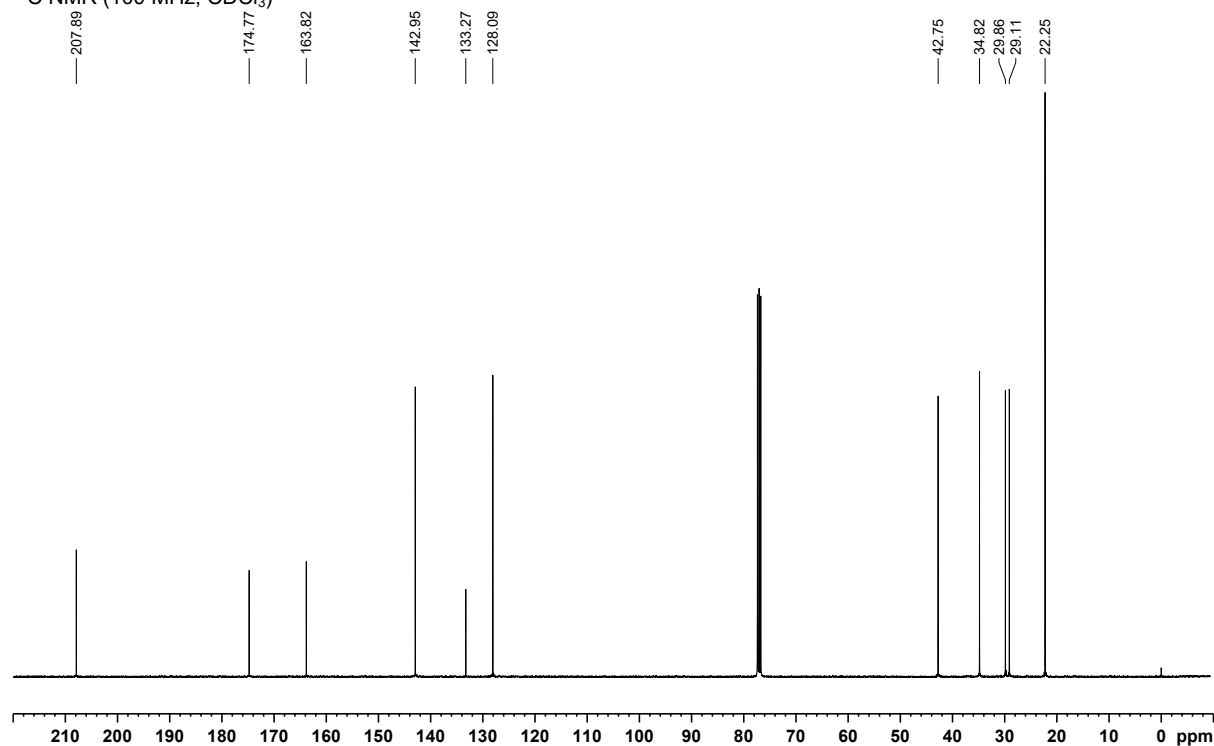
### 3-(2-Isobutylthiazol-5-yl)cyclopent-2-enone 143



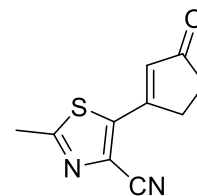
$^1\text{H}$  NMR (400 MHz,  $\text{CDCl}_3$ )



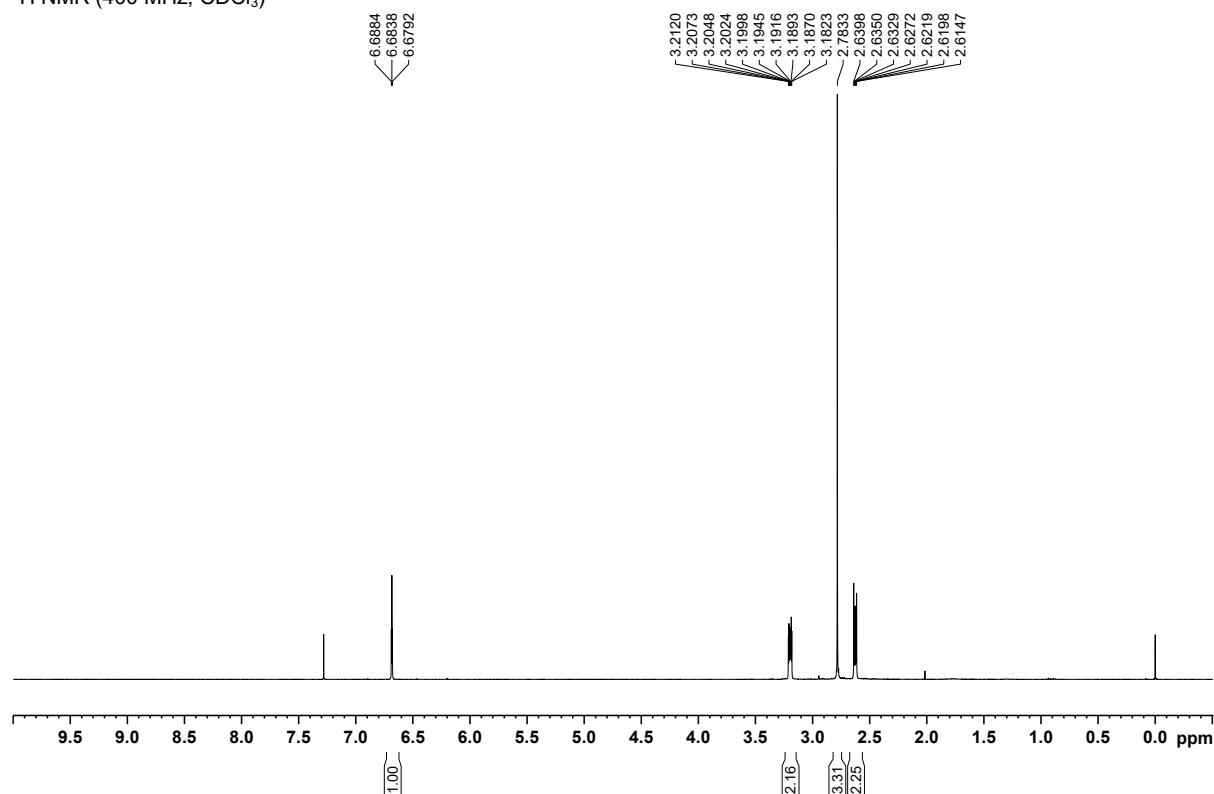
$^{13}\text{C}$  NMR (100 MHz,  $\text{CDCl}_3$ )



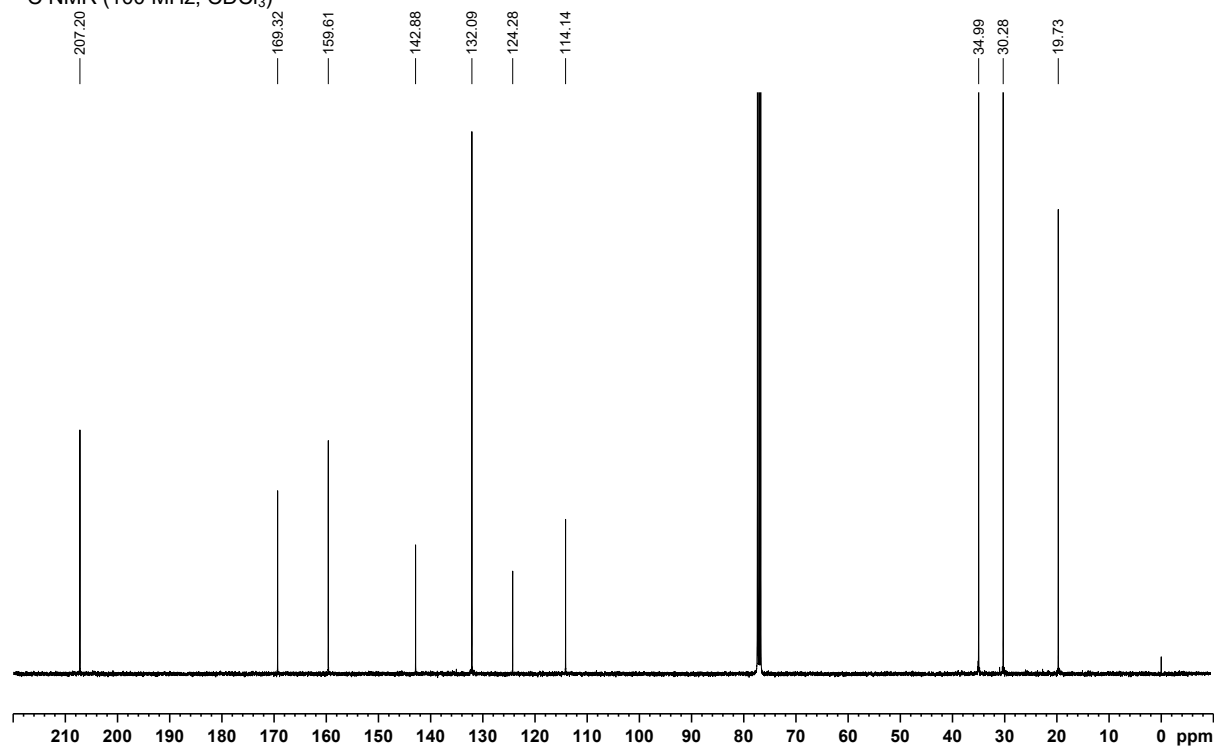
# 2-Methyl-5-(3-oxocyclopent-1-en-1-yl)thiazole-4-carbonitrile 144



$^1\text{H}$  NMR (400 MHz,  $\text{CDCl}_3$ )

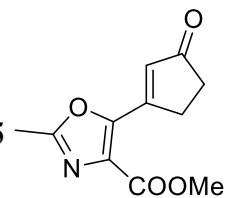


$^{13}\text{C}$  NMR (100 MHz,  $\text{CDCl}_3$ )

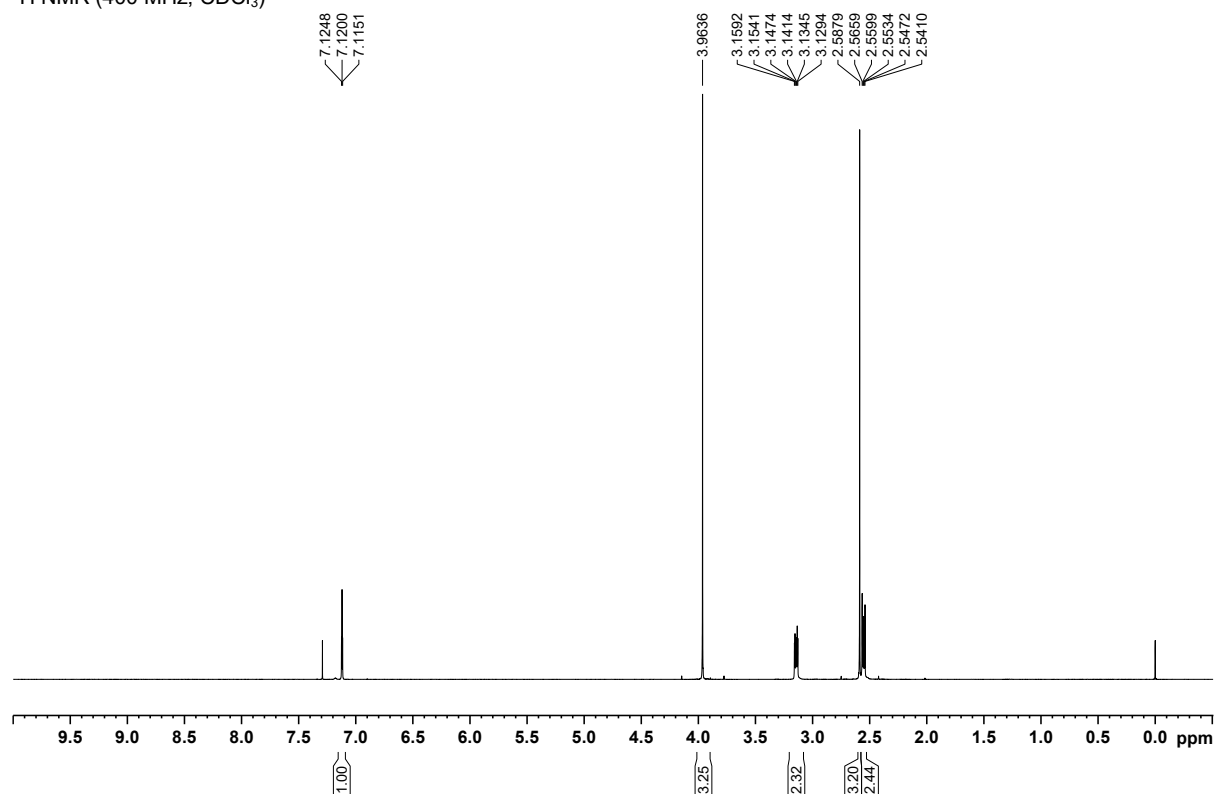




**Methyl 2-methyl-5-(3-oxocyclopent-1-en-1-yl)oxazole-4-carboxylate 145**



$^1\text{H}$  NMR (400 MHz,  $\text{CDCl}_3$ )



$^{13}\text{C}$  NMR (100 MHz,  $\text{CDCl}_3$ )

